

---

[All ETDs from UAB](#)

[UAB Theses & Dissertations](#)

---

1987

## Computer Controlled Partial Ischemia In The Rat Brain.

Richard John Boehme Jr  
*University of Alabama at Birmingham*

Follow this and additional works at: <https://digitalcommons.library.uab.edu/etd-collection>

---

### Recommended Citation

Boehme, Richard John Jr, "Computer Controlled Partial Ischemia In The Rat Brain." (1987). *All ETDs from UAB*. 4327.

<https://digitalcommons.library.uab.edu/etd-collection/4327>

This content has been accepted for inclusion by an authorized administrator of the UAB Digital Commons, and is provided as a free open access item. All inquiries regarding this item or the UAB Digital Commons should be directed to the [UAB Libraries Office of Scholarly Communication](#).

## INFORMATION TO USERS

The most advanced technology has been used to photograph and reproduce this manuscript from the microfilm master. UMI films the original text directly from the copy submitted. Thus, some dissertation copies are in typewriter face, while others may be from a computer printer.

In the unlikely event that the author did not send UMI a complete manuscript and there are missing pages, these will be noted. Also, if unauthorized copyrighted material had to be removed, a note will indicate the deletion.

Oversize materials (e.g., maps, drawings, charts) are reproduced by sectioning the original, beginning at the upper left-hand corner and continuing from left to right in equal sections with small overlaps. Each oversize page is available as one exposure on a standard 35 mm slide or as a 17" x 23" black and white photographic print for an additional charge.

Photographs included in the original manuscript have been reproduced xerographically in this copy. 35 mm slides or 6" x 9" black and white photographic prints are available for any photographs or illustrations appearing in this copy for an additional charge. Contact UMI directly to order.



300 North Zeeb Road, Ann Arbor, MI 48106-1346 USA



**Order Number 8801891**

**Computer controlled partial ischemia in the rat brain**

**Boehme, Richard John, Jr., Ph.D.**

**The University of Alabama in Birmingham, 1987**

**U·M·I**

300 N. Zeeb Rd.  
Ann Arbor, MI 48106



**PLEASE NOTE:**

In all cases this material has been filmed in the best possible way from the available copy. Problems encountered with this document have been identified here with a check mark .

1. Glossy photographs or pages
2. Colored illustrations, paper or print \_\_\_\_\_
3. Photographs with dark background
4. Illustrations are poor copy \_\_\_\_\_
5. Pages with black marks, not original copy \_\_\_\_\_
6. Print shows through as there is text on both sides of page \_\_\_\_\_
7. Indistinct, broken or small print on several pages
8. Print exceeds margin requirements \_\_\_\_\_
9. Tightly bound copy with print lost in spine \_\_\_\_\_
10. Computer printout pages with indistinct print \_\_\_\_\_
11. Page(s) \_\_\_\_\_ lacking when material received, and not available from school or author.
12. Page(s) \_\_\_\_\_ seem to be missing in numbering only as text follows.
13. Two pages numbered \_\_\_\_\_. Text follows.
14. Curling and wrinkled pages \_\_\_\_\_
15. Dissertation contains pages with print at a slant, filmed as received
16. Other \_\_\_\_\_  
\_\_\_\_\_  
\_\_\_\_\_

**U·M·I**



**COMPUTER CONTROLLED PARTIAL ISCHEMIA IN THE RAT BRAIN**

by

**RICHARD J. BOEHME, JR.**

**A DISSERTATION**

**Submitted in partial fulfillment of the requirements for the degree of  
Doctor of Philosophy in the Department of Biomedical Engineering  
in the Graduate School, The University of Alabama  
at Birmingham**

**BIRMINGHAM, ALABAMA**

**1987**

**DEDICATION**

**To Julia, Ashley, Bo, and Eudoxie Robinson**

ABSTRACT OF DISSERTATION  
GRADUATE SCHOOL, UNIVERSITY OF ALABAMA AT BIRMINGHAM

Degree Doctor of Philosophy Major Subject Biomedical Engineering

Name of Candidate Richard J. Boehme, Jr.

Title Computer Controlled Partial Ischemia in the Rat Brain

---

**ABSTRACT**

A system permitting computer control of partial ischemia in the normotensive rat brain was developed. Bilateral subclavian artery occlusion in the rat makes the input of blood to the brain solely dependent on carotid artery input. The studies were performed under constant perfusion pressure. Perfusion pressure is defined as the difference between carotid blood pressure (Circle of Willis pressure as measured anterogradely from the right carotid artery) and venous pressure (measured retrogradely from the right jugular vein). Control of perfusion pressure was effected by partial compression of the left common carotid artery by a servo system which compresses the carotid artery with a balloon. The system can produce a range of partial ischemic states maintaining perfusion pressures from 20 mmHg to 4 mmHg with an accuracy of  $\pm 0.6$  mmHg. The hydrogen clearance method is fully automated and used to determine cerebral blood flow at four different anatomical locations bilaterally (cortex, hippocampus, thalamus, and substantia nigra). Three groups of male Sprague-Dawley rats (300-450 grams)

were studied at constant perfusion pressures of 12 mmHg (N = 7), 9 mmHg (N = 2), and 7 mmHg (N = 7) to determine the relationships among cerebral blood flow, perfusion pressure, and EEG activity with anatomical location. There were significant regional flow differences. In general, the left hemisphere had significantly higher flows at all anatomical sites than the right hemisphere. Flow reductions were most severe in the thalamus and substantia nigra while the cortex was least affected of all the anatomical areas. A linear relationship between EEG and flow was found at flows less than 30 ml/100g/min. An EEG silence threshold was not found. At 7 mmHg perfusion pressure, all flows in the right hemisphere decreased to zero in  $137 \pm 43$  minutes. When initial cerebral blood flow levels fell between 8 and 12 ml/100g/min, they invariably collapsed in the 7 mmHg perfusion pressure group. However, all anatomical areas within this "threshold flow" range recovered slowly in the 9 and 12 mmHg perfusion pressure groups. This suggests that perfusion pressure is more important in determining the fate of flow within an anatomical structure than the absolute flow itself.

Abstract Approved by: Committee Chairman Virginia Capbell  
Program Director Frederic C. Shyng  
Date 8/27/87 Dean of Graduate School Anthony Bamed

## **ACKNOWLEDGEMENTS**

The methodologies developed and studies performed in the dissertation were done as an MD/PhD candidate at the University of Alabama School of Medicine in Birmingham. The area of cerebral vascular disease was suggested to me by Dr. Julio Garcia and I am grateful to him for welcoming me into the Neuropathology Laboratory and introducing me to Dr. Karl Conger.

I especially want to acknowledge and thank Dr. Conger for his guidance, suggestions, and encouragement throughout this period. His influence has greatly stimulated my interest in research and I feel that the techniques that I have learned from him will have a very positive impact on my medical career.

I am very grateful to Dr. Louis C. Sheppard and Dr. Charlie W. Scott for allowing me to participate in their programs and providing me with financial support throughout this period. I want to thank the Department of Pathology for its support.

I would like to acknowledge Dr. Conger and Dr. Tony Hudetz for their concept of modulating the cerebral vascular blood supply through one input. I want to thank Jim Roesel for bringing the balloon technique, which was developed by Dr. Stanley Digerness and Bill Tracy, to the laboratory and Bill Tracy for making the balloon mold on his lathe. I also want to thank Dr. Andras Eke for bringing the servo literature to our attention.

I would like to acknowledge Ed Strong for the design of the blood pressure, hydrogen, EEG, and computer interface circuitry. I would like to thank Dr. James H. Halsey for lending us two Grass recorders and the EEG and blood pressure boxes and Dr. Carpenter for giving me some surgical retracters and the heating element to conduct experiments.

I would especially like to thank Dr. Joe Beckman for his consultation on the statistical workup of the experimental results. I also want to thank Dr. Virginia Campbell, Dr. Beckman, and Dr. Micheal Anderson for their timely reviews of this manuscript. The photographic material included is a result of the care and skill of Ralph Roseman.

Finally, I am eternally grateful to my wife, Julia, and children, Ashley and Bo. Without their continued support and understanding, none of this would have been possible.

## TABLE OF CONTENTS

	Page
ABSTRACT.....	iii
ACKNOWLEDGEMENTS.....	v
LIST OF TABLES.....	ix
LIST OF FIGURES.....	x
LIST OF ABBREVIATIONS.....	xiv
INTRODUCTION.....	1
METHODS.....	7
ANIMAL MODEL.....	15
ANESTHESIA.....	24
HYDROGEN CLEARANCE METHOD.....	31
PERFUSION PRESSURE CONTROL.....	67
EEG MEASUREMENT.....	91
EXPERIMENTAL PROTOCOL.....	95
RESULTS.....	101
DISCUSSION.....	136
APPENDICES	
A THEORETICAL CONSIDERATIONS FOR THE CLEARANCE AND POLAROGRAPHIC EQUATIONS OF THE HYDROGEN CLEARANCE METHOD.....	144
B PLATINUM ELECTRODE ARRAY CONSTRUCTION.....	149

**TABLE OF CONTENTS (continued)**

<b>C LATEX BALLOON MANUFACTURE .....</b>	<b>155</b>
<b>D COMBINED EXPERIMENTAL RESULTS .....</b>	<b>156</b>
<b>BIBLIOGRAPHY.....</b>	<b>185</b>

## LIST OF TABLES

Table		Page
<i>ANESTHESIA</i>		
4-1	Comparison of LCBF with anesthetic regimens within the same animal .....	27
<i>HYDROGEN CLEARANCE METHOD</i>		
5-1	Stereotaxic coordinates for the eight electrode locations including target nucleus .....	39
<i>RESULTS</i>		
9-1	Blood gasses and hematocrit for all animals in the study .....	102
9-2	Pre-ischemic pressures .....	103
9-3	Pre-ischemic CBF levels .....	104
9-4	Ischemic pressures .....	112
9-5	Average CBF as a function of perfusion pressure and anatomical location after partial occlusion was initiated .....	119
9-6	Average EEG activity as a function of perfusion pressure and anatomical location after partial occlusion was initiated .....	128
9-7	Slopes for EEG regression lines .....	135

## LIST OF FIGURES

Figure	Page
<b>METHODS</b>	
2-1 The current system .....	8
2-2 In-vivo arrangement of the balloon compression technique.....	10
2-3 Console display during the experiment.....	12
<b>ANIMAL MODEL</b>	
3-1 Cerebral blood supply in the rat .....	16
3-2 Anatomical relationship of the subclavian arteries .....	19
3-3 Perfusion pressure control during bilateral subclavian occlusion .....	21
<b>ANESTHESIA</b>	
4-1 The anesthetic and hydrogen gas delivery system .....	25
<b>HYDROGEN CLEARANCE METHOD</b>	
5-1 LCBF determination from an exponential hydrogen clearance curve .....	35
5-2 Stereotaxic location for platinum electrodes .....	37
5-3 Simple circuit for measuring tissue hydrogen concentration level with platinum electrodes.....	42

**LIST OF FIGURES (continued)**

<b>Figure</b>	<b>Page</b>
5-4 Schematic diagram of platinum electrode polarization and current measuring circuit.....	45
5-5 Computer interface schematic.....	49
5-6 Hydrogen concentration profile for serial LCBF determinations.....	57
5-7 Hydrogen concentration profile during a 7 mmHg perfusion pressure experiment.....	60
5-8 Summary of conditions.....	65

**PRESSURE CONTROL SUBSYSTEM**

6-1 In-vivo arrangement of the balloon and cuff.....	68
6-2 Pressure monitoring system mechanical.....	70
6-3 Computer control interface schematic.....	73
6-4 Pressure monitoring interface circuitry.....	75
6-5 Power supply and electronic controlling circuit for the servo-motor.....	78
6-6 Bi-directional servo control syringe.....	81
6-7 In-vitro test of servo-balloon system.....	85
6-8 In-vivo test of servo-balloon system.....	88

**EEG MEASUREMENT**

7-1 Frequency response curves for the active EEG filter.....	93
--	----

**EXPERIMENTAL PROTOCOL**

8-1 Bilateral electrode array implant.....	96
--	----

## LIST OF FIGURES (continued)

Figure	Page
<b>RESULTS</b>	
9-1 Perfusion control experiment .....	105
9-2 Control of perfusion pressure at 12 mmHg and 7 mmHg .....	107
9-3 Control of perfusion pressure at 9 mmHg. ....	109
9-4 Bilateral substantia nigral CBF at 12 mmHg and 7 mmHg perfusion pressure. ....	113
9-5 Bilateral thalamic-substantia nigral fast EEG at 12 mmHg and 7 mmHg perfusion pressure .....	115
9-6 CBF comparison between right and left hemispheres for all anatomical locations and perfusion pressures. ....	117
9-7 CBF ratio for each anatomical location at 12 mmHg, 9 mmHg, and 7 mmHg perfusion pressures. ....	120
9-8a Right hemispheric CBF versus time at 7 mmHg perfusion pressure .....	123
9-8b Initial CBF versus rate of change in CBF ..	123
9-9 Initial CBF versus rate of change in CBF ..	125
9-10 Percent slow and fast EEG activity as a function of perfusion pressure and anatomical location for each hemisphere. ....	129
9-11 Combined EEG-CBF relationship for the cortical-hippocampal areas .....	131
9-12 Combined EEG-CBF relationship for the thalamic-substantia nigral areas .....	133
<b>PLATINUM ELECTRODE ARRAY CONSTRUCTION</b>	
B-1 Platinum electrode construction. ....	150
B-2 Platinum electrode array .....	153

**LIST OF FIGURES (continued)**

<b>Figure</b>	<b>COMBINED EXPERIMENTAL RESULTS</b>	<b>Page</b>
D-1	Control of perfusion pressure at 12 mmHg and 7 mmHg .....	157
D-2	Bilateral hippocampal CBF at 12 mmHg and 7 mmHg perfusion pressure.....	159
D-3	Bilateral thalamic CBF at 12 mmHg and 7 mmHg perfusion pressure.....	161
D-4	Bilateral substantia nigral CBF at 12 mmHg and 7 mmHg perfusion pressure.....	163
D-5	Bilateral cortical CBF at 12 mmHg and 7 mmHg perfusion pressure.....	165
D-6	Bilateral cortical-hippocampal fast EEG at 12 mmHg and 7 mmHg perfusion pressure .....	167
D-7	Bilateral thalamic-substantia nigral fast EEG at 12 mmHg and 7 mmHg perfusion pressure .....	169
D-8	Bilateral cortical-hippocampal slow EEG at 12 mmHg and 7 mmHg perfusion pressure .....	171
D-9	Bilateral thalamic-substantia nigral slow EEG at 12 mmHg and 7 mmHg perfusion pressure .....	173
D-10	Control of perfusion pressure at 9 mmHg.....	175
D-11	Bilateral cortical and hippocampal CBF at 9 mmHg perfusion pressure .....	177
D-12	Bilateral thalamic and substantia nigral CBF at 9 mmHg perfusion pressure .....	179
D-13	Bilateral cortical-hippocampal fast and slow EEG at 9 mmHg perfusion pressure ..	181
D-14	Bilateral thalamic-substantia nigral fast and slow EEG at 9 mmHg perfusion pressure .....	183

## LIST OF ABBREVIATIONS

<b>%</b>	<b>percent</b>
<b>a.</b>	<b>artery</b>
<b>A/D</b>	<b>analog to digital</b>
<b>AC</b>	<b>alternating current</b>
<b>Ag</b>	<b>silver</b>
<b>amps</b>	<b>amperes</b>
<b>BAL</b>	<b>balloon pressure</b>
<b>BP</b>	<b>blood pressure</b>
<b>br.</b>	<b>branch</b>
<b><sup>14</sup>C</b>	<b>carbon 14</b>
<b>CBF</b>	<b>cerebral blood flow</b>
<b>cc</b>	<b>cubic centimeter(s)</b>
<b>CNS</b>	<b>central nervous system</b>
<b>D/A</b>	<b>digital to analog</b>
<b>DC</b>	<b>direct current</b>
<b>DSC</b>	<b>deenergized shut/cycles</b>
<b>DSNS</b>	<b>deenergized shut/normally shut</b>
<b>e-</b>	<b>electron</b>
<b>EEG</b>	<b>electroencephalogram</b>
<b>F</b>	<b>flowmeter</b>

### LIST OF ABBREVIATIONS (Continued)

<b>g</b>	<b>gram(s)</b>
<b>H<sup>+</sup></b>	<b>hydrogen ion</b>
<b>H<sub>2</sub></b>	<b>hydrogen</b>
<b>Hct</b>	<b>hematocrit</b>
<b>Hz</b>	<b>hertz</b>
<b>K</b>	<b>kilo</b>
<b>kg</b>	<b>kilograms</b>
<b>L</b>	<b>left</b>
<b>LCBF</b>	<b>local cerebral blood flow</b>
<b>mA</b>	<b>milliamperes</b>
<b>mg</b>	<b>milligrams</b>
<b>min</b>	<b>minutes</b>
<b>ml</b>	<b>milliliters</b>
<b>mm</b>	<b>millimeters</b>
<b>mmHg</b>	<b>millimeters of mercury</b>
<b>mV</b>	<b>millivolts</b>
<b>N<sub>2</sub>O</b>	<b>nitrous oxide</b>
<b>N(n)</b>	<b>number</b>
<b>NO</b>	<b>normally open</b>
<b>ns</b>	<b>not significant</b>
<b>NS</b>	<b>normally shut</b>
<b>O<sub>2</sub></b>	<b>oxygen</b>
<b>P</b>	<b>pressure transducer</b>
<b>P<sub>a</sub>O<sub>2</sub></b>	<b>arterial oxygen pressure</b>
<b>P<sub>a</sub>CO<sub>2</sub></b>	<b>arterial carbon dioxide pressure</b>
<b>PCP</b>	<b>phencyclidine</b>

### LIST OF ABBREVIATIONS (Continued)

pCO <sub>2</sub>	P <sub>a</sub> CO <sub>2</sub>
pO <sub>2</sub>	P <sub>a</sub> O <sub>2</sub>
PP	perfusion pressure
PT	pressure transducer
R.	right
RC	resistance capacitance
SBP	systemic blood pressure
SD	standard deviation
SE	standard error
T <sub>1/2</sub>	half life
uF	microfarrads
um	microns
V	volts
VDC	direct current voltage
VP	venous pressure

## **INTRODUCTION**

**Circulatory disorders are the main cause of death and disability in the United States. As many as 50% of the annual deaths (or approximately 1 million Americans) each year are a result of having the condition of systemic hypertension, cardiovascular disease, or stroke (Garcia, 1985). Circulatory disorders of the central nervous system result from a blood supply insufficient for the functional metabolic rate of the tissue. When the deficiency of blood flow results from a functional constriction or actual occlusion of a vessel a state of ischemia exists. Hemorrhage or edema resulting from alterations in the blood vessels of the brain can also cause a deficiency in the blood supply because the increase in fluid volume within the rigid intracranial space results in a lower perfusion pressure (the difference between arterial blood pressure and intracranial pressure). Previous studies have demonstrated that the majority of strokes have one of three etiologies. Seventy-five percent result from a brain infarction, which is parenchymal ischemic destruction resulting from the occlusion of the supplying vessel, usually an artery, eleven percent from brain hemorrhage, and five percent from non-traumatic subarachnoid hemorrhage (Garcia, 1985). Collectively, ischemic and hemorrhagic strokes are the most common focal neurologic disease in adults and account for approximately 10% of the annual deaths in the United States (Garcia, 1985).**

The human syndrome of stroke can be described as a condition manifested by a localized neurologic deficit such as hemiplegia, vertigo, numbness, aphasia, or unilateral blindness caused by an acute vascular lesion in the brain such as hemorrhage, embolism, thrombosis, or rupturing aneurysm (Garcia, 1985, Dorland, 1984). This condition of severe partial ischemia may be transient, but often it is followed by progressive and permanent neurologic damage. Thus, there is time for therapeutic intervention after the onset of severe partial ischemia, but the number of available therapeutic protocols are limited, partly because the mechanisms that cause ischemic tissues to die are incompletely understood. Therefore, it is appropriate to develop a model of severe partial ischemia in which the mechanisms of circulatory failure can be elucidated and therapeutic interventions can be studied. In physical chemistry, it is possible to put constraints on experiments (for example, constant pressure or constant temperature) in order to have absolute control over the conduct of the experiment. It is felt that the rate of progress in elucidating the mechanisms of circulatory failure during severe partial ischemia would be markedly accelerated if similar constraints could be applied to the study of stroke.

The main idea in studying the phenomena of cerebral infarction resulting in stroke is to consistently reproduce the physiological events leading to a cerebral infarction in a live animal and to infer the results to man. In order to study different therapeutic protocols a cerebral infarct must be consistently produced in a live animal which is constant in size and in anatomical location. This is an obvious requirement in that the main question to be answered is "Does the drug regimen reduce infarct size?". Thus, the first objective of the system to be developed is that it must have control over the hemodynamic properties of the cerebral vascular bed such

that the induced hemodynamic changes are reproducible and yield a consistent infarct. Because cerebral infarction results from an inadequate blood supply, one of the main objectives in this research is to control the blood supply to the cerebrum. This involves making the brain's blood supply totally dependent on the input from one arterial vessel and subsequently modulating the input from this vessel. It should be noted that in order to produce an infarct, the arterial input pressure must be lowered significantly. Since perfusion pressure is equal to the difference between the arterial input pressure and the intracranial pressure, perfusion pressure will also be lowered. By measuring, modulating, and controlling the perfusion pressure with a computer it is felt that the hemodynamics of the cerebral vascular bed will be reproducible and will thus yield consistent infarcts.

The second objective of this research is to develop an animal model in which consistent ischemic lesions can be generated resulting from a significant decrease in perfusion pressure in order to study the mechanisms of circulatory failure and to evaluate different therapeutic regimes, while maintaining the animal in a physiological condition that mimics or resembles that which normally exists in man before, during, and after a stroke. Garcia (1983) states that the analysis of the physiological and morphological parameters which change during the time course of a brain infarct require an animal model in which (a) a single-artery can be reversibly occluded, (b) the vascular occlusion results in predictable changes in blood flow, (c) barbituates are not used at the time of the arterial occlusion, (d) the resulting parenchymal lesion should closely resemble a human brain infarction, and (e) the method of arterial occlusion should allow for subsequent reperfusion.

An obstacle in stroke research today is the lack of a suitable animal model. The design of a severe partial ischemic animal model using the rat

and resulting in a reproducible, regional ischemic lesion within the cerebrum has not been previously accomplished. This is due in part to the efficiency of the intracranial collateral circulation within the rat which results in the inability to lower the perfusion pressure to a level which will cause ischemic brain damage when a single extracranial vessel or group of vessels are occluded. Thus, some previous animal models have employed systemic insults such as hypotension (Menelow, 1984), hypoxia (Levine, 1960; Brown, 1968; Salford, 1973), or drug administration in addition to extracranial vessel occlusion in order to produce consistent ischemic lesions. The additional systemic variant may cause generalized metabolic derangement with or without compromise of other organ systems. This greatly complicates the analysis of the resulting data.

Intracranial approaches have been used but their success has also been limited. The procedure of Tamura et al. (1981), which involves the ligation of the proximal middle cerebral artery (MCA) through a subtemporal approach, is very difficult to perform and even though it has been reported to result in consistent ischemic changes, the animal's brief survival time limits it to acute experiments (Hossmann et al, 1983). The procedure involves a craniectomy and subdural manipulations which may result in traumatic damage to the cerebrum instead of purely ischemic damage. Also, the reperfusion option is unavailable because the MCA ligation is permanent. Coyle's (1982) procedure involves MCA ligation above the rhinal fissure which is technically less difficult and affords longer animal survival than that of Tamura's, but it does not produce cerebral infarction in young Wistar rats. Chen et al. (1986) uses MCA ligation followed by successive occlusion of the right and left common carotid arteries and reports consistent ischemic infarct size. However, the model described by Chen et al. (1986) does not allow

reperfusion in the infarcted area and the infarct size varies directly with the length of ischemia.

Other models use permanent ligation of major extracranial vessels in order to achieve ischemic conditions. The model of Pulsinelli et al. (1979) requires monopolar cautery on the vertebral arteries through the alar foramina bilaterally with subsequent occlusion of both common carotid arteries. This method may be simple to perform but the resulting ischemic damage has been inconsistent and has been the subject of a great deal of criticism (Furlow, 1982). The inconsistencies of Pulsinelli's results probably stem from the fact that visual confirmation of the permanent occlusion of the vertebral arteries is not performed and therefore, some viable vertebral artery input may exist in a number of animals on a random basis. Todd et al. (1986) uses the Pulsinelli method but visually verifies that the vertebral arteries have been occluded. Verification is accomplished by drilling out the alar foramina with a high speed dental drill and exposing the vertebral arteries lying within the foramen transversarium. The hemodynamic results of Todd et al. (1986) are consistent for animals weighing 200-300 grams, but we have been unable to consistently reproduce his results, especially in animals weighing in excess of 300 grams. Kameyama et al. (1985) uses a variation of the Pulsinelli method in which the basilar artery is permanently ligated instead of the vertebral arteries. Kameyama's reported results are more consistent than Pulsinelli's, but once again, we have not been able to consistently lower perfusion pressure to ischemic levels using his method, especially for the larger animals. In fact, ischemic perfusion pressure levels have not been achieved consistently in our laboratory using either the Pulsinelli or Kameyama methods for any rat species, especially for animals weighing in excess of 250-300 grams. Thus, the criticism (Furlow, 1982) that

these methodologies only work for animals of a particular inbred strain with a certain weight limit is supported by our results.

In addition to the above arguments, all of the previously mentioned models are very limited in the fact that they can only achieve one level of occlusion; i.e., there is no way to modulate the amount of severity of the ischemic episode. It should also be noted that these models do not employ the use of carotid blood pressure (CBP) or perfusion pressure measurements during ischemic episodes and the correlations within these models are only made to systemic blood pressure (SBP). It is felt that hemodynamic correlations made on the basis of carotid perfusion pressure will be more consistent than that made to systemic perfusion pressure.

Thus, the goal of this research is to develop a system in which the animal model follows the requirements set forth above; the animal's perfusion pressure can be lowered to a level which will result in ischemic damage; that different levels of perfusion pressure within the ischemic range can be reached and maintained under computer control while allowing reperfusion in the infarcted area.

## **METHODS**

Our previous work with animal models required that the animals be subjected to systemic hypotension and heparinization in order to maintain computer control over the desired range of perfusion pressures. An improved system of modulating cerebral perfusion pressure without the use of hemorrhagic hypotension is shown in Figure 2-1. With the development of a new animal model (discussed below) in which both subclavian arteries are occluded, the animal is made sufficiently dependent on carotid artery input to permit modulation of ischemia. This is accomplished by occluding one common carotid and partially occluding the contralateral common carotid artery under computer control. To partially occlude the carotid artery, a balloon partial occlusion technique is developed (balloon manufacturing technique given in Appendix C) in which a plastic cylinder is placed around the left common carotid artery. A latex balloon connected to a computer controlled servo-pump is then inserted into the cylinder (see Figure 2-2). The servo-pump is interfaced to the computer in order that the actual perfusion pressure is closely matched to the desired perfusion pressure.

The three pressure transducers employed within this system provide four continuous signals to the computer which are then displayed to the investigator (see Figure 2-3). The perfusion pressure signal is simply the difference between the CBP and the venous pressure (VP). Unlike the VP in

FIGURE 2-1  
THE CURRENT SYSTEM

Carotid blood pressure (CBP), venous pressure (VP), and systemic blood pressure (SBP) are monitored continuously by the computer via pressure transducers. Perfusion pressure (PP) is monitored continuously by taking the difference between CBP and VP with a transducer mixer. Balloon compression is used to modulate the input of blood into the cerebrum. A plastic cylinder is placed around the left common carotid artery, which is the only input of blood into the cerebrum. A latex balloon connected to a computer controlled servo-pump is inserted into the cylinder. The servo circuitry which drives the servo-motor compares the desired perfusion pressure to the actual perfusion pressure. If the actual perfusion pressure is too high, then the servo circuitry will drive the servo-pump to increase balloon pressure, which results in lowering the perfusion pressure. The servo-pump operates in the opposite direction when the perfusion pressure is too low. In this system, perfusion pressure can be controlled down to approximately 4 mmHg (see Figure 2-3). Local hydrogen concentration is detected by platinum electrodes implanted into the cerebrum (see Methods section) and the resultant signal is received and processed by an IBM-AT computer to yield LCBF (Aukland et al., 1964; Haining et al., 1968) at the anatomical site being monitored. EEG is also monitored at the electrode sites.

# THE SYSTEM

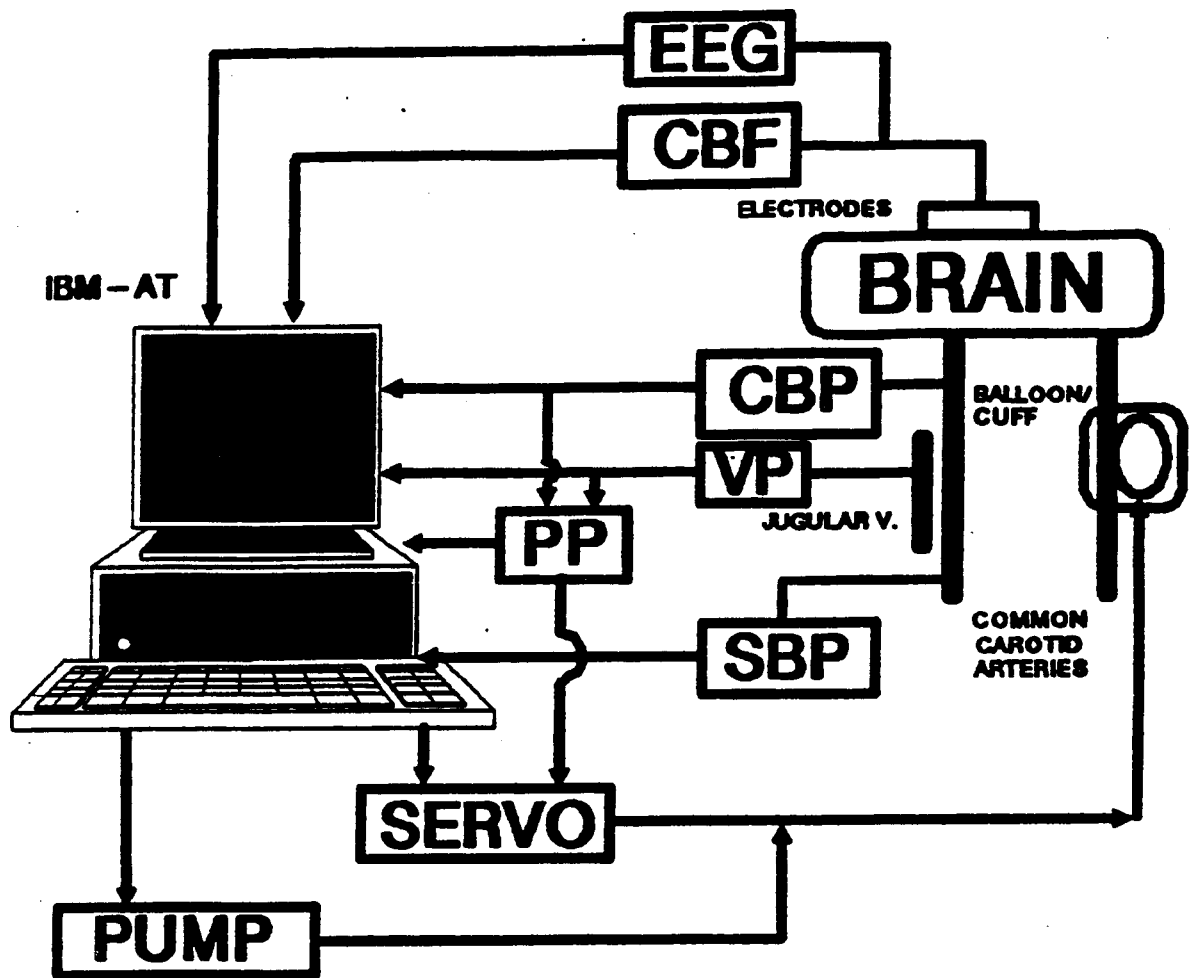


**FIGURE 2-2****IN-VIVO ARRANGEMENT OF THE BALLOON COMPRESSION TECHNIQUE**

**Balloon compression is used to modulate perfusion pressure to the desired level and maintain it there throughout the entire experiment. In this photograph, the plastic cylinder (or cuff) is placed around the left common carotid artery. The balloon which is connected to a computer controlled servo-pump is placed within the cylinder such that the common carotid artery can be compressed between the balloon and the cuff.**



**FIGURE 2-3**  
**CONSOLE DISPLAY DURING THE EXPERIMENT**

During the experiment, the investigator has a continuous display of the more significant aspects of the system such as time, pressures, EEG levels, and hydrogen concentration on the console screen. This allows the investigator to quickly assess the current status of the experiment and the animal in order to make any rapid adjustments if necessary. Also shown on the console screen are a number of INKEY selections that allow the operator to control the experiment. An example of an INKEY is "A" when depressed will allow the operator to change the time interval between hydrogen flow determinations (see Hydrogen Clearance Method section).

H AUTO HZ  
I(W) ZERO HZ HZ(D)OFF (E) EEG CHANNEL 3  
J(Q) HZ FILE  
TIME 515.38 HZ = 0.26 0.29 0.89 0.88 AVG = 0.149 0.888

P(Z) HYDROGEN CFILE HYDROGEN FILING INACTIVE LAST FILE =  
H(J) ZERO OZ (7) AUTO SLOPE ON  
TIME = 515.38 HZ = 0.88 0.16 0.39 0.88

U AUTOREGULATORY DATABASE  
L COMP LOCKS CBU OR PRESSURE

I(N) ZEROS ICP G RANGE ((K) ZEROS SBP, CBP, 2HZ & 7HZ  
R RECOVERS BASELINES 0 CAL. SBP, CBP & ICP  
F(X) ZERO CO2 U CAL. CO2  
2HZ= 25.1 25.0 25.0 25.8 7HZ= 21.5 21.4 21.5 21.4  
SBP= 188.8 CUFF= 188.8 SBP-BAL= 0.8  
CBP= 89.4 UP = 25.1 CBP-UP= 64.3 PP= 20.2  
(1) BP ALARM OFF (2) HYDROGEN RATE  
(3) WRITE DATABASE (4) PLOT DATABASE  
(5) INPUT PRESSURE LOCKS (6) START PRESSURE RUN

the hemorrhagic technique, the VP in this system is significant (on the order of 5 mmHg) relative to ischemic perfusion pressure levels.

In order to better understand the hemodynamic properties of cerebral infarction, local cerebral blood flow (LCBF) is measured at four different anatomical sites bilaterally giving a total of eight measurement sites. The hydrogen clearance method is fully automated within this system to obtain these flows. The investigator has control over the automatic features of the hydrogen clearance method through the use of INKEYS which are continually displayed on the console screen (see Figure 2-3). In addition to displaying the different INKEY selections, the control program also displays different items on the console screen that are of particular interest to the investigator such as SBP, CBP, VP, perfusion pressure, EEG levels, hydrogen voltage levels for each channel, and desired perfusion pressure. Since the hydrogen clearance method requires that platinum electrodes be implanted into the tissue in which blood flow measurements are to be made, EEG measurements are readily made. Thus, brain electrical activity can also be studied at the different anatomical sites during ischemia.

Now that the general system has been described, each part of this system will be covered in more detail.

## **THE ANIMAL MODEL**

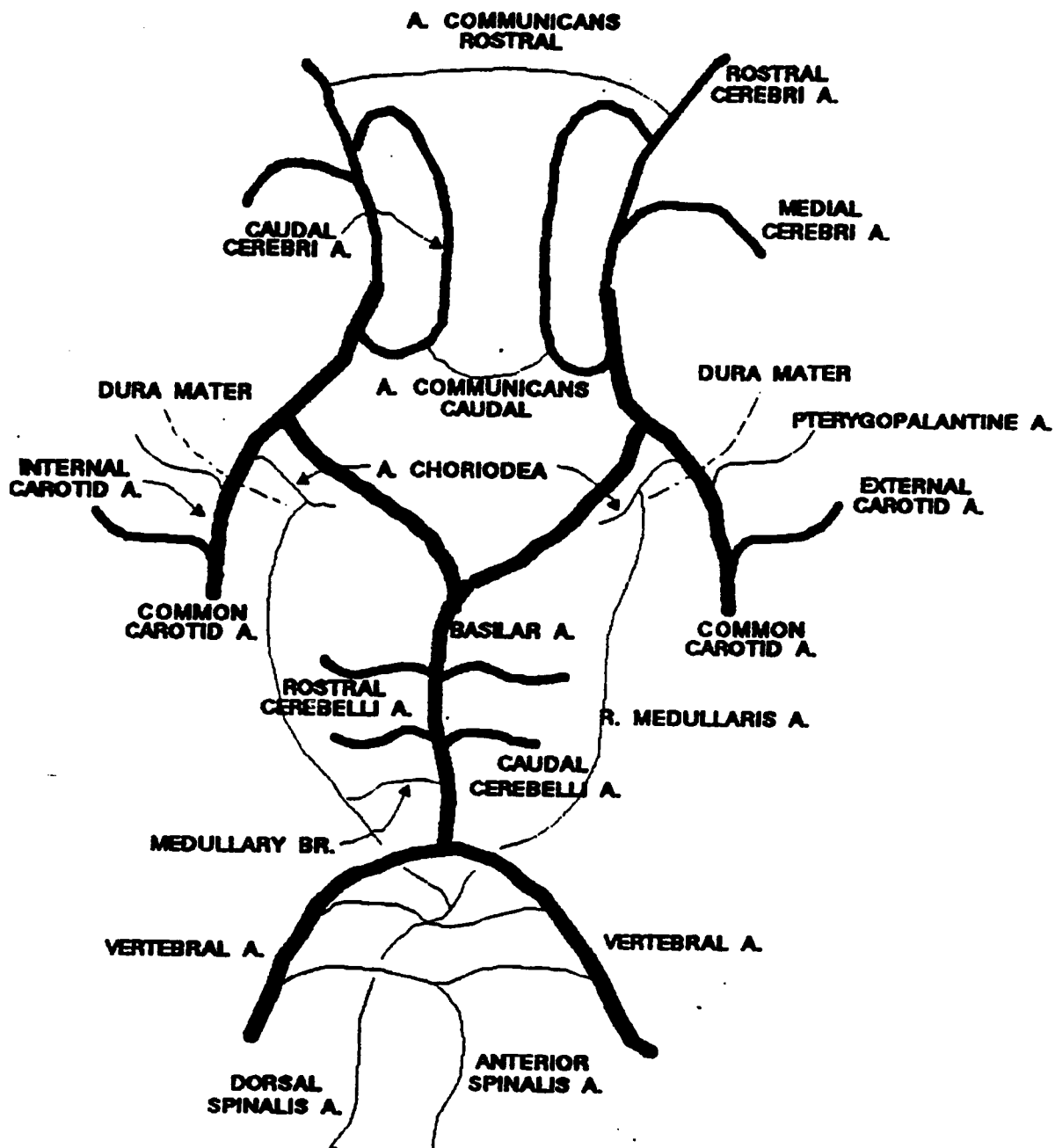
The rat is chosen as the experimental subject for this system because it affords a wide range of advantages when modelling human cerebrovascular disease which other animal species cannot. First, unlike the gerbil, cat, and dog, the rat's intracranial circulation is very similar to that of man (Yamori et al., 1976). For example, Figure 3-1 shows that the anatomical relationship of the major cerebral vessels in the rat closely resembles the Circle of Willis in man. Second, there is abundant neurochemical data for this animal (Iversen et al., 1978; Roberts et al., 1978; Siesjo, 1978; Brown and Cooper, 1979). Third, the rat is the most studied animal in stroke in recent years. Thus, there is a wealth of information readily available for this animal. Fourth, the rat is large enough for physiological monitoring but small enough for easy handling and housing within the laboratory. And finally, the purchase and maintenance cost is relatively low. Therefore, a large number of animals can be used in the development of this system as well as to provide an adequate number for statistical analysis in the studies that are performed.

In the development of the animal model, the first objective is to make cerebral blood flow dependent on one major vessel for its blood supply. Once this has been accomplished, then it will be possible to control the perfusion pressure via the arterial input pressure by modulating the input of this one major vessel. The second objective is to develop an animal

**FIGURE 3-1****CEREBRAL BLOOD SUPPLY IN THE RAT**

**One of the reasons that the rat is chosen as the experimental subject for this system is that its cerebral blood supply closely resembles that of man. Note that the Circle of Willis in man is essentially the same as in the rat. However, the rat has an extensive collateral supply system that makes it very difficult to lower perfusion pressure via an extracranial artery to a level resulting in ischemic damage.**

## CEREBRAL BLOOD SUPPLY IN THE RAT



preparation which control to perfusion pressure is achievable, surgical trauma is minimized, and the normal physiological state of the animal is maintained. There are two reasons why it is felt that the normal physiological state of the animal is maintained within this system. First, the balloon compression technique (described above) is being used which does not require the use of drugs or other systemic insults to be implemented, and secondly, no drugs other than those used for anesthesia and muscle paralysis (discussed below) are being used. Thus, the major considerations in developing the animal preparation are to perform the shortest surgical preparation with the least amount of trauma in order to maximize animal survival and to have a prepared animal such that its perfusion pressure can be lowered and controlled in the "ischemic range" (i.e. a perfusion pressure level which will result in ischemic damage). The last consideration of being able to lower the perfusion pressure to a level that will result in ischemic damage is the major limitation of most of the previous animal models, especially the models that used extracranial vessels to limit blood flow to the cerebrum. Because the balloon compression technique requires that an extracranial artery be controlled in order to induce ischemic damage, a new animal model had to be developed in order to avoid having to employ systemic insults to augment the perfusion pressure drop. Also, the new animal model should work in animals weighing in excess of 300 grams.

A surgical technique was developed which permits modulation of the perfusion pressure using an extracranial artery on rats of any species up to weights of at least 450 grams (This technique has not been performed on any animals weighing more than 450 grams). This technique involves bilateral reversible clipping ligation of the subclavian arteries (see Figure 3-2) through an open thoracotomy with permanent ligation of one common carotid artery

**FIGURE 3-2****ANATOMICAL RELATIONSHIP OF THE SUBCLAVIAN ARTERIES**

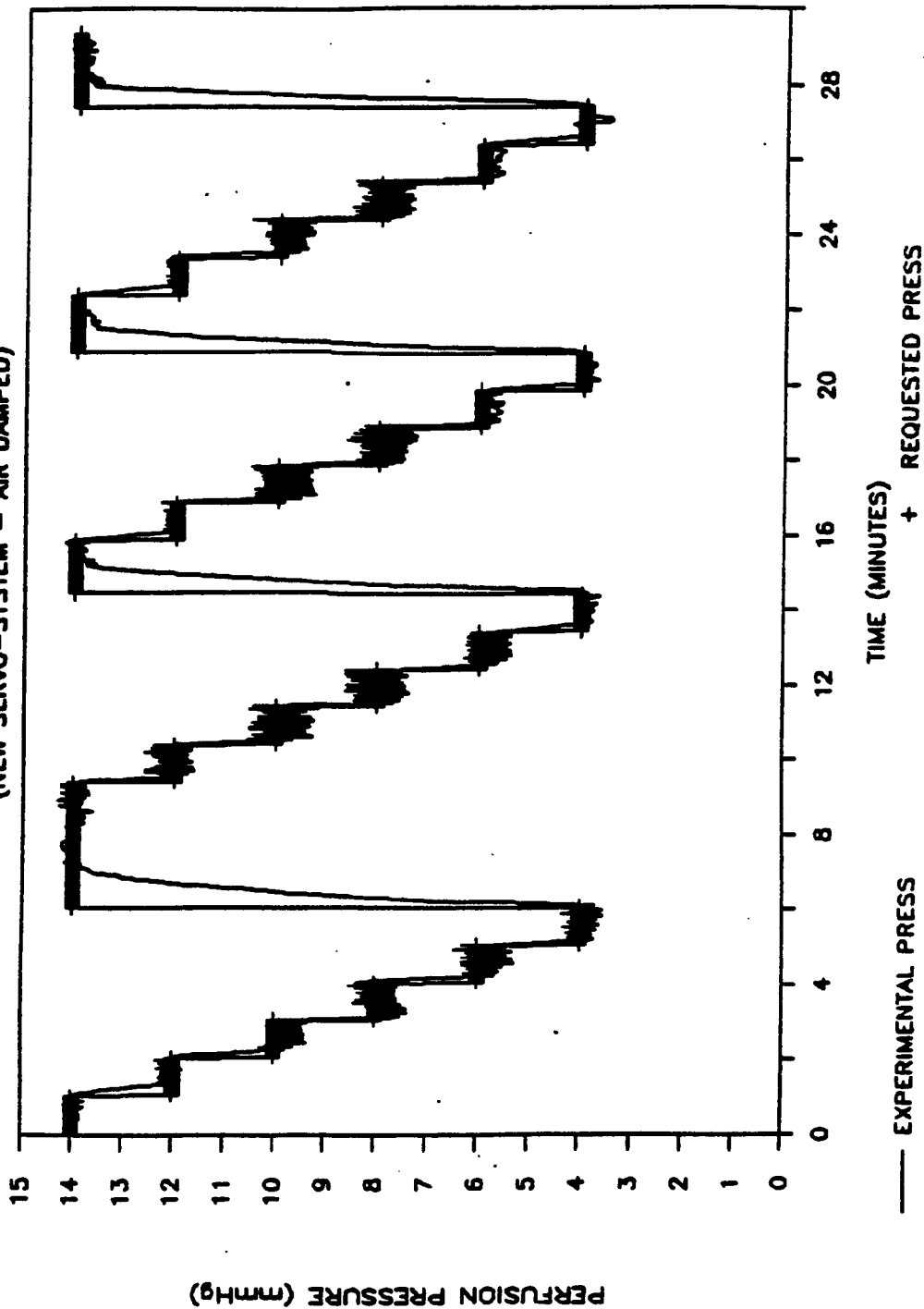
With the exception of the anterior and dorsal spinalis arteries, the entire blood supply to the cerebrum in the rat comes from the subclavian and common carotid arteries. Since the contribution to the total blood supply by the anterior and dorsal spinalis arteries is small, this animal model is based on the occlusion of both subclavian arteries and one common carotid artery while modulating the input of blood to the cerebrum with the remaining common carotid artery. In order to occlude the subclavian arteries, an open thoracotomy must be performed since they are within the chest cavity. The right subclavian artery branches off the innominate artery while the left subclavian artery branches off the aortic arch and are identified by the letters (c) and (f), respectively. This illustration is from the Laboratory Manual of the Anatomy of the Rat by H. R. Hunt (1924).



**FIGURE 3-3**  
**PERFUSION PRESSURE CONTROL DURING**  
**BILATERAL SUBCLAVIAN OCCLUSION**

Previous animal models were mostly limited in that the efficient collateral circulation in the rat prevented consistent ischemic damage from occurring when trying to lower perfusion pressure via occlusion of an extracranial artery. The new animal model which uses bilateral subclavian occlusion clearly provides the perfusion pressure range necessary to obtain consistent ischemic damage. One of the results from the studies performed using this system was that CBF collapsed at a perfusion pressure around 7 mmHg. Thus, this animal model provides the opportunity to study the entire ischemic range from mild partial ischemia to total ischemia.

# BILATERAL SUBCLAVIAN OCCLUSION (NEW SERVO-SYSTEM - AIR DAMPED)



— EXPERIMENTAL PRESS

+ REQUESTED PRESS

for CBP and SBP measurements (see surgical preparation), followed by partial compression of the contralateral carotid via the servo-driven balloon for induction of an ischemic state (see Figure 6-2). This method allows control of perfusion pressure through the entire desired ischemic range. The results of a typical perfusion pressure control experiment which clearly shows that the perfusion pressure can be effectively controlled down to 4 mmHg are shown in Figure 3-3. Total occlusion of the remaining viable carotid artery with the balloon after bilateral subclavian occlusion usually yields a perfusion pressure on the order of 1-3 mmHg. The only input of blood flow to the brain in this animal model is through the anterior spinalis artery which receives its blood supply from the descending aorta. Obviously, this supply of blood to the brain is minimal.

The surgical preparation is described in the animal preparation section and includes the bilateral subclavian technique briefly described above. In addition to the range of control over the perfusion pressure, this technique has other advantages worth mentioning. First, the procedure is not invasive with respect to the CNS. Thus, there is no cerebral trauma induced which could be mistaken for ischemic damage when interpreting the morphologic results. Second, reperfusion is clearly an option since the decompression of the balloon and removal of the microclips will allow reflow through the major arteries supplying the brain. Third, no systemic insults such as hypoxia or hypotension are required. Fourth, in keeping with Garcia's (1983) criteria listed earlier the only drugs required for this technique are the anesthetic agents and the muscle paralytic agent. Fifth, the surgical preparation time is approximately 1.5 hours and the preparation itself results in a very low mortality rate (about 5%). Thus, this technique fulfills all the desired goals and objectives for this system.

## **ANESTHESIA**

Even though anesthesia is normally not present in people when they experience a stroke, it is necessary in this system for humane reasons and in order to perform the surgical preparation on the animal. In order not to complicate the results of the studies the anesthetic regimen should have minimal physiological effects on the animal in addition to inducing a state of unconsciousness. During the development of the current system, two anesthetic regimens were evaluated and the anesthetic regimen chosen for this system consists of administering a 70% nitrous oxide, 29% oxygen, and 1% halothane gas mixture. The anesthetic delivery system is shown in Figure 4-1 and includes the hydrogen gas arrangement used for blood flow measurements. The hydrogen gas arrangement is discussed in the hydrogen clearance method section.

The other anesthetic regimen under consideration consisted of the dissociative anesthetic agent ketamine and the muscle relaxant Rompun. Being a derivative of phencyclidine (PCP) and thus having its effects at the level of perception in the cortex, ketamine is classified as a dissociative anesthetic agent. Also, ketamine is administered by injection. This is unlike the halogenated agents such as halothane which are believed to exert their effect at the reticular formation of the brainstem and are administered by gas inhalation. Ketamine is a desirable agent in that SBP is usually constant

FIGURE 4-1

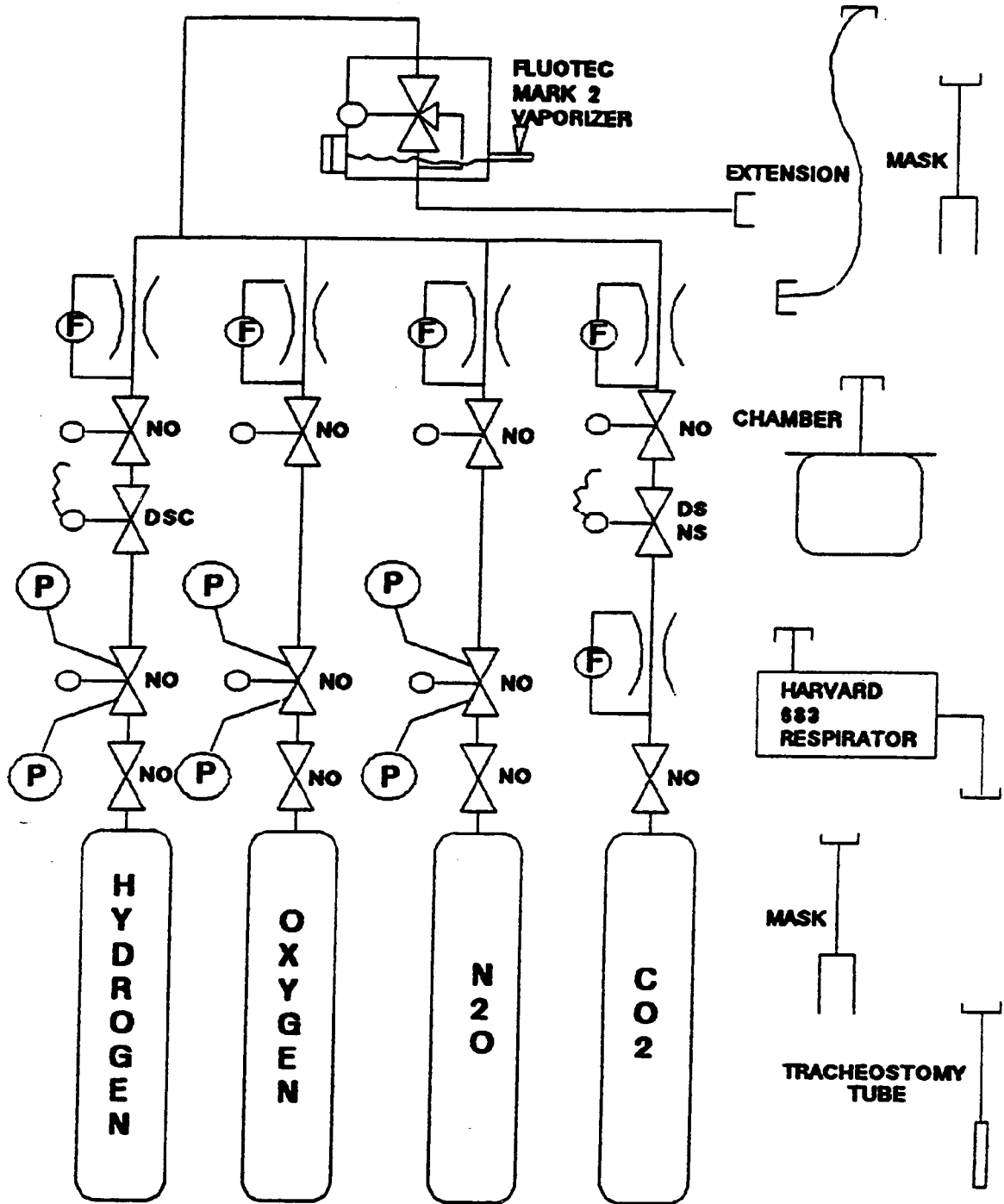
## THE ANESTHETIC AND HYDROGEN GAS DELIVERY SYSTEM

Anesthesia and hydrogen are delivered to the animal within the same system since they consist of a gas/vapor mixture and a gas, respectively. The valve positions shown in this illustration represent the normal configuration during an experiment. The flowmeters provide a mechanical indication for the flowrate of each gas in liters/min. The sum of all the individual flowrates represents the total flowrate reaching the halothane vaporizer. By knowing the total flowrate, the vaporizer throttle valve can be set appropriately in order to deliver the proper amount of halothane to the animal. The throttle valves are set so that the total flow is approximately 4-5 liters/minute and 70% of the total flow is nitrous oxide, 29% of the total flow is oxygen, and the remaining 1% is from the vaporized halothane. The tubing from the gas cylinders to the output side of the vaporizer is constructed of copper to prevent hydrogen gas accumulation. If hydrogen gas was allowed to accumulate in tubing made of plastic, then there would still be hydrogen delivery to the animal when the solenoid valve terminated hydrogen flow to the animal via diffusion from the plastic tubing. This would introduce errors in determining cerebral blood flow (CBF) from the hydrogen washout curves.

The adapter can be connected to one of three items, an extension tube, a chamber, and the respirator. The chamber is used to house the conscious animal during the induction of anesthesia. Once anesthesia has been induced, the adapter is then connected to the respirator for the duration of the experiment. With the respirator set at the appropriate stroke volume and rate, anesthetic gasses are delivered to the animal either through a mask (before the tracheostomy procedure is performed) or the tracheostomy tube. The respirator decreases the amount of gas flow to the animal from liters/minute to milliliters/minute. The unused gas is discharged into a well ventilated space away from the experimental space. The extension is used when performing the stereotactic implant procedure in another surgical preparation room.

When hydrogen gas is administered for subsequent flow determinations (see Hydrogen Clearance Method section), its delivery is controlled remotely from the computer via the solenoid isolation valve. The throttle valve is set so that hydrogen is delivered at approximately 3% of the total concentration which provides an adequate signal being generated at the platinum electrodes. NO = normally open; P = pressure measuring device; F = flowmeter; DSNS = deenergized shut/normally shut; DSC = deenergized shut/cycles; CO<sub>2</sub> = carbon dioxide; N<sub>2</sub>O = nitrous oxide.

### GAS DELIVERY SYSTEM



or elevated when used during surgery whereas halothane can produce a profound lowering in SBP which could result in death. Even though ketamine is reported to increase blood flow to many organs, including the brain, as a result of the increase in SBP, the ketamine/rompun regimen severely lowers blood flow in the cerebrum. This is shown in Table 4-1. During the pre-ischemic phase of the studies while using the ketamine/rompun regimen, the LCBF's would not come close to literature values. This prompted the examination of the two anesthetic regimens shown in Table 4-1. This clearly demonstrates that the ketamine/rompun regime has a serious effect of lowering LCBF at the monitored sites within the cerebrum and thus would clearly complicate the results of studies done with this system if this anesthetic regimen were used. This is not to say that ketamine alone would also produce these results, but the combination of ketamine and rompun do.

TABLE 4-1

COMPARISON OF LCBF WITH ANESTHETIC REGIMENS  
WITHIN THE SAME ANIMAL

ANIMAL	HALOTHANE/NITROUS OXIDE				KETAMINE/ROMPUN			
	LCBF (ml/100g/min)							
	E1	E2	E3	E4	E1	E2	E3	E4
610 70	60	78	50	39	36	35	30	
611 71	64	100	NA	27	25	33	26	
613 80	100	100	76	30	47	43	31	

NA = not available

Three animals were used to compare the effects of the two different anesthetic regimes on LCBF. LCBF was measured at four different anatomical sites, E1, E2, E3, and E4 representing the hippocampus, thalamus, substantia nigra, and cortex, respectively. The values for LCBF's resulting from the halothane/nitrous oxide regime closely match literature values in these areas while the LCBF's resulting from the ketamine/rompun regime were approximately 50% of literature values.

Unfortunately, rompun, a muscle relaxant, is required in addition to the ketamine to produce surgical anesthesia because ketamine alone at 44 mg/kg (the recommended dose) does not. Therefore, the halogenated agent halothane is the agent of choice for this system and its use has resulted in obtaining pre-ischemic LCBF's very close to literature values. Switching to a gas delivery system did not complicate the development of this system because a gas delivery system is required to administer hydrogen to the animal for blood flow determinations and to administer oxygen to the animal via the respirator to control blood gasses.

Halothane is a potent anesthetic agent with properties that allow a smooth and rapid transition from consciousness to a state of surgical anesthesia with abolition of response to painful stimuli. It is a popular anesthetic agent in that the depth of anesthesia can be rapidly changed, the animal's conscious state can be restored very quickly when the administration of the vapor gas is terminated, and the toxic side effects are minimal after consciousness has been regained. However, the margin of safety associated with its use is very narrow which could result in profound circulatory depression and blood pressure collapse. Thus, the appropriate sign for the depth of anesthesia is the rate of depression of SBP and the animal's response to surgical manipulation (i.e. blood pressure increases, movement, and even awakening) (Gilman et al, 1980).

Since the system being developed obtains information on cerebrovascular hemodynamics, the effects of halothane on the nervous system should be noted. The cerebral vessels dilate with a corresponding increase in blood flow if arterial pressure is not lowered too greatly (Wollman et al., 1964). Also, halothane increases cerebrospinal fluid pressure (Lassen and Christensen, 1976) and impairs cerebral autoregulation (Miletich et al.,

1976) if doses of 2% or greater are used. However, there is no indication that halothane interferes with energy metabolism in the brain unless excessive doses are administered (Smith and Wollman, 1972; Michenfelder and Theye, 1975). Even though halothane has few physiological effects on the nervous system in addition to inducing a state of anesthesia, it is desirable to maintain the level of halothane as low as possible.

Nitrous oxide is used in the anesthetic regimen in order to augment the anesthetic effect of halothane, thus reducing the amount of halothane necessary to induce and maintain a level of surgical anesthesia. In the presence of 70% nitrous oxide in oxygen, the concentration of halothane necessary to induce and maintain surgical anesthesia is approximately one half of that required when using oxygen and halothane alone. Like other anesthetic agents, nitrous oxide administration results in analgesia, unconsciousness, and depression of the reflexes while not exerting any toxic side effects to the central nervous system (Gillman, 1980). Autoregulation is unaffected and cerebral blood flow is still responsive to changes in carbon dioxide at levels of 70% nitrous oxide (Wollman et al., 1965). Thus, the anesthetic regime consisting of 70% nitrous oxide, 29% oxygen, and 0.8-1% halothane during the surgical preparation should maintain the normal physiological state of the animal with the exception of unconsciousness and the lack of response to painful stimuli throughout the experiment.

The two other drugs used in this system are d-Tubocurare and atropine. Atropine is administered to the animal in order to minimize respiratory tract secretions. If this is not done, the animal stands a greater chance of becoming acidotic from decreased oxygen exchange due to the increased secretions. Atropine has a central nervous system (CNS) effect usually confined to a slight increase in the rate and occasionally depth of breathing

resulting from the bronchiolar dilation and the subsequent increase in physiologic "dead space" (Gillman, 1980). The muscle paralytic agent d-Tubocurarine is given to the animal just after the animal is placed on the respirator to prevent the animal from fighting against the respirator. Thus, blood gasses are more easily controlled. d-Tubocurarine has virtually no effect on the CNS because of its inability to penetrate the blood-brain barrier effectively (Gillman, 1980).

## **HYDROGEN CLEARANCE METHOD**

The hydrogen clearance method is used to measure LCBF in this system because it has distinct advantages over other techniques for blood flow measurement. First, the method is very inexpensive and relatively easy to implement and maintain. The electronic circuitry is simple and many electrodes can be manufactured without much difficulty. Hydrogen gas is readily obtained and has no unusual storage requirements. Second, blood flow measurements can be made in any tissue where a platinum electrode can be implanted. This method has been used to measure blood flow in the brain (Aukland et al., 1964), heart (Aukland et al., 1967), intestine (Mishima et al., 1979), pancreas (Nagata et al., 1979), spinal cord (Senter et al., 1978), uterus (Klingenberg, 1974), skeletal muscle (Aukland et al., 1964), kidney (Aukland et al., 1964), tongue (Fazekas et al., 1978), and bone marrow (Whiteside et al., 1977). It has also been previously used to measure blood flow in ischemic tissue (Fein et al., 1975; Halsey et al., 1970, 1971, and 1977; Jamieson et al., 1973; Meyer et al., 1972; and Morawetz et al., 1978). Third, many flows can be obtained serially at each electrode site over a long period of time. In comparison, the microsphere technique can only yield a maximum of six flows per experiment due to the number of radioisotopes available and the <sup>14</sup>C-iodoantipyrine technique can yield only terminal flows profiles. Fourth, this method is compatible with performing subsequent

morphological studies on the tissue being monitored. Fifth, since the blood flow is determined from the rate of hydrogen clearance from the tissue and not the absolute level of the hydrogen within the tissue, electrodes do not have to be calibrated to the absolute hydrogen concentration. Finally, this methodology can be fully automated, as will be documented below.

Basically, the hydrogen clearance method consists of (1) inserting a positively polarized platinum electrode into a tissue bed, (2) administering hydrogen by inhalation, (3) detecting the current generated from hydrogen reduction at the electrode which is proportional to the concentration gradient between the tissue and the electrode surface, (4) allowing the hydrogen to be cleared from the arterial blood, and (5) then monitoring the exponential clearance rate of hydrogen from the tissue. Blood flow at the tip of the implanted electrode is then calculated from the slope of the clearance rate curve in units of ml/100g/min.

Detection of hydrogen as a simple tracer substance in the cerebral cortex by means of a platinum electrode was first accomplished by Misrahy and Clark (1956). The detection was based on the potentials generated by the spontaneous oxidation of inhaled hydrogen gas. Clark and Bargeron (1959) similarly constructed intravascular electrodes to detect left to right cardiac shunts in children. The potentiometric technique used in these applications could qualitatively measure a change in blood flow. However, this application was limited because it was neither linear nor selective to hydrogen concentration changes.

Hyman (1961) first observed that the current response of a platinum electrode to hydrogen in solution is linear with hydrogen concentration. Aukland, Bower, and Berliner (1964) modified the technique introduced by Hyman (1961) by polarizing the platinum electrode to the potential of a

standard calomel electrode. The results of this technique not only confirmed the observations of Hyman (1961) but also showed that the effects of substances such as oxygen,  $H^+$ , and ascorbate had an acceptably small influence on the hydrogen generated current at the platinum electrode.

Assuming that hydrogen gas is in rapid diffusion equilibrium between the tissue and venous blood, and the arterial concentration of the hydrogen gas is zero when desaturation begins, the local blood flow per volume of homogeneously perfused tissue can be calculated based on the Fick principle in the equation described by Kety (1951):

$$C_i = C_{i0}e^{-kt} \quad (1)$$

where,

$C_i$  = the hydrogen concentration in tissue at time  $t$ ,

$C_{i0}$  = the hydrogen concentration in tissue at the beginning of desaturation,

$k = F/W\lambda$ ; the blood flow per tissue volume divided by the  
blood:tissue partition coefficient in ml/min/ml  
(or  $\text{min}^{-1}$ ),

$\lambda$  = the blood:tissue partition coefficient,

$W$  = a defined tissue volume, and

$t$  = time after desaturation begins (minutes).

Rearranging the terms and taking the natural logarithm yields

$$\ln(C_i/C_{i0}) = -(F/W\lambda)t. \quad (2)$$

Since the partition coefficient,  $\lambda$ , for hydrogen has been found to be unity both for the brain (Fieschi et al., 1965) and for the kidney (Aukland et al., 1964) and if  $T_{1/2}$ , the half-life, is substituted for  $t$ , equation (2) will read:

$$\ln(2)/T_{1/2} = F/W = f \quad (3)$$

where  $f$  is the blood flow per volume in ml/g/min. The  $T_{1/2}$  is readily determined by measuring the rate of hydrogen voltage (measure of

hydrogen concentration) decline after hydrogen gas inhalation is terminated. The value of  $f$  is usually multiplied by 100 in order to yield  $f$  in units of ml/100g/min which is the normal convention for reporting LCBF. An illustrative example for determining the local blood flow per volume from a sample curve can be found in Figure 5-1. Appendix A contains a more complete description of the theoretical considerations for the hydrogen clearance equations and its electro-chemical detection at an implanted platinum electrode.

Platinum electrode construction is a critical step in performing the hydrogen clearance technique for obtaining reproducible blood flow measurements. Because an invasive implantation procedure is required to measure blood flow at some desired tissue location, these electrodes should be as small as possible to minimize the rheologic distortions due to tissue injury. However, the electrodes should remain resilient to any damage that may occur during the implant procedure.

Electrodes of 2 mm in diameter were originally used by Aukland et al. (1964) and since then have diminished in size to 200-250 microns (Morawetz et al., 1978; Fein et al., 1975; Pasztor et al., 1973; and Kummer et al., 1984), 75 microns (Halsey et al., 1970, 1971, and 1977; and Jamieson et al., 1973), and smaller sizes (Young, 1980). The platinum electrodes manufactured and used here have an outer diameter between 100 and 125  $\mu\text{m}$ .

In this study, the hippocampus, ventro-dorsal thalamus, substantia nigra, and the cortex were chosen as cerebral sites of bilateral electrode placement. The exact tissue coordinates according to the stereotaxic atlas of the rat brain by Pellegrino (1979) are shown in Table 5-1 and illustratively in Figure 5-2. Because the X and Y coordinates of the four anatomical structures on each side of the cerebrum are relatively close to one another, the four

## FIGURE 5-1

LCBF DETERMINATION FROM AN EXPONENTIAL  
HYDROGEN CLEARANCE CURVE

LCBF is determined from an exponential hydrogen clearance curve. The ordinate is the natural logarithm of the hydrogen concentration measured in volts while the abscissa is time in minutes. The  $T_{1/2}$  is determined by finding the time it takes the hydrogen concentration to fall to 1/2 its value. In the example given,  $T_{1/2}$  is 2.0 minutes which yields an LCBF of 34.7 cc/100 gms/min.

### LCBF DETERMINATION FROM AN EXPONENTIAL HYDROGEN CLEARANCE CURVE

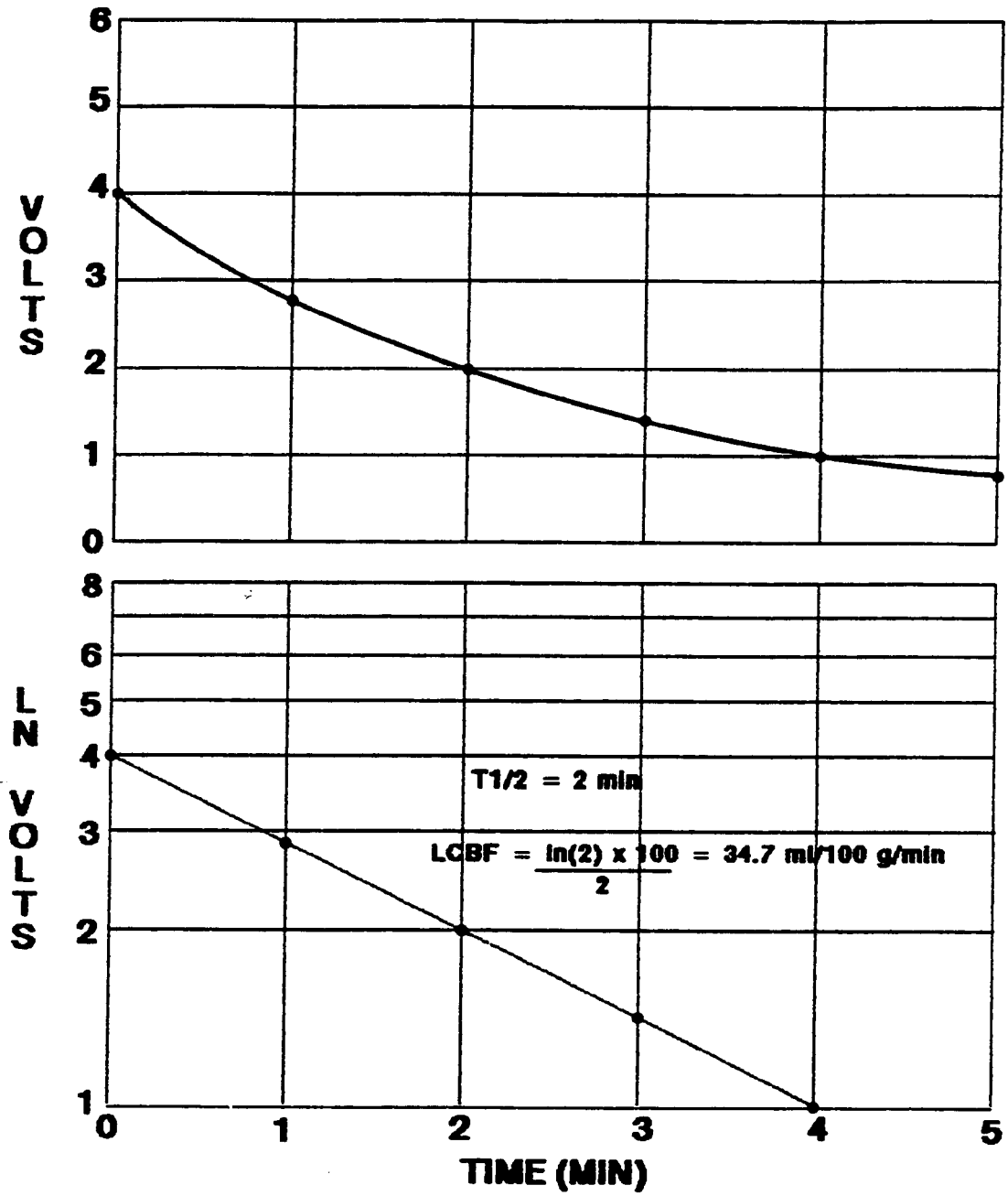


## FIGURE 5-2

## STEREOTAXIC LOCATION FOR PLATINUM ELECTRODES

The X and Y coordinates are shown for the eight electrodes including the major landmarks. Table H1 gives the Z length (depth) and the target nucleus for each electrode. The coordinates are obtained from the stereotaxic atlas of the rat brain by Pellegrino (1979).

## STEREOTACTIC LOCATION FOR ELECTRODES

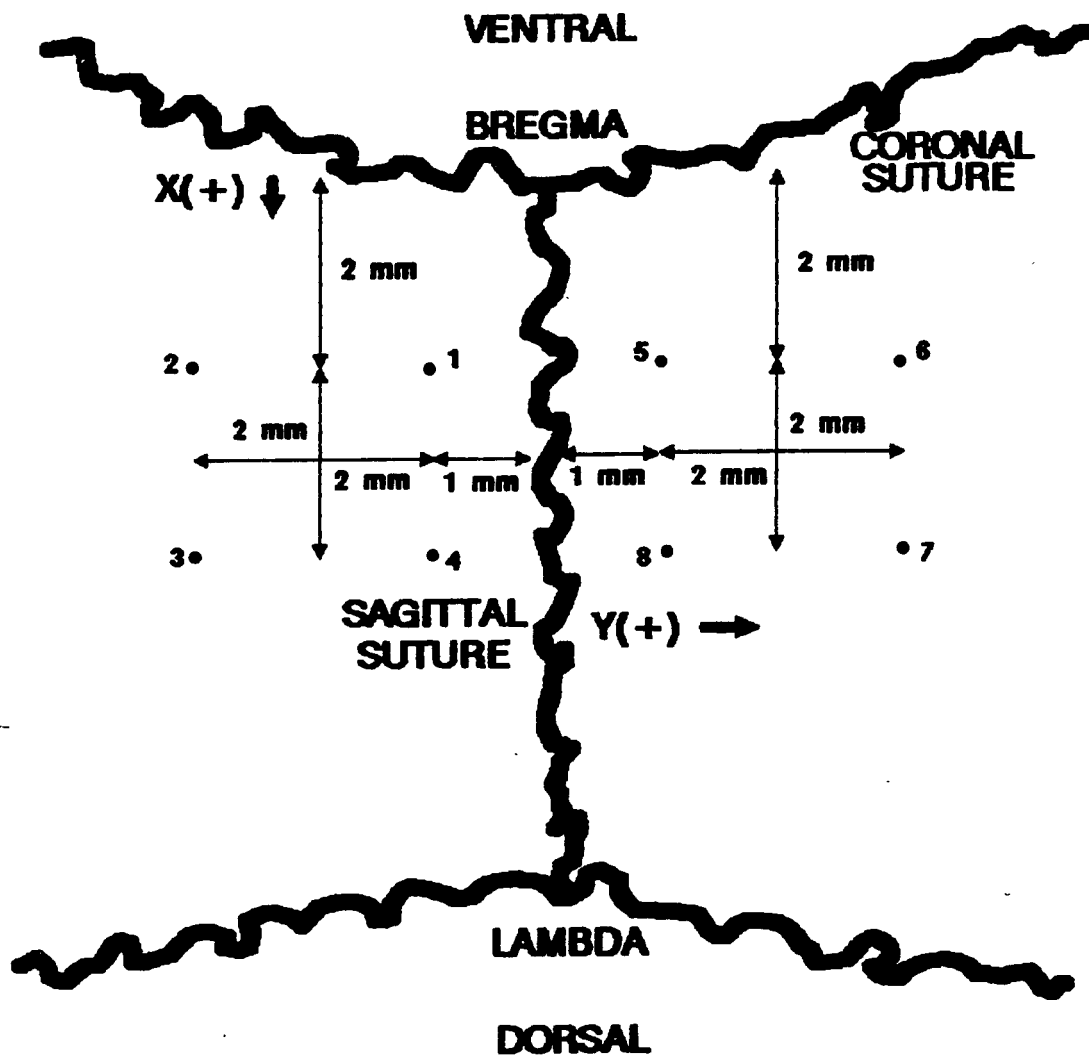


TABLE 5-1  
STEREOTAXIC COORDINATES FOR THE EIGHT ELECTRODE LOCATIONS  
INCLUDING TARGET NUCLEUS

Electrode	Distance (mm)			Nucleus
	X	Y	Z	
1	2.0	1.0	4.0	Hippocampus
2	2.0	3.0	6.0	VD Thalamus
3	4.0	3.0	9.0	Substantia Nigra
4	4.0	1.0	1.0	Cortex
5	2.0	-1.0	4.0	Hippocampus
6	2.0	-3.0	6.0	VD Thalamus
7	4.0	-3.0	9.0	Substantia Nigra
8	4.0	-1.0	1.0	Cortex

X = distance from bregma  
Y = distance from sagittal suture  
Z = depth

electrodes for these locations are manufactured as a single array. Thus, the ease of placement is achieved by reducing the number of implantable items from eight separate electrodes to two arrays consisting of four electrodes each. The method of construction for one electrode array is described in Appendix B.

The basic principle of hydrogen polarography is that hydrogen can be oxidized to form 2 hydrogen ions and 2 electrons ( $H_2 \rightarrow 2H^+ + 2e^-$ ; Will, 1963). When a substance such as platinum is placed within the vicinity of this reaction electrons will flow towards the acceptor surface, thus generating current flow. If the platinum electrode is positively polarized with respect to the reference electrode (Silver electrode in this case), and inserted into some medium containing hydrogen ( $H_2$ ), the hydrogen molecules closest to the platinum electrode will dissociate, first causing more hydrogen molecules from the bulk area to diffuse toward the electrode. Thus, a concentration gradient is established between the bulk medium and the electrode surface. As the polarization potential is increased, the above reaction is in effect intensified (Adams, 1969); causing more and more hydrogen molecules to be

dissociated at the electrode surface per time and thereby increasing the current generated. However, there will come a point at which any further increase in polarization potential will cause the depletion of hydrogen molecules at the electrode surface to exceed the rate of migration of hydrogen molecules from the bulk medium. At this point, the current generated at the electrode surface is limited by the diffusion coefficient of hydrogen in the medium and therefore, further increases in polarization voltage will result in a constant current plateau until the voltage is such that the current will increase as a result of the electrolysis of water. When this condition exists, the current generated at the electrode is proportional to the hydrogen concentration in the bulk medium according to Faraday's Law and Fick's Law (Adams, 1969). A more detailed description of the equations involved is found in Appendix A. The current plateau for hydrogen normally occurs over the polarization voltage range of +240 mV to +800 mV (Young, 1980).

Besides linearity, the selectivity of the polarized platinum electrode for hydrogen alone is the other consideration in setting the polarization voltage. The possibility that any chemical substance can contribute electrons to or take electrons away from a polarized electrode becomes significant if the electrode voltage is matched to the potential energy holding the electron to the chemical substance. Thus, the polarized electrode will oxidize or reduce substances that have potential energy barriers similar to the polarization voltage resulting in current contributions from these substances. As mentioned before, Aukland et al. (1964) show that the effects of ascorbate, oxygen, and hydrogen ion are acceptably small when the polarization potential is +250 mV. But Young (1980) argues that ascorbate will contaminate the signal if polarization potentials on the order of +500 mV

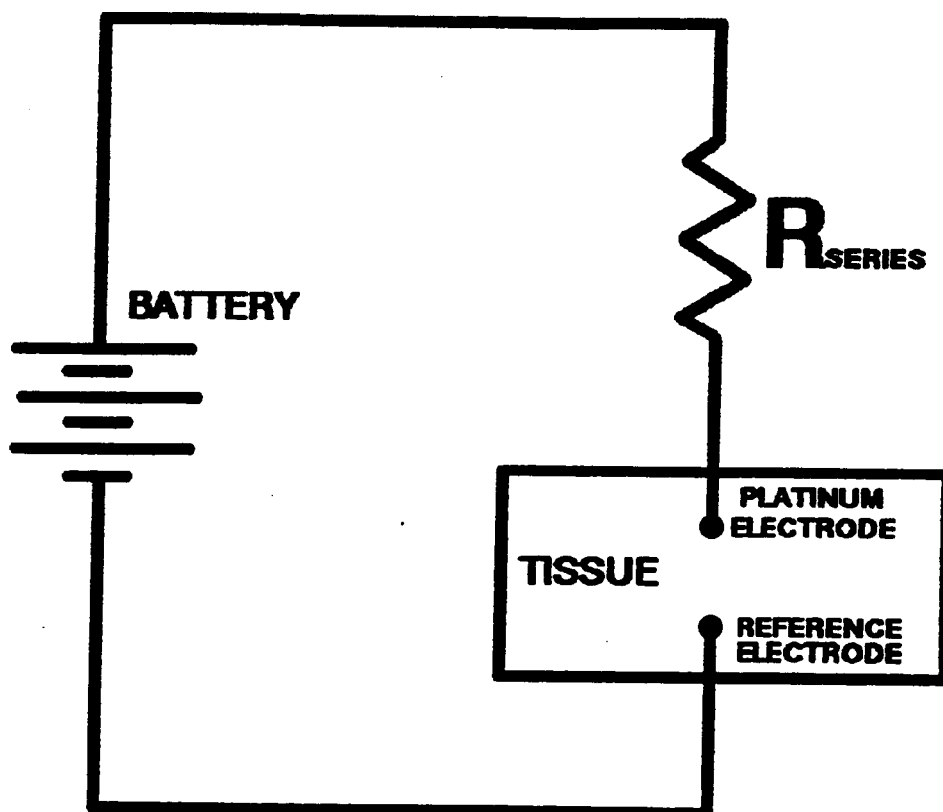
are used for electrodes detecting hydrogen in the brain since ascorbate levels are much higher in the brain than in other body tissues (Martin, 1961; Schaus, 1957; and Flamm et al., 1978) and ascorbate sensitivity is maximized at this level. However, the magnitude of this contamination is very small considering that 0.1 mM ascorbate contributes 0.25% of the total signal detected by a +250 mV platinum electrode (Aukland et al., 1964) when the sensitivities of hydrogen and ascorbate are similar (Aukland et al., 1964; Adams, 1969; and Ball, 1937). Unlike ascorbate, the signal noise contribution of oxygen becomes significant when the polarization potential approaches -100 mV (Young, 1980). With these considerations, the polarization voltage set for each platinum electrode is +600 mV. This polarity has been used by other investigators (Halsey et al., 1977; Fein et al., 1975; Jamieson et al., 1973; and Roseblum, 1977) in ischemic cerebral tissue studies.

The earlier circuits of Aukland et al. (1964) utilized a battery in series with a resistor to provide both the polarization potential and the means to measure the current output of the platinum electrode (see Figure 5-3). The voltage drop across  $R_s$  is proportional to the electrode current while a value of  $R_s$  equal to or greater than 105 ohms resulted in enhanced sensitivity of the platinum electrode to hydrogen. However, the voltage drop across the resistor would change the polarization potential applied to the platinum electrode which resulted in significant changes in electrode sensitivity to hydrogen for relatively small changes in polarization potential (Aukland et al., 1964; and Willis et al., 1974). To minimize the error in the flow determinations caused by the fluctuation in polarization potential, Willis et al. (1974) describes a circuit in which the electrode polarization potential at all electrode currents encountered during flow measurements is held

## FIGURE 5-3

**SIMPLE CIRCUIT FOR MEASURING TISSUE HYDROGEN  
CONCENTRATION LEVEL WITH PLATINUM ELECTRODES**

The basic concept of hydrogen polarography is depicted here. The battery supplies a polarization potential to the platinum electrode and the electrode current is measured as a voltage drop across the series connected resistor.

**SIMPLE HYDROGEN POLAROGRAPHIC CIRCUIT**

constant. The circuit used in this system is a modification of the circuit described by Willis et al.(1974) and is illustrated in Figure 5-4.

The circuit in Figure 5-4 is essentially a high impedance circuit because the generated electrode current (on the order of nanoamperes) at the + 600 mV polarization potential yields impedance values in the megohm range. Thus, great care is required to prevent signal distortion resulting from electronic noise or signal loss. Some of the precautions include proper grounding of the animal and the circuitry to the reference electrode, adequate insulation around the copper wires between the electrodes (platinum and reference) and the circuitry, and separate power sources for different equipment within the system to minimize electronic noise.

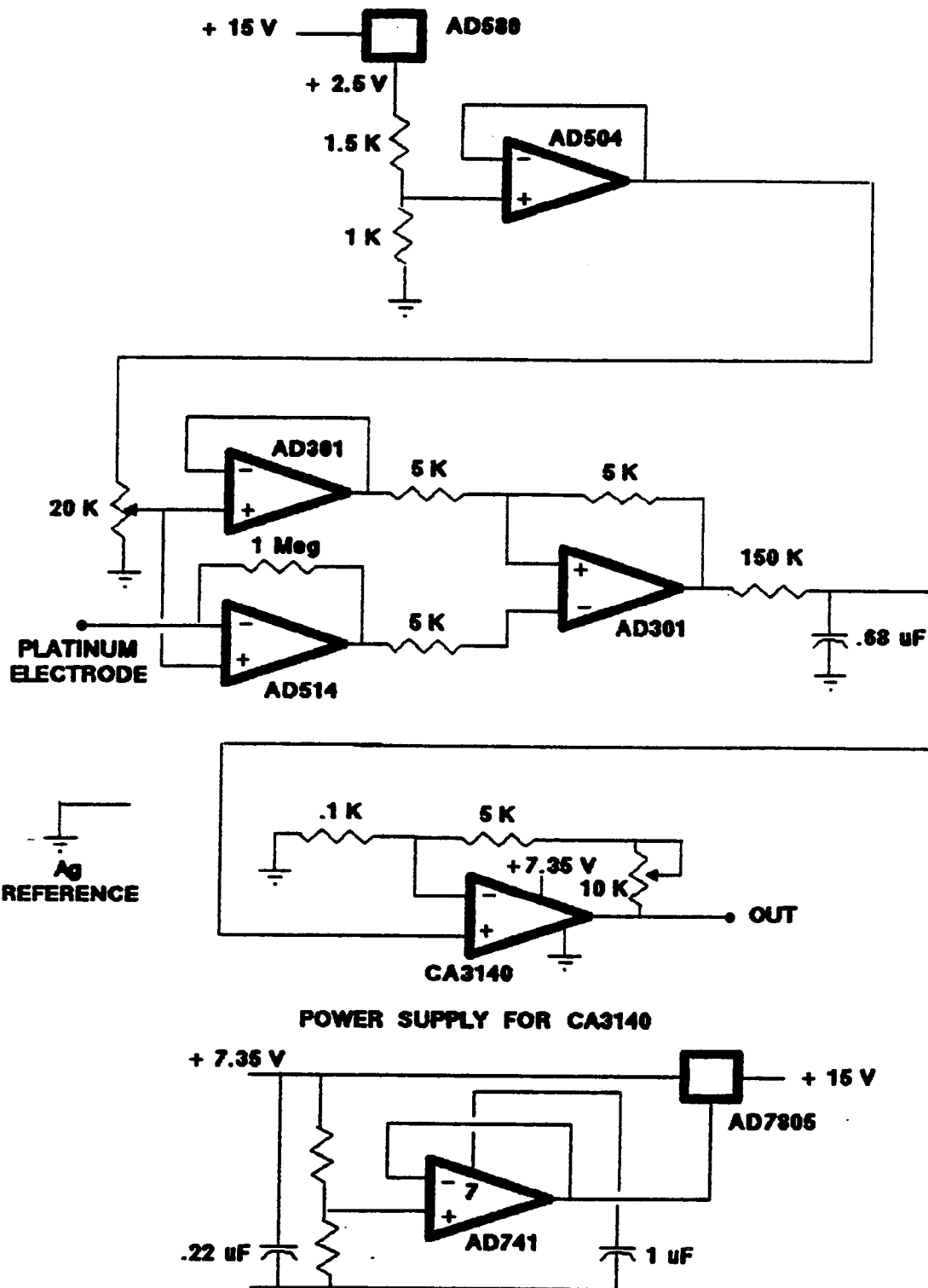
An Analog Device Model 920 dual power supply box (+ 15 volt 200 mA) provides all eight circuits with + 15 volts DC. This signal is transformed in two locations to 2.5 volts by an LM580 voltage rectifier and to 7.35 volts by an AD7805 voltage rectifier. A 1 volt signal is generated from the 2.5 volt signal through a voltage divider and fed into a voltage follower (AD504 operational amplifier) to provide a stable polarization potential. The output of the voltage follower is divided by a 20K ohm potentiometer to yield the + 600 mV polarization potential. This is fed into the non-inverting end of the AD514 operational amplifier. Measurement of the electrode current and polarization of the electrode with a constant voltage (+ 600 mV) is accomplished by the AD514. A 1.0 megohm resistor is inserted in the feedback loop while the hydrogen electrode is connected between the summing point and ground. The AD514 keeps the voltage at the summing point equal to the voltage at the non-inverting input, thus balancing the current flow in the electrode circuit by a current flow in the feedback loop of equal magnitude. This maintains a constant polarization potential for all

FIGURE 5-4

**SCHEMATIC DIAGRAM OF PLATINUM ELECTRODE  
POLARIZATION AND CURRENT MEASURING CIRCUIT**

This circuit provides a constant polarization potential to the platinum electrode for the range of electrode currents encountered during flow measurements and measures the electrode current resulting from the hydrogen concentration. The AD514 operational amplifier detects the electrode current by measuring the voltage drop across the 1 Megohm resistor. The AD301(a) high impedance non-inverting voltage follower serves to minimize the loading of the electrode circuit by the polarization voltage while the AD301(b) unity gain differential amplifier removes the polarization potential from the output signal of the AD514. The additional signal gain is provided by the CA3140 operational amplifier. See text for further details.

## PLATINUM ELECTRODE POLARIZATION AND CURRENT MEASURING CIRCUIT



electrode currents encountered in flow determinations. The voltage drop across the 1.0 megohm resistor is proportional to electrode current according to Ohm's law. The common mode electrode polarization potential is removed from this signal (output of AD504) by the AD301 unity gain differential amplifier while the AD301 high impedance non-inverting voltage follower minimizes the loading of the electrode circuit by the polarization voltage signal. The output of the AD301 unity gain differential amplifier is amplified by the CA3140 amplifier which establishes the overall circuit sensitivity to +5.0 volts DC per microampere of electrode current by adjusting the 10K ohm potentiometer in the feedback loop. A single silver reference electrode inserted subcutaneously in the animal will suffice for all eight platinum electrodes. The output signal from this circuit is limited to the range of zero volts to +5.0 volts by the CA3140 amplifier because possible damage may result to the DTX311 Analog/Digital Converter (discussed below) since its input range is zero to +5.0 volts. This is accomplished by biasing the seventh terminal of the CA3140 with 7.35 VDC power supply which comes from the LM7805 voltage regulator and AD741 operational amplifier arrangement.

The output signals of the eight CA3140 amplifiers are fed to the computer through the first eight channels of an iSBX bus compatible analog/digital converter (DTX311 from Data Translation, Inc., Marlborough, MA) (See Figure 5-5). The DTX311 acquires analog signals from the user interface and converts them into digital code which can be processed by the host computer (IBM-AT). The DTX311 provides 16 single-ended or 8 differential input channels and can be configured for unipolar or bipolar input ranges. The input range for this system is unipolar 0 to +5 volts. This is why the overall circuit sensitivity described above is set to +5.0 volts. The

DTX311 is interfaced to the IBM-AT bus through one of the three iSBX connectors on the DT2806 Multi-Function Input/Output Subsystem Board (Data Translation). With this arrangement, electrode voltages representing hydrogen concentration within the tissue being monitored can be recorded with respect to time in discrete files by the computer. Thus, the computer can be programmed to collect "flow" files during the washout phase and then calculate the blood flow at each electrode site automatically.

Hydrogen gas delivery to the animal is under computer control by a solenoid isolation valve (Dayton Corp). The solenoid valve is in the "OPEN" position when energized with 110 VAC and is in the "SHUT" position when deenergized. A General Electric solid state relay (rated at 120 VAC and 5 Amps) switches the power to the solenoid either "ON" or "OFF". The solid state relay receives its switching signal from channel 1 of a 24 channel DPDT relay output accessory board (Model ERB-24 from Metrabyte Corp., Stoughton, MA) (see Figure 5-5). The switching signal from channel 1 of the ERB-24 is under computer control which addresses the ERB-24 through the DTX350 Digital Input/Output Module (Data Translation) connected to the DT2806. When the appropriate conditions exist, the computer initiates an output signal that addresses the appropriate register on the DT2806 causing the channel 1 DPDT relay to switch the solid state relay resulting in a change in power (either energized or deenergized) felt at the solenoid.

In the current system, the hydrogen clearance method is fully automated and controlled through an IBM-AT computer to minimize some of the limitations of the method and to make the method more consistent, reliable, and reproducible. In general, after the baselines and gains have been set for each electrode channel, the animal is permitted to inhale hydrogen along with the anesthetic gases (about 2 - 3% of the gas mixture)

FIGURE 5-5  
COMPUTER INTERFACE SCHEMATIC

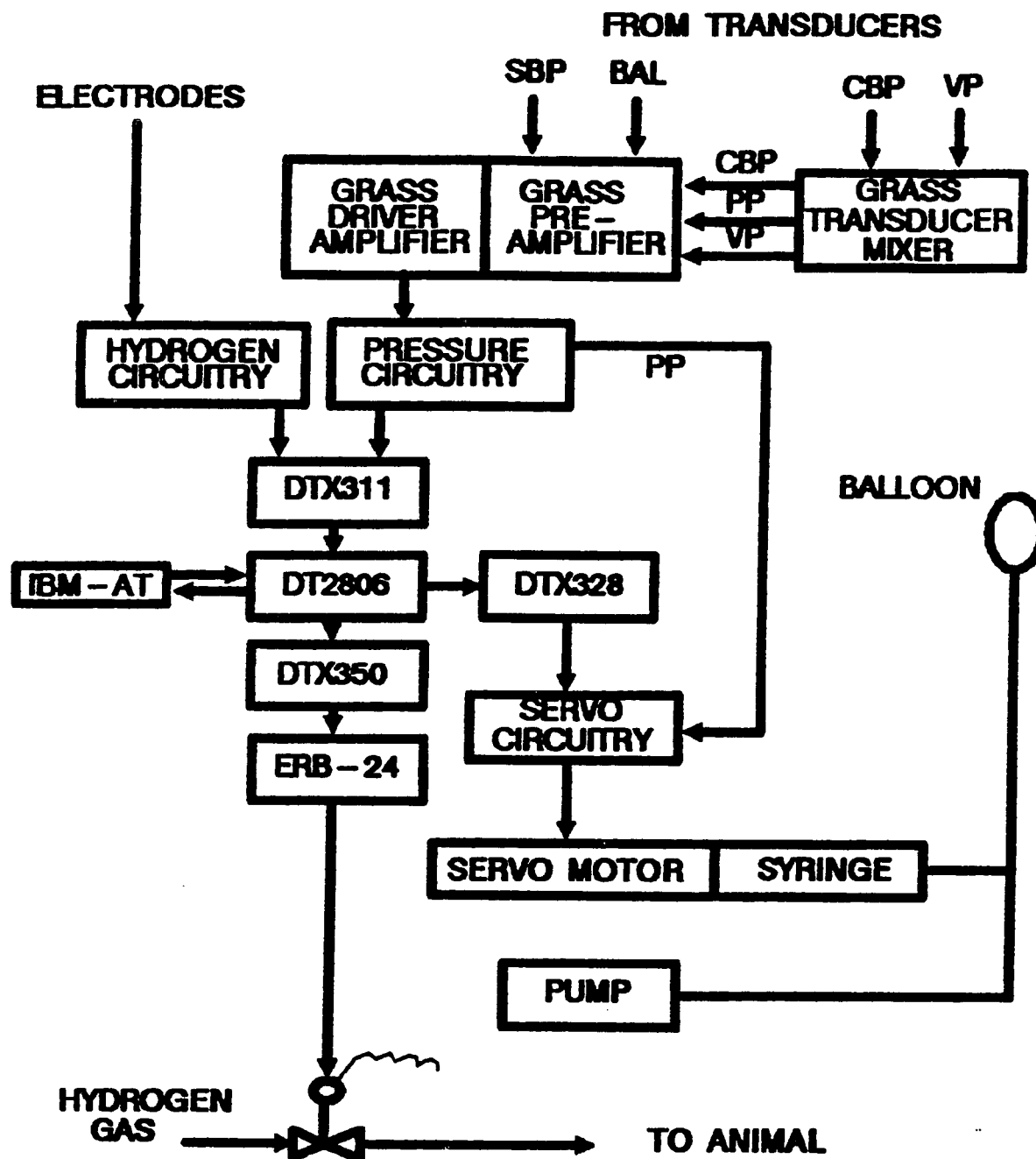
The general scheme in which the signals are generated, collected, and processed is shown here. All pressure signals originate from transducers while all hydrogen concentration signals originate from the platinum electrodes. The hydrogen concentration signals are generated by the circuitry described in Figure 5-4 and made available to the computer through the first eight channels of the DTX311 Analog/Digital converter and the DT2806 Multi-Function Input/Output board.

The difference in the CBP and VP pressure signals are obtained from a Grass Transducer Mixer. The resulting perfusion pressure voltage along with the CBP and VP are sent to the Grass Pre-amplifiers. The pre-amplifiers also receive the pressure signals for SBP and the balloon. The pre-amp amplifies these signals and outputs them to the Grass driver amplifiers. The driver amplifier powers the pens to give a hard copy of the signals being received and provides some damping to the signals before they are sent to the pressure circuitry. The pressure circuitry provides damping, sensitivity, and baseline adjustment to the signals and is described in detail in the pressure control section. The pressure signals are made available to the computer through five of the sixteen channels of the DTX311 Analog/Digital converter and the DT2806 Multi-Function Input/Output board.

The DTX311 and the DT2806 enables the operator to process the signals through a computer program. The hydrogen concentration signals are continuously displayed and used to calculate LCBF for each electrode while the pressure signals are continuously displayed. The DTX328 Digital/Analog converter converts the desired perfusion pressure digital signal to an analog signal in order that it can be compared to the actual perfusion pressure in the servo circuitry. The difference in these two signals causes the servo motor to be activated resulting in the appropriate change in balloon pressure.

The computer also generates switching signals at times specified by the control program which are sent to the ERB-24 DPDT Relay Output Accessory board via the DTX350 Input/Output Module. This enables the operator to control the hydrogen input to the animal by a solenoid control isolation valve. Also, a greater capability of monitoring four channels of EEG (instead of one) during experiments is provided by multiplexing through the ERB-24 (not shown in this figure). See text for details.

## COMPUTER INTERFACE SCHEMATIC



while the computer continuously monitors the electrode voltages for each channel. When tissue saturation occurs, the computer initiates a signal which deenergizes the solenoid valve for controlling hydrogen input causing it to "SHUT" and thereby terminating hydrogen input to the animal. During the washout phase the computer periodically collects flow information consisting of electrode voltage and time from each channel and writes this information to a flow file. When the electrode voltage for any channel falls to some value predetermined by the operator, the computer terminates data collection and reenergizes the solenoid valve for subsequent resaturation. The computer now has a flow file consisting of the voltage versus time relationships for each electrode which represents the exponential washout curve for each electrode. As described before in Figure 5-1, the computer then calculates the LCBF in ml/100g/min by a least square fit at each electrode site. Then, a hard copy of all the flows is immediately made by the printer and the flows are stored on hard disk in a database file created for each experiment. This process repeats itself when the animal is resaturated with hydrogen gas.

A computer program written in the BASIC language allows the operator to set up certain conditions under which the hydrogen method is to be executed automatically during the experiment. The conditions that can be set include (1) baselines, (2) the lowest electrode voltage allowed before termination of flow information collection occurs and resaturation begins, (3) the time between flow collections, (4) the automatic slope function, (5) the percent drop in hydrogen concentration before flow information is collected, and (6) the rate of flow collection. These are discussed in detail in the following sections. The automatic conditions are addressed by the operator by selecting and depressing the appropriate INKEY on the computer keyboard. As described before, the different INKEY selections are normally

displayed on the computer screen continuously during an experiment. This allows the operator to INPUT the appropriate value for the desired condition. For example, assume the operator desires to change the time between flow measurements from 15 minutes to 25 minutes. After referring to the computer screen, the operator selects and depresses the key with the letter "A" on it. In response to this action the console screen will clear and the computer will write a message like "Time between H2 flows ... (0) To Stop?" The operator will then type in 25 followed by depressing the ENTER key. The original screen display will reappear and from now on if all the other conditions are satisfied flows will be collected at 25 minute intervals instead of 15 minute intervals. In addition to the conditions that can be set for automatic operation, there is an INKEY which will allow the operator to energize or deenergize the solenoid control valve for hydrogen isolation. This is very useful when initially setting the baselines and gains for each electrode channel.

#### (1) Baselines

The baselines and gains for the hydrogen signal range of each electrode channel are set such that the voltage signal corresponding to complete saturation is maximized while keeping the voltage signal corresponding to zero hydrogen concentration "close" to zero. This is done to maximize the signal difference during the washout phase in order to obtain a more accurate clearance curve from which the flow determinations are made. It should be emphasized, however, that the system sensitivity limitation described above in monitoring the voltage signals from the eight different electrode channels is from zero to + 5.0 volts. Thus, any generated electrode voltage signal above + 5.0 volts or below zero volts will sent to the computer as + 5.0 volts or zero volts, respectively, because the AD3140 amplifier in the

hydrogen circuitry is set up to send out a maximum voltage signal of + 5.0 volts and a minimum voltage signal of zero volts. Therefore, any generated electrode voltage signal outside of this range is essentially off scale and cannot be used for hydrogen flow determinations.

Obviously, an off scale signal during the washout phase will invalidate that particular flow. However, a more serious problem arises if all the electrode baselines are set to zero volts and the baselines shift downward. This will result in unknown baselines that are off scale and will certainly invalidate all the flows obtained for the affected channels for that experiment. To circumvent this problem an INKEY pair was created and is described in the following example. After the electrodes have been connected to the circuitry and allowed to stabilize while the animal is in a state of complete hydrogen desaturation, an artificial voltage baseline corresponding to zero electrode voltage output for each electrode is set to approximately 0.4 to 0.5 volts. At this point, the INKEY "T" is depressed which will take the artificial baseline value for each electrode channel and subtract this value from all future voltage readings for each channel. In effect, each channel has been "zeroed" (i.e. shifted to zero volts corresponding to zero hydrogen concentration) at some on scale value while not affecting the signal range. Individual channel gains are then set to give 3.0 to 3.5 volt readings at all electrodes in the hydrogen equilibrated animal.

If it becomes necessary to reset the baselines for some reason (e.g. after a major adjustment in the gain settings) the current zeroes must be removed before the baseline zeroes are reset. This is done by depressing the INKEY "W". The baseline zeroes are then reset as described above.

## (2) Lowest Electrode Voltage

After the baselines have been zeroed as described above, it is now possible for the computer to obtain negative voltage readings during the hydrogen washout phase if the baselines have shifted downward. This is undesirable because the computer takes the natural logarithm of all the voltages obtained during its calculation of LCBF at each electrode. In essence the program will "bomb" when the negative voltage is encountered during the natural logarithm calculation. This is avoided by selecting the INKEY "2" which will clear the console screen, take the operator to the "hydrogen rate" subroutine, and display additional INKEY selections. One of these selections is INKEY "D"; when depressed, this will allow the operator to INPUT the minimum or bottom voltage allowable during hydrogen flow collection for any channel. During hydrogen washout the electrode voltages will all tend to zero until the lowest voltage reading reaches the minimum or bottom voltage set by the operator. When this happens, the computer automatically terminates hydrogen flow file collection, begins calculation of the LCBF's at each electrode site, and energizes the solenoid valve for subsequent resaturation with hydrogen gas. Throughout these studies we have used 0.6 to 0.3 volts as the minimum voltage signal to terminate the washout phase and to recommence the saturation phase. It is the lowest electrode voltage signal that allows the computer to perform the hydrogen method many times without interruption as long as the other conditions are satisfied.

### (3) Time Between Flows

This INKEY initiates the automatic hydrogen clearance method and it is briefly described above. The time between each flow is calculated from the instant the previous washout begins. The time table for automatic flow collection is as follows: At time zero the solenoid valve is deenergized, marking the beginning of the washout phase. The computer calculates the

average hydrogen signal among all the channels and when this signal falls a certain percentage of the average hydrogen signal for complete saturation (see the percent drop section below), the computer starts collecting the hydrogen flow file. This continues until the lowest electrode voltage is obtained which terminates the washout phase. Resaturation commences and continues until 15 minutes have elapsed from the initiation of the previous washout phase (i.e. when the solenoid valve was previously deenergized). Then, if the autoslope function is satisfied (discussed below) a new washout phase will commence for subsequent flow determination because the time requirement has been satisfied.

The values that are currently used for this interval are 15 minutes and 25 minutes. The 15 minute interval is used when normal control flows are being obtained while the 25 minute interval is used when perfusion pressure has been lowered to less than 12 mmHg. The reason for the two different values for the two different conditions is that it takes hydrogen considerably longer to clear and resaturate at the very low perfusion pressures than it does at the higher pressures due to the difference in the flow.

To stop the automatic flow collection sequence a zero is entered for the time between hydrogen flows. This prevents the washout phase from starting regardless of the autoslope function.

#### (4) Automatic slope function (autoslope)

Two conditions must be satisfied in order to commence the washout phase when the hydrogen clearance method is in the automatic collection mode. The first condition is the "time between flows" criterion and the second is the "autoslope" function. Basically, the autoslope function is employed to ensure that complete hydrogen saturation exists before the washout phase begins. Each time the computer makes a pass through the

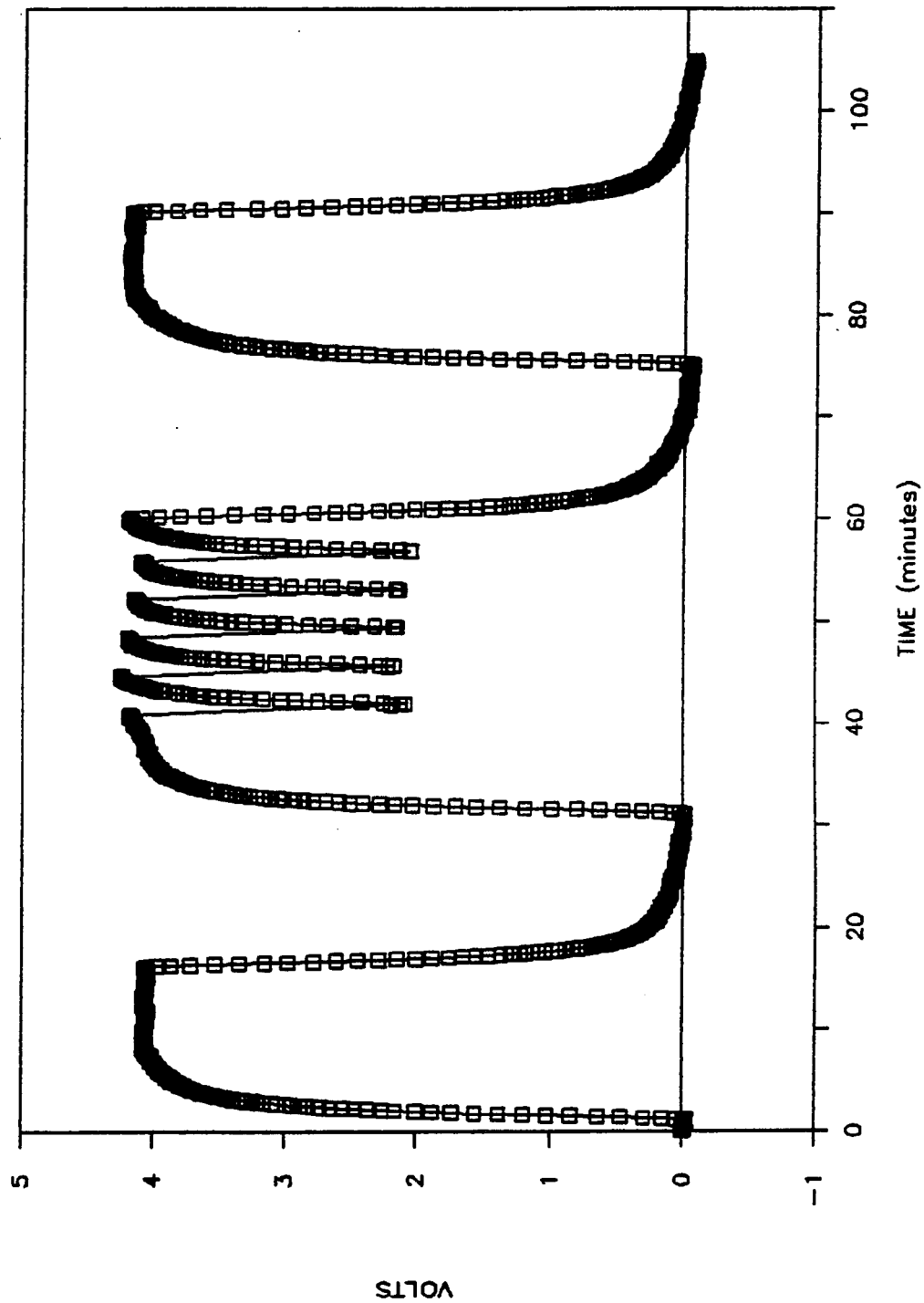
program it updates the electrode voltage signal from each channel and the averaged voltage signal from all eight channels. These voltage signals are continuously displayed on the console screen. The autoslope function evaluates the rate of change in the averaged voltage signal and displays this value to four significant digits on the console screen. This value is also updated on each computer pass. When a state of complete hydrogen saturation or desaturation exists, this value will be small. The value of 0.030 volts/min is chosen for the autoslope limit in this system which was less than 1% of full signal strength and represents background noise. Therefore, as long as the autoslope function is implemented and the rate of the averaged electrode voltage signal is greater than 0.030 volts/time then the washout phase cannot be started. The INKEY associated with this condition functions only to activate or deactivate this function. Therefore, the operator can choose whether or not to have this capability during experiments, but not to change its value.

This function is extremely useful because it consistently and correctly determines when hydrogen saturation exists without involving the operator. Thus, the time between flow collections is minimized and a more reproducible and reliable state of saturation exists before each washout phase is commenced. Also, this function can determine when a state of desaturation exists after non-ischemic studies in order to determine how much each electrode channel baseline has shifted during the experiment. Figure 5-6 shows a typical hydrogen profile obtained for one channel during a recent experiment. Thus complete hydrogen saturation existed before all washout phases were commenced for flow determination (as indicated by the voltage plateaus) and that the hydrogen electrode voltage signal returned to its original baseline within 1% when the experiment was over.

**FIGURE 5-6**  
**HYDROGEN CONCENTRATION PROFILE**  
**FOR SERIAL LCBF DETERMINATIONS**

During the course of an experiment the computer maintains a continuous file of electrode voltage (hydrogen concentration) for each platinum electrode. In an experiment consisting of only serial LCBF determinations the automatic slope function clearly prevented the washout phase from occurring until the condition of hydrogen saturation was met. Also note that there was no shift in hydrogen baseline at the end of the experiment.

# VALIDATION OF SERIAL CBF DETERMINATIONS



This is significant in that it demonstrates that the baselines do not normally shift in this system and the requirement for complete hydrogen saturation is satisfied before each flow determination is made.

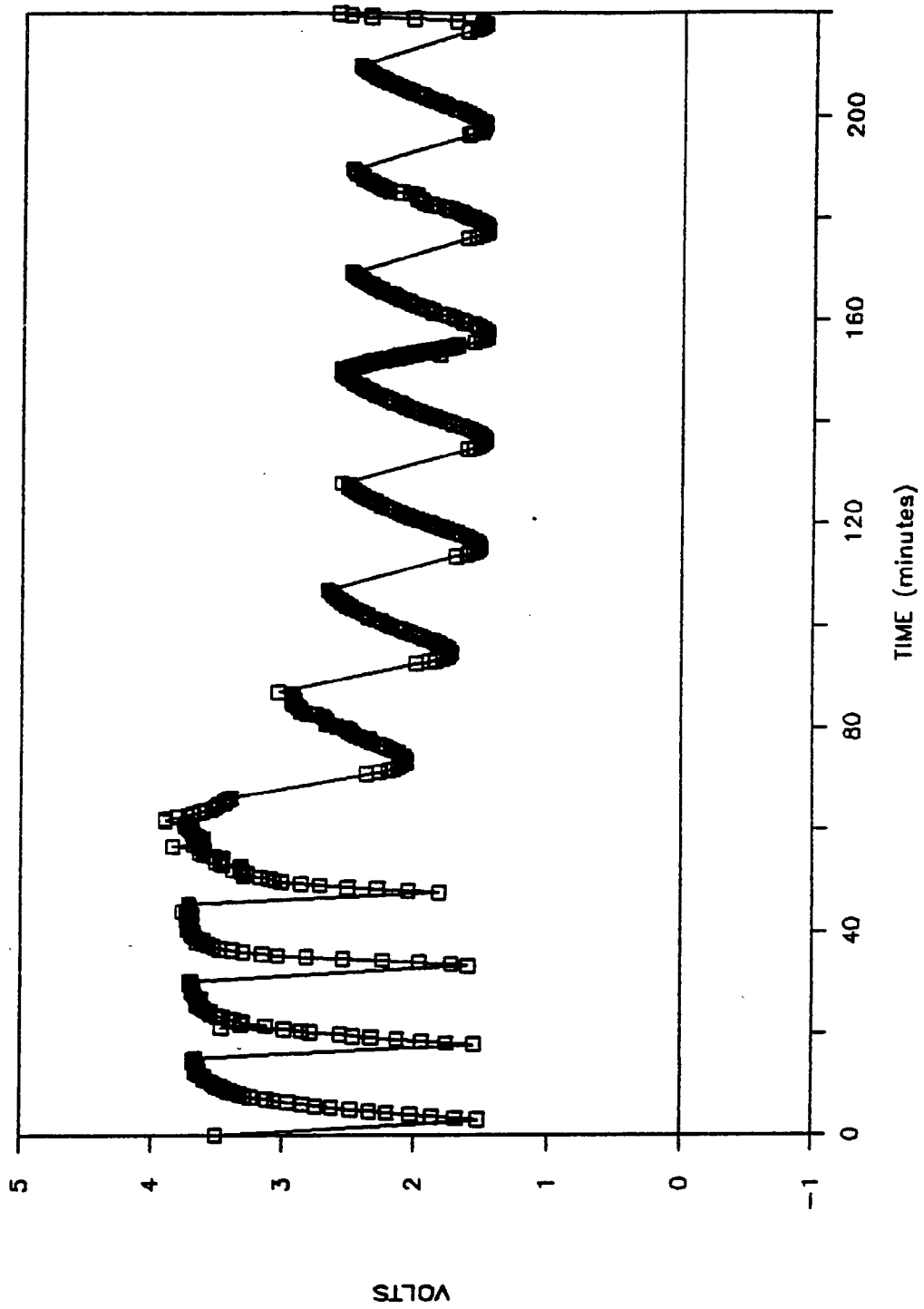
For ischemic studies (when perfusion pressure is lowered to  $<9$  mmHg) the autoslope function is not very useful in determining how much the baseline has shifted at the end of the experiment because in areas where the flow has collapsed to less than 3 to 4 ml/100g/min hydrogen becomes essentially "trapped" in the tissue being monitored. Therefore, its removal becomes increasingly dependent on its diffusion out of the tissue. The electrode voltages will return to their original baselines, but at a much slower rate than the rate set for the autoslope function. Thus, the operator must monitor the slow decline in electrode voltage over a long period of time in order to determine how much the baseline has shifted.

A possible explanation of the phenomenon of the trapped hydrogen is as follows: before the perfusion pressure is lowered to  $<9$  mmHg the animal exists in a state of complete hydrogen saturation. After the perfusion pressure is lowered the capillaries in the vicinity of the tissue electrode which had originally brought the hydrogen to that location slowly collapse one by one due to the decreased blood flow. As a result, the hydrogen turnover is very small due to the decrease in local flow and to the lower number of functional capillaries (essentially a change in hemodynamics). This may also explain why the electrode voltage saturation plateaus are lower during the ischemic time course as compared to pre-ischemic levels (see Figure 5-7). Then when it comes time to completely desaturate the animal of hydrogen by reperfusion, the available number of functional capillaries within the electrode vicinity has decreased and thus the mode of hydrogen exodus has

**FIGURE 5-7**  
**HYDROGEN CONCENTRATION PROFILE DURING**  
**A 7 mmHg PERFUSION PRESSURE EXPERIMENT**

This curve is typical for experiments performed at 7 mmHg. Even though hydrogen saturation exists before any flow determination, the saturation plateaus are lower than those before occlusion was enacted. This may be the result of altered hemodynamics after severe partial occlusion has been enacted. Also note that the hydrogen baseline has not shifted and this is typical for all these experiments.

# HYDROGEN CONCENTRATION VS TIME



been limited even though flow has increased in the functional capillaries as a result of the reperfusion. Therefore, the only mode of exodus for hydrogen in tissue not being served by a functional capillary is by diffusion. This concept is supported by the eventual clearance of tissue hydrogen (i.e., electrode baseline recovery) only after prolonged periods of time (see Figure 5-7) at the termination of the experiment.

#### (5) Percent Drop

The "percent drop condition" refers to the percent drop in the averaged electrode voltage signal from complete saturation before initiating hydrogen flow file collection. There are two considerations as to why this condition exists. The first is that one of the assumptions in deriving the hydrogen clearance equations is that the arterial concentration of hydrogen is zero during clearance. Fieschi et al. (1969), Halsey et al. (1977), and Jamieson et al. (1973) have reported that 95% of the hydrogen is cleared from the major arteries within one minute while others (Lubbers et al., 1969; and Stosseck, 1970) have reported that the clearance of hydrogen from the pial arteries lags considerably (up to several minutes) behind the major arteries. Since no further hydrogen is being administered to the tissue, Fick's law is not violated, but Young (1980) argues that significant hydrogen transfer can occur between different tissue compartments through the vascular space and thus influence hydrogen clearance by capillaries downstream. However, if all the tissue compartments are completely saturated and some time is allowed to elapse after hydrogen inhalation termination before hydrogen flow file information is collected then the pial artery concentration of hydrogen will be greatly reduced and its influence on downstream hydrogen clearance will be greatly minimized. The saturation requirement is accomplished by the autoslope function described above.

The second consideration is that some critics of the hydrogen clearance method argue that introducing an electrode into the brain parenchyma may result in a zone of devitalized cells constituting a diffusion barrier (Brock et al., 1967; and Aukland, 1964). Aukland (1964) studied these effects and reports that for a membrane of 0.2 mm, 0.4 mm, and 0.6 mm, the electrode response deviates from the hydrogen concentration during the first 1 second, 16 seconds, and 1 minute, respectively, of clearance. After this initial deviation, however, the electrode response does reflect the hydrogen concentration despite these diffusion barriers (Aukland, 1964). Thus, it is appropriate to introduce a pause between hydrogen inhalation termination and hydrogen measurement.

Instead of incorporating a specific time requirement before hydrogen flow file collection commences, a percent drop in the averaged electrode signal is used because it is assumed that the time requirement will change when going from normal flow conditions to ischemic flow conditions. The percent drop for this system is 15% and it was determined as follows: Hydrogen flows were obtained at different values for percent drop at constant systemic pressure and the resulting clearance curve was evaluated for any significant breakpoints (Jones et al., 1984). From this, it was empirically determined that for drops of 10% or less, the clearance curve was not linear (when plotted logarithmically) while nearly all the clearance curves with drops of 15% or more were linear. Thus, 15% was chosen in order to maximize the amount of the clearance curve to be evaluated for flow determination. It takes nearly 1 minute under normal flow conditions for a 15% drop to occur after hydrogen inhalation termination and approximately 4 minutes for this drop to occur under flow conditions resulting from a perfusion pressure of 7 mmHg. Even though an INKEY exists for this option,

this value of 15% has been left unaltered throughout all the experiments performed.

#### **(6) Rate of Flow File Collection**

Since the rate at which the computer collects flow files as data points for the hydrogen clearance curve is automatically calculated and executed by the computer, the INKEY associated with this option is never used. However, a brief description is provided for this capability.

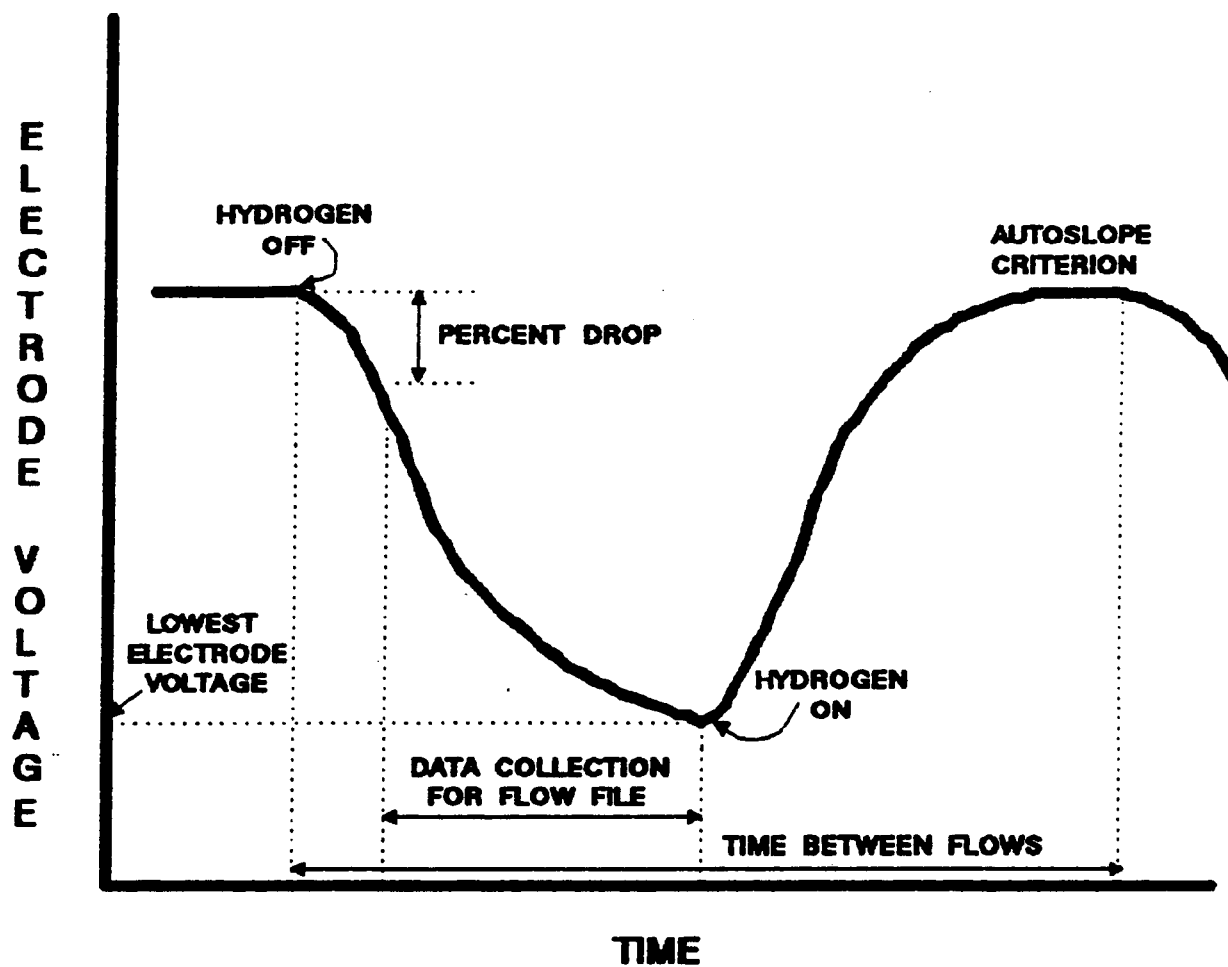
The computer has the ability to write flow information (electrode voltage and time) to a file on every pass it makes through the control program. However, since hydrogen clearance is dependent on flow rate, a potential disparity in file lengths exists for normal flow and ischemic flow files. Specifically, the files would be very large since it can take up to 15 minutes for hydrogen to clear under such restraints. Thus, to have comparable flow file dimensions and to reduce file length, the computer calculates a collection rate based on the hydrogen clearance rate during the initial 10% drop. This results in evenly spaced data points on the clearance curve from the beginning of hydrogen flow file collection to the point at which an averaged voltage signal of 60% of the original signal at the beginning of the washout phase exists. At this point, the collection rate is automatically halved because the linear change in the magnitude of the electrode voltages is not as great as it was at the beginning of flow file collection.

Figure 5-8 is provided to give a graphical representation of some of the automatic conditions described above.

**FIGURE 5-8****SUMMARY OF CONDITIONS**

The automatic conditions that the operator has control over for the conduct of the hydrogen clearance method is presented here graphically. Each condition shown is discussed fully in the text.

## SUMMARY OF CONDITIONS



## **PRESSURE CONTROL SUBSYSTEM**

The newly developed animal model provides modulation of perfusion pressure throughout the ischemic range by controlling the input of blood to the cerebrum from one extracranial artery. This is a very important aspect of the system in that modulating perfusion pressure throughout the ischemic range without systemic insults such as hypoxia or hypotension requires some form of mechanical compression on an arterial supply. Because the technique for mechanical compression takes up a finite space and the rat is rather small, an artery lying outside of the cranium must be used. Perfusion pressure control is provided by making the brain's blood supply dependent on the input from the left common carotid artery (described in Animal Model section). To partially occlude the common carotid artery, a balloon partial occlusion technique is developed (balloon manufacturing technique given in Appendix C) in which a plastic cylinder is placed around the left common carotid artery. A latex balloon connected to a computer controlled servo-motor driven syringe is then inserted into the cylinder (see Figure 6-1). The servo-motor is interfaced to the computer so that the actual perfusion pressure is closely matched to the desired perfusion pressure.

The pressure signals for SBP, CBP, VP, and perfusion pressure originate from cannulas inserted into the right common carotid artery and the right jugular vein (see Figure 6-2). Perfusion pressure is obtained by taking the

**FIGURE 6-1****IN-VIVO ARRANGEMENT OF THE BALLOON AND CUFF**

To provide remote compression on the left common carotid artery, a balloon connected to the computer controlled servo-pump is inserted into a plastic cylinder placed around the vessel. Also shown are the two cannulas inserted into the right common carotid artery for SBP and CBP monitoring and the single cannula inserted into the jugular vein for VP monitoring.

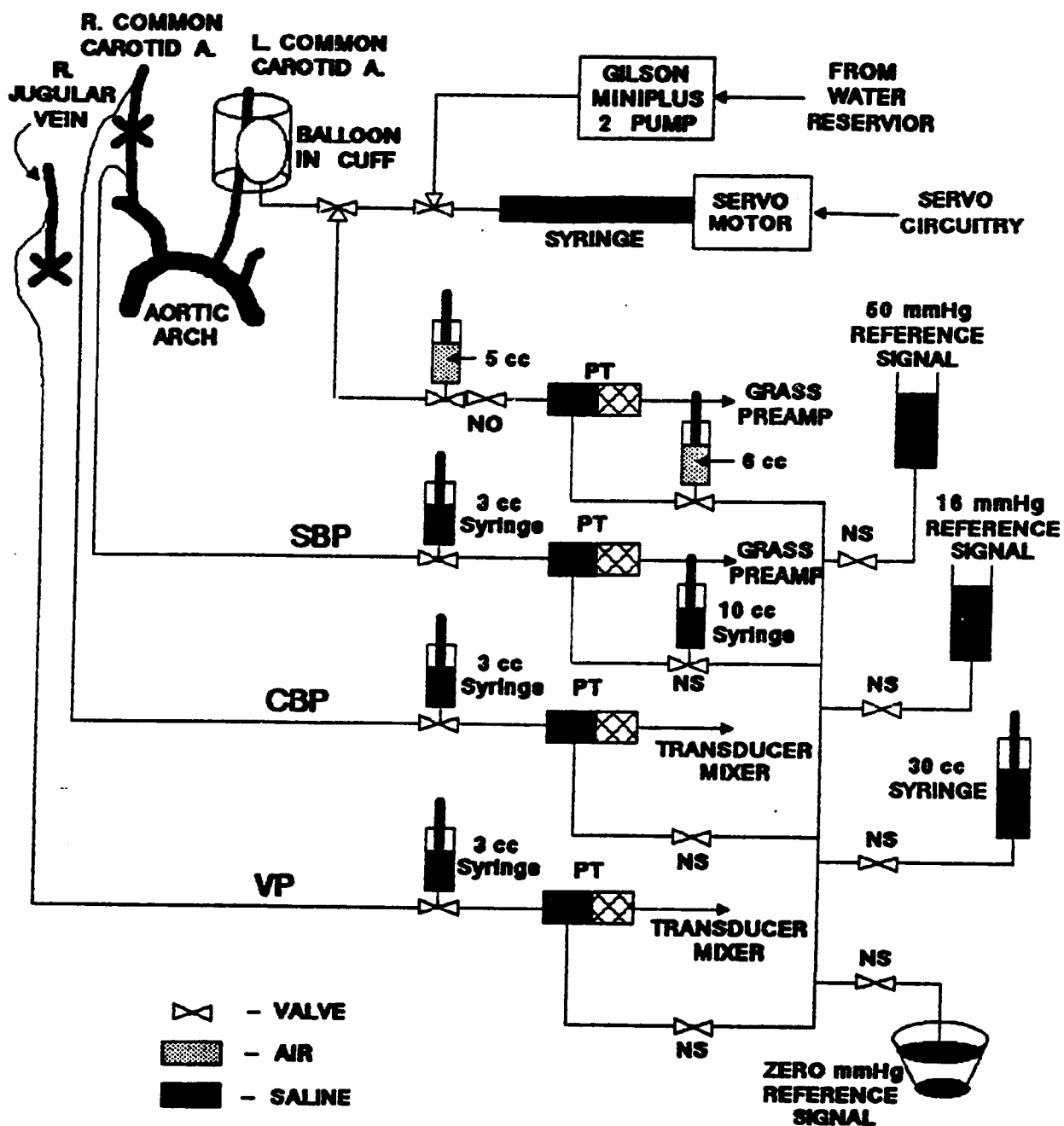


**FIGURE 6-2****PRESSURE MONITORING SYSTEM MECHANICAL**

SBP, CBP, and VP are obtained directly from the animal while perfusion pressure is obtained indirectly from the difference between CBP and VP. The pressure transducers convert the mechanical signals into electrical signals for further processing. A reference system is provided for transducer calibration.

The servo-controlled syringe adds or takes water out of the balloon to modulate balloon pressure. A Gilson Miniplus 2 Pump serves as an infinite reservoir in order to provide a greater pressure range for the balloon. This is necessary when changing the balloon pressure more than can be provided by the servo syringe itself. PT = pressure transducer; NO = normally open; NS = normally shut.

## PRESSURE MONITORING SYSTEM - MECHANICAL



difference between the CBP and VP signals within the Grass Transducer Mixer (see Figure 6-3) and balloon pressure is obtained through a three-way valve connected downstream of the syringe on the balloon line. The cannulas for SBP, CBP, and VP are completely filled with normal saline which serves as a continuous medium to transmit the pressure within the animal to the appropriate pressure transducer. The normal saline is heparinized 20 units/ml to prevent the occurrence of blood clotting within the cannulas during the experiment. Potential backflow of blood from the animal's vessel to the transducer is corrected by flushing the blood back into the animal by a 3 cc syringe provided in each line. The mechanical portion of this subsystem also has three reference signals (50, 16, and zero mmHg) used to calibrate the pressure transducers. A 30 cc syringe reservoir replenishes fluid loss from evaporation in the reference lines and from flushing.

The four pressure transducers convert the mechanical pressure signal to a voltage signal for further processing. The SBP and balloon pressure signals are sent directly to the Grass pre-amplifier while the CBP and VP signals are sent to the Grass Transducer Mixer to generate the perfusion pressure signal (see Figure 6-3). The Grass pre-amplifier receives all of the pressure signals, amplifies them, and sends them to the Grass Driver Amplifier which provides a hard copy of all the pressure signals on chart recording paper.

Because the input rating to the DTX311 Analog/Digital converter is from zero to 5 volts (discussed previously in the Hydrogen Clearance Method section), the pressure signals from the Grass Driver Amplifier must be processed in a similar fashion to that occurring at the last stage of the hydrogen circuitry. The schematic diagram for this circuitry is shown in Figure 6-4. The first half of the AD747 operational amplifier provides baseline and gain adjustments to the incoming signal. The second half of the AD747 serves

FIGURE 6-3

## COMPUTER CONTROL INTERFACE SCHEMATIC

The general scheme in which the pressure signals are generated, collected, and processed is shown here. The hydrogen signal processing and control is described in the Hydrogen Clearance Method section. All pressure signals originate from transducers while all hydrogen concentration signals originate from the platinum electrodes. The difference in the CBP and VP pressure signals is obtained by a Grass Transducer Mixer. The resulting perfusion pressure along with the CBP and VP are sent to the Grass Pre-amplifier. The pre-amplifier receives all the pressure signals, amplifies them, and sends them to the Grass driver amplifier. The driver amplifier powers the pens to give a hard copy of the signals being received and provides some damping to the signals before they are sent to the pressure circuitry. The pressure interface circuitry provides damping, overall sensitivity, and baseline adjustment to the signals and is described in detail in the pressure control section. The pressure signals are made available to the computer through five of the sixteen channels of the DTX311 Analog/Digital converter and the DT2806 Multi-Function Input/Output board.

The DTX311 and the DT2806 enables the operator to process the signals through a computer program. The DTX328 Digital/Analog converter converts the desired perfusion pressure digital signal to an analog signal in order that it can be compared to the actual perfusion pressure in the servo circuitry. The difference in these two signals causes the servo motor to be activated resulting in the appropriate change in balloon pressure.

## COMPUTER INTERFACE SCHEMATIC

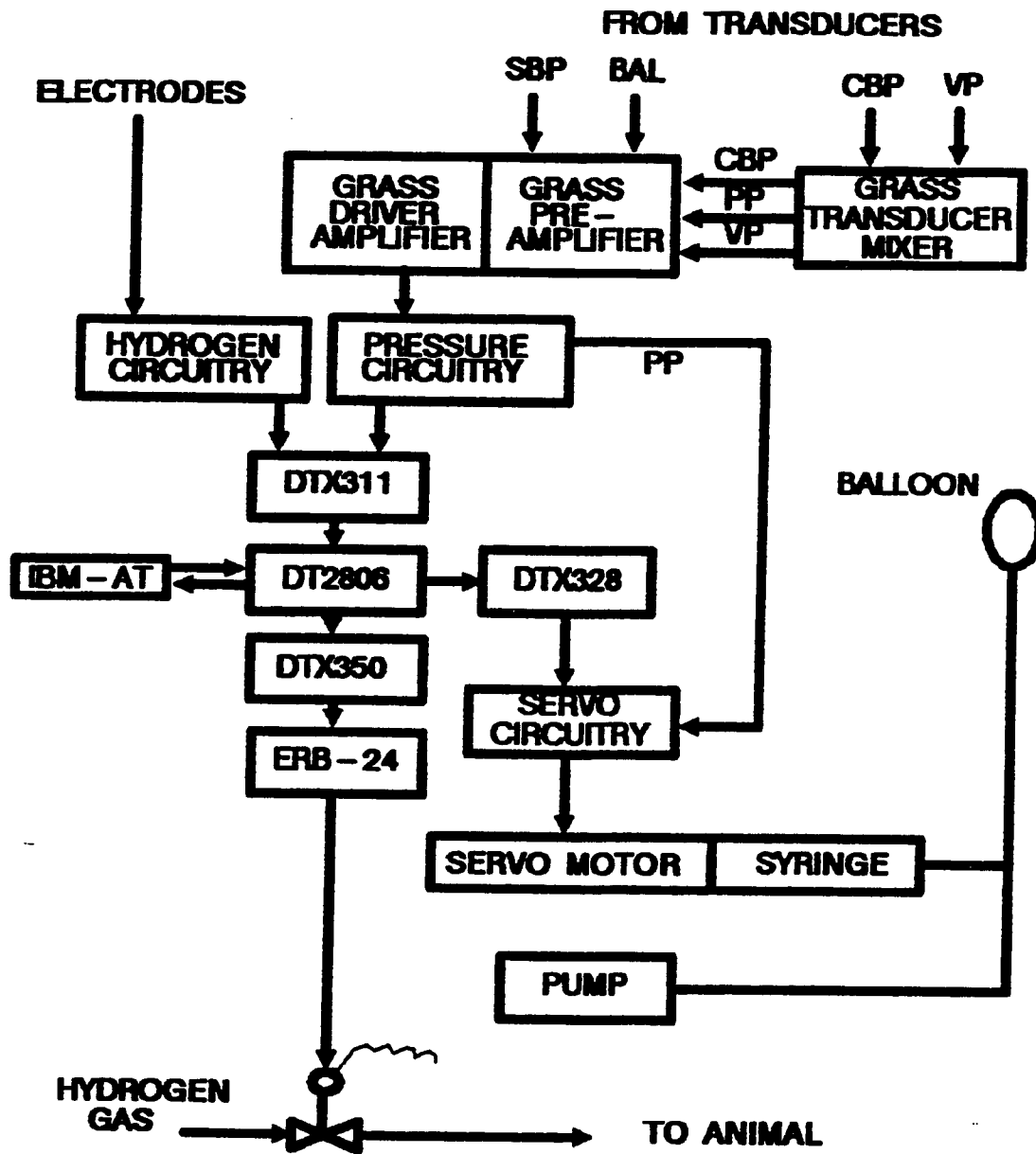
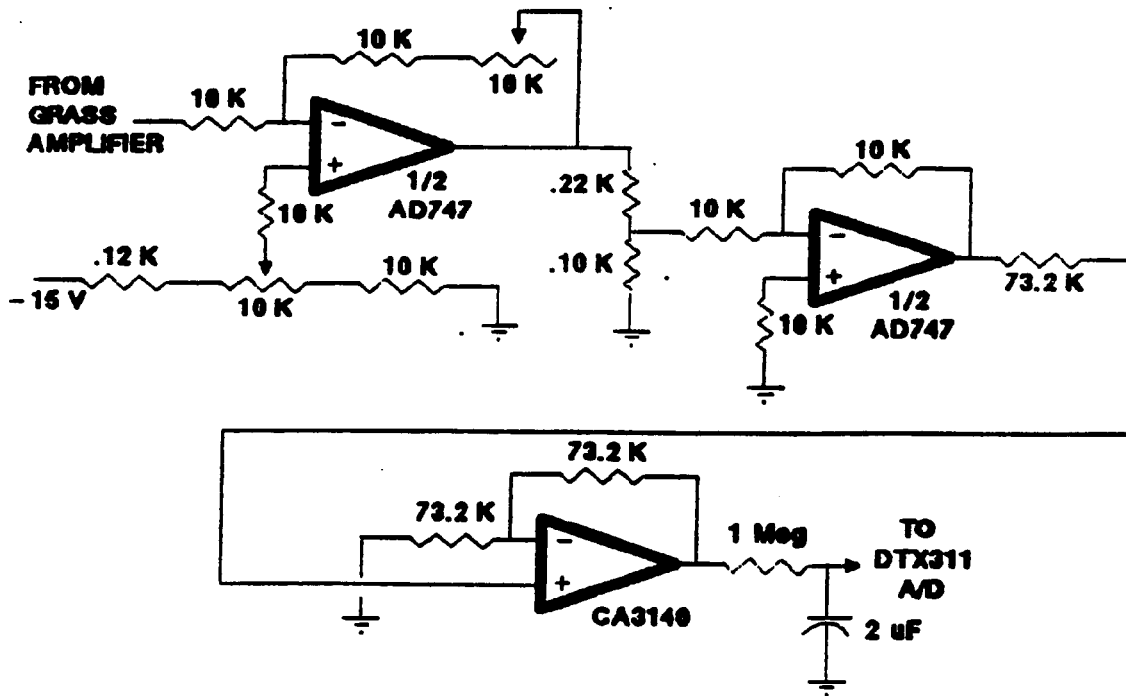


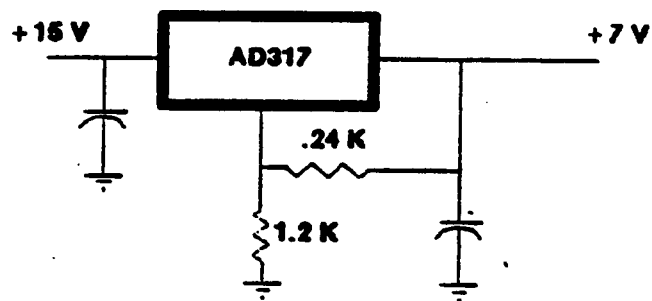
**FIGURE 6-4****PRESSURE MONITORING INTERFACE CIRCUITRY**

As with the hydrogen signals, the pressure signals from the Grass Driver Amplifier must also be processed in order to be fed into the DTX311 Analog/Digital Converter. The two amplifiers within the AD747 provide gain and baseline adjustment to the incoming signal. As before, the CA3140 provides the sensitivity for the circuit. Each of the five pressure channels has an RC filter connected to the output of the CA3140 amplifier. The capacitance for channels corresponding to SBP, CBP, VP, and balloon pressure is 2  $\mu\text{F}$  while that for perfusion pressure is 0.68  $\mu\text{F}$ .

## FIVE CHANNEL GRASS TO A/D INTERFACE



### POWER SUPPLY FOR CA3140



as a unity gain amplifier. As described before, the CA3140 operational amplifier limits the output to between zero and 5 volts. However, unlike the hydrogen circuitry, the signal is sent through an RC filter on the output side of the CA3140 to minimize the oscillations in the signal due to perturbations such as the animal's heart rate. The output signals of the five CA3140 amplifiers are fed to the computer through five channels of an iSBX bus compatible analog/digital converter DTX311. As described previously in the Hydrogen Clearance Method section, the DTX311 acquires the analog signals, converts them to digital code, and then sends them to the host computer for processing via the DT2806 Multi-Function Input/Output Subsystem Board. In addition to being fed to the computer via the DTX311, the perfusion pressure signal is also sent to the servo circuitry (see below) to be compared to the "desired" perfusion pressure.

The desired perfusion pressure originates as a digital signal created by the computer from the input value chosen by the operator. To compare the desired and actual perfusion pressures, the desired perfusion pressure signal must be converted to an analog signal. This function is performed by the DTX328 Digital/Analog Converter connected to the DT2806 and the output signal is fed to the servo circuitry in Figure 6-5.

Hester et al. (1983) describes a system for servo-controlling renal perfusion pressure in dogs through a Dacron-reinforced inflatable silastic occluder placed around the aorta from which the circuitry shown in Figure 6-5 is modified. While input signals in Hester's system originate from the Grass Polygraph recorder, the input signals in the current system originate from the computer and the pressure circuitry. The desired perfusion pressure voltage is then inverted in a unity gain amplifier while the actual perfusion pressure is fed through a voltage follower in order to minimize the loading of the

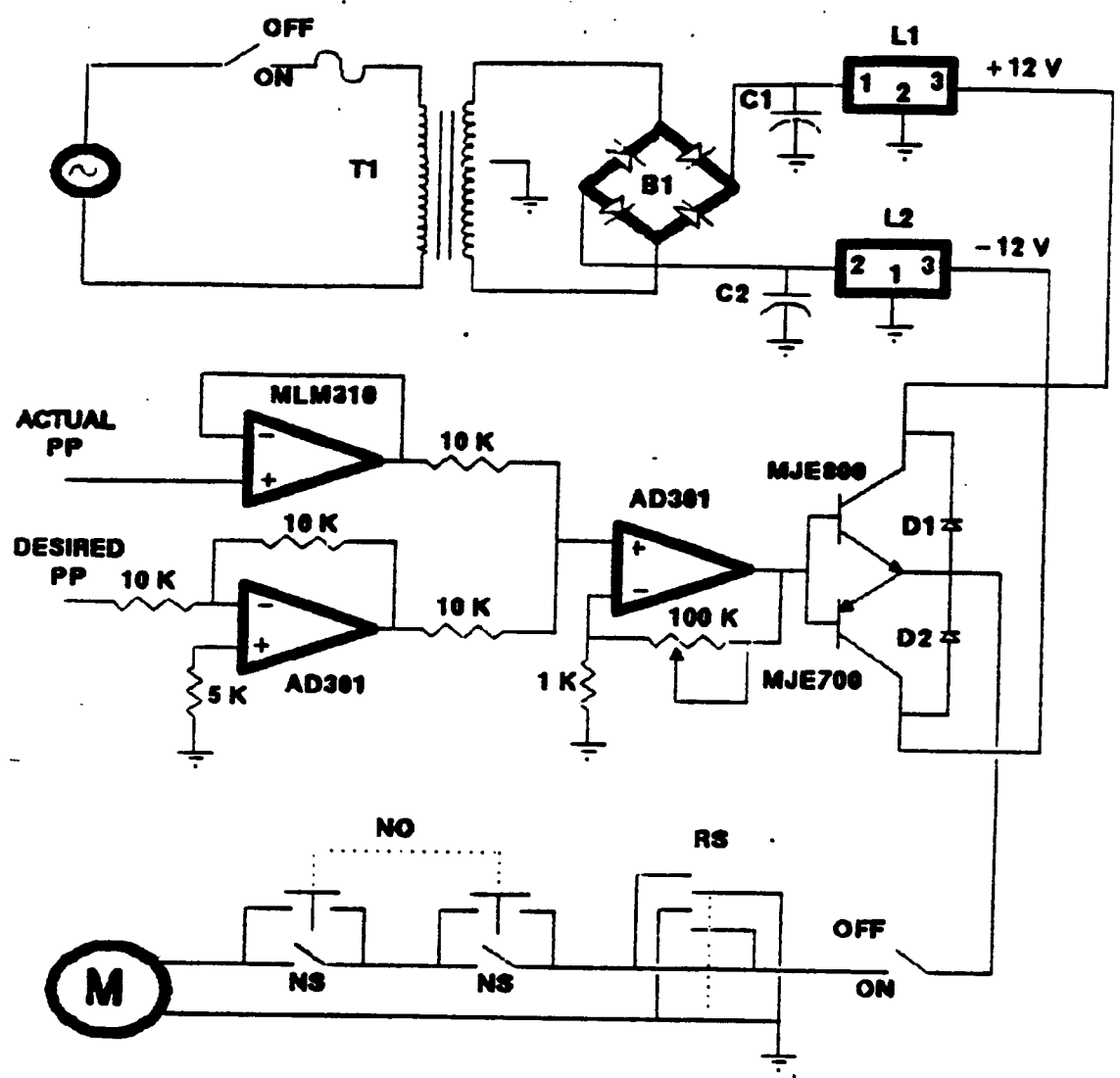
FIGURE 6-5

**POWER SUPPLY AND ELECTRONIC CONTROLLING CIRCUIT  
FOR THE SERVO-MOTOR**

The power supply of this circuit is provided via a 40-Volt center tap transformer, bridge rectifier, and two voltage regulators. The output from the transformer is applied to a bridge rectifier (B1). The output of the bridge rectifier is applied to the input of the voltage regulators L1 and L2 to supply a positive and negative 12 volts to the power transistors. The capacitors are used to filter the output.

The electronic controlling circuit consists of three operational amplifiers. The AD301 unity gain amplifier inverts the desired perfusion pressure signal while the MLM310 amplifier serves as a voltage follower for the actual perfusion pressure signal. The AD301 summing amplifier obtains the difference between the actual and desired perfusion pressure and amplifies this signal according to the current gain setting. A 100K potentiometer connected between the output and the inverting end of the summing amplifier affects the gain setting for the summing amplifier. Thus, the response of the servo-motor can be modulated to the difference between actual and desired perfusion pressure (i.e the "dead" space can be varied). See text for further details. T1 = 40V center tap transformer; B1 = bridge rectifier; L1 = LM7812 positive voltage regulator; L2 = LM7912 negative voltage regulator; C1 = C2 = 3000 uF 25 VDC capacitors; D1 = D2 = 50 V diodes; M = 12 VDC motor (Micro Mo Electronics, model 2233); NO = normally open; NS = normally shut.

### SERVO CIRCUITRY



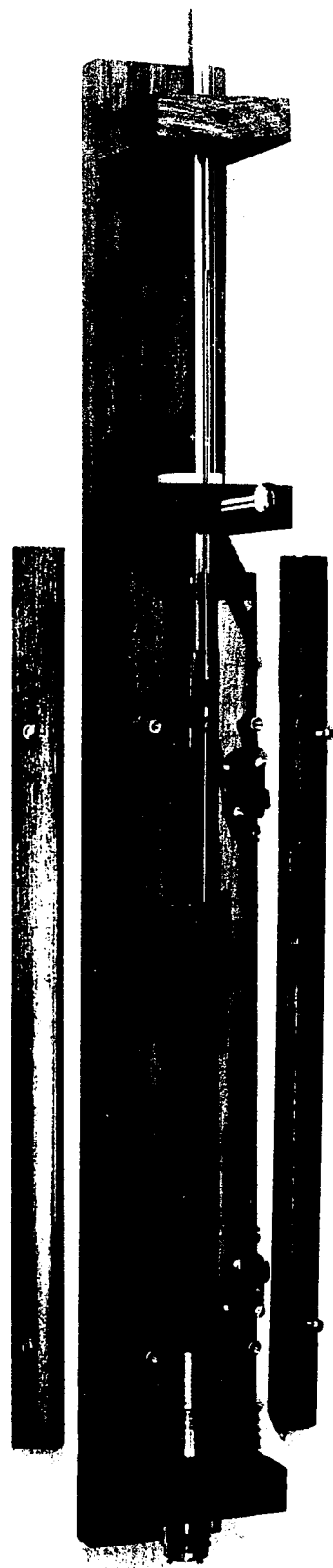
circuit. The two signals are summed in the AD301 summing amplifier yielding a signal representing the difference between the two input signals. The gain of the summing amplifier depends upon the potentiometer setting of the feedback resistor. For positive output voltages from the summing amplifier, the MJE800 transistor conducts, the MJE700 transistor is turned off, and current flows from the +12 volt source through the motor. When negative outputs occur, the MJE800 transistor is turned off, the MJE700 transistor conducts, and current flows from the -12 volt source through the motor. When the desired perfusion pressure signal equals the actual perfusion pressure signal both transistors are turned off because there is no voltage output from the summing amplifier. Two 50-volt diodes are placed between the collector and emitter of the transistors to protect the transistors. Thus, through negative feedback from the CBP and VP transducers, the servo-motor rotates in such a way as to minimize the difference between the actual perfusion pressure and the desired perfusion pressure.

The servo-motor (Micro Mo Electronics, model 2233) rotates a threaded rod in either direction depending upon the polarity of the current being supplied to the windings. In the case of a zero voltage output from the summing amplifier, the servo-motor does not rotate. A reversing switch is provided in the circuitry to change the polarity of the current supply to the motor if it becomes necessary to reverse directions. To prevent motor damage from overload due to mechanical binding of the pusher block (see Figure 6-6) two micro switches connected in series with the motor and power supply automatically shut the motor off before the pusher block has travelled its full path. A bypass switch is installed to override the microswitches so that the pusher block can be recentered after full travel.

FIGURE 6-6

## BI-DIRECTIONAL SERVO CONTROL SYRINGE

The servo-motor is mounted in a walnut block for stability and connected to a threaded rod via an aluminum coupler. The pusher block is connected to a bicycle spoke that travels within a hollow glass tube. The pusher block travels back and forth along the threaded rod due to the rotating servo-pump. The displacement or infusion of water within the hollow glass tube resulting from the movement of the bicycle spoke changes the pressure within the balloon which is connected to the glass rod by means of a PE-50 tube (not shown). The perfusion pressure is directly affected by the balloon pressure. Two microswitches serve to limit the travel of the pusher block to prevent mechanical binding at either end of the threaded rod.



A unique feature in the servo circuitry is that the response of the servo-motor to the difference between the actual and desired perfusion pressures can be controlled by adjusting the gain of the AD301 summing amplifier through a potentiometer connected between the output and the inverting side of the amplifier. A very high gain setting results in a rapid motor response rotating at a maximum angular velocity from a very small difference between actual and desired perfusion pressures while a small gain setting has the opposite effect. Thus, the gain setting directly influences the operating "dead" space of the motor. In effect, the system can be damped by modulating the response of the servo-motor to the difference between the desired perfusion pressure and the actual perfusion pressure.

The servo-motor and a 54.6:1 gearhead (Micro Mo Electronics) are connected to a 10/32 threaded rod via an aluminum coupler and mounted in a walnut block as shown in Figure 6-6. The rod is threaded through an aluminum extender at the base of a walnut pusher block, which fastens to a 14 gauge bicycle spoke. The bicycle spoke serves as a plunger for the glass tube, which is securely mounted in walnut blocks. The bicycle spoke and glass tube arrangement is called the syringe. The connection between the glass tube and the bicycle spoke is water tight while allowing the spoke to travel freely within the glass tube. The displacement or infusion of water in the glass tube serves to change the pressure in the balloon placed within the cuff around the left common carotid artery.

The range of balloon pressure modulation corresponds to the total travel of the pusher block. When initiating partial compression on the left common carotid artery, the balloon pressure must be increased from approximately 5 mmHg to greater than SBP to affect perfusion pressure.

Unfortunately, the pressure range of the syringe cannot accomplish this initial change in pressure. Therefore, a Gilson Miniplus 2 Pump is connected to the balloon line to supply the extra water volume necessary for this initial change in pressure. The pump is operated manually until the perfusion pressure falls to within the range that can be handled by the syringe. Then the pump is secured and the syringe takes over in controlling the perfusion pressure.

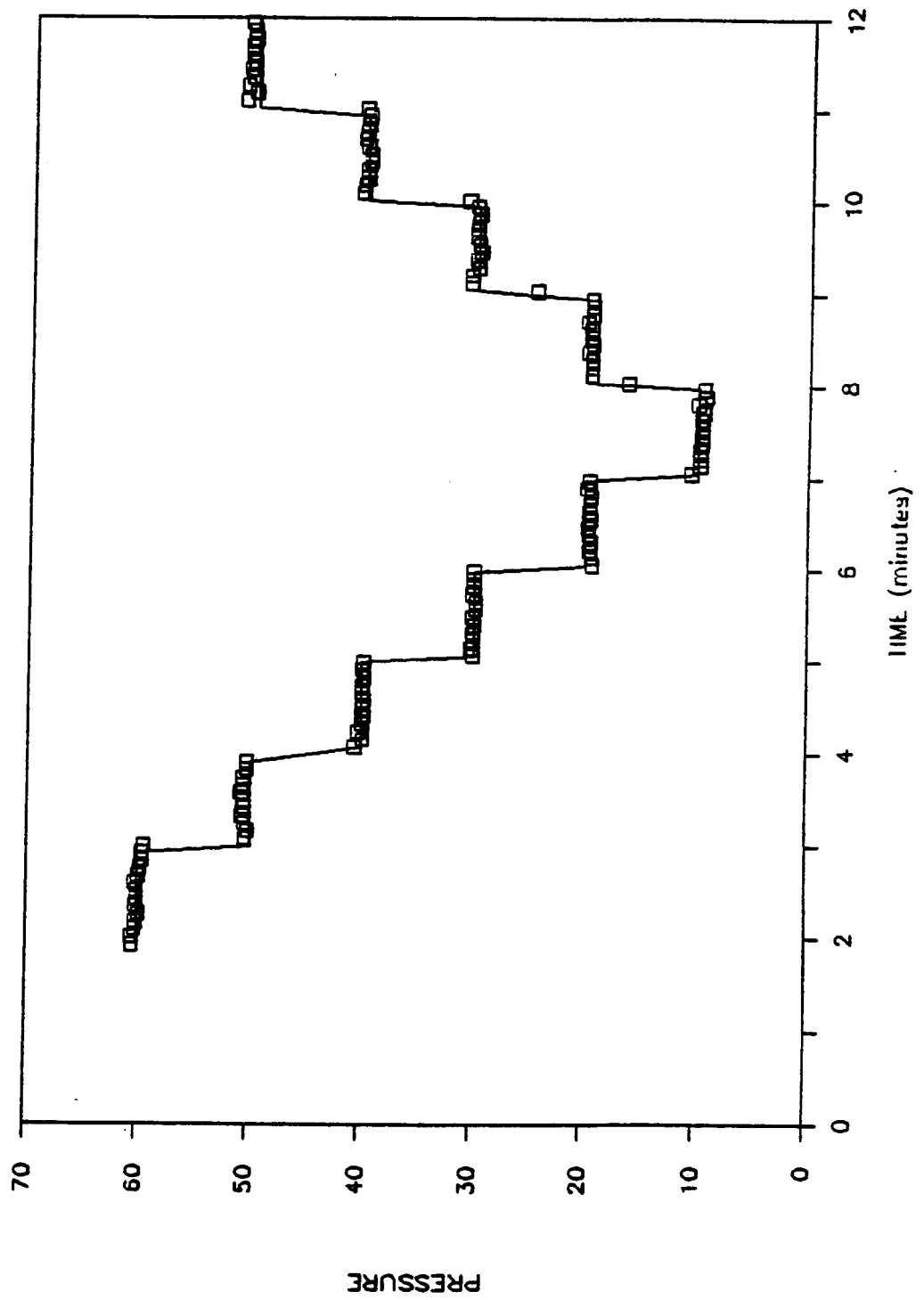
When the syringe is maintaining the perfusion pressure at the requested level, it is often desirable to have the pusher block centered on the threaded rod. Thus, in the event of any unexpected pressure perturbation, the syringe will have the maximum pressure range in either direction available to offset the pressure change. The pusher block is centered on the threaded rod by operating the Gilson pump manually at slow speed to withdraw or infuse water. The infusion of water into the balloon will be felt by the system as a decrease in perfusion pressure which will cause the system to respond by moving the pusher block towards the servo-motor. On the other hand, the withdrawal of water from the balloon will be interpreted as an increase in perfusion pressure which will result in the pusher block being moved towards the syringe.

Initial testing of the pressure control subsystem was done in-vitro by connecting the syringe output to the CBP transducer and setting the VP transducer to 0.0 mmHg with the zero mmHg reference and then setting the desired perfusion pressure to different levels. The results of the system's response during the in-vitro test were quite satisfactory and are shown in Figure 6-7. However, the first in-vivo test was quite unsatisfactory because the system was trying to respond to many perturbations such as the animal's heart rate, the pulse pressure, and the respirator which resulted in a

**FIGURE 6-7****IN-VITRO TEST OF SERVO-BALLOON SYSTEM**

The results of the in-vitro test of the balloon-servo system is presented here. The straight lines represent requested perfusion pressure while the boxes represent the actual perfusion pressure at which the balloon-servo system was controlling to.

# IN VITRO TEST OF SERVO-BALLOON SYSTEM



perfusion pressure that oscillated by as much as 3-4 mmHg on either side of the desired perfusion pressure. To minimize the oscillatory response of the system to these perturbations, both mechanical and electrical damping is employed. The electrical damping consists of perfusion pressure signal modulation by the RC filter in the pressure monitoring interface circuitry (see Figure 6-3) and by changing the servo-motor's response to the difference between the desired and actual perfusion pressure levels with the 1.0 megohm potentiometer in the electronic controlling circuit for the servo-motor (see Figure 6-4). The mechanical damping consists of increasing the amount of air within the balloon line.

The major consideration in selecting the appropriate damping are twofold. First, it is desirable to maintain a relatively quick system response during periods of unexpected excursions in the animal's mean arterial blood pressure. Yet, it is also desirable to minimize the system's oscillatory response during steady state (steady state refers to the animal's mean arterial blood pressure being constant over some period of time). Thus, an increase in damping will result in slower system response while a lower damping level will result in more pronounced oscillations.

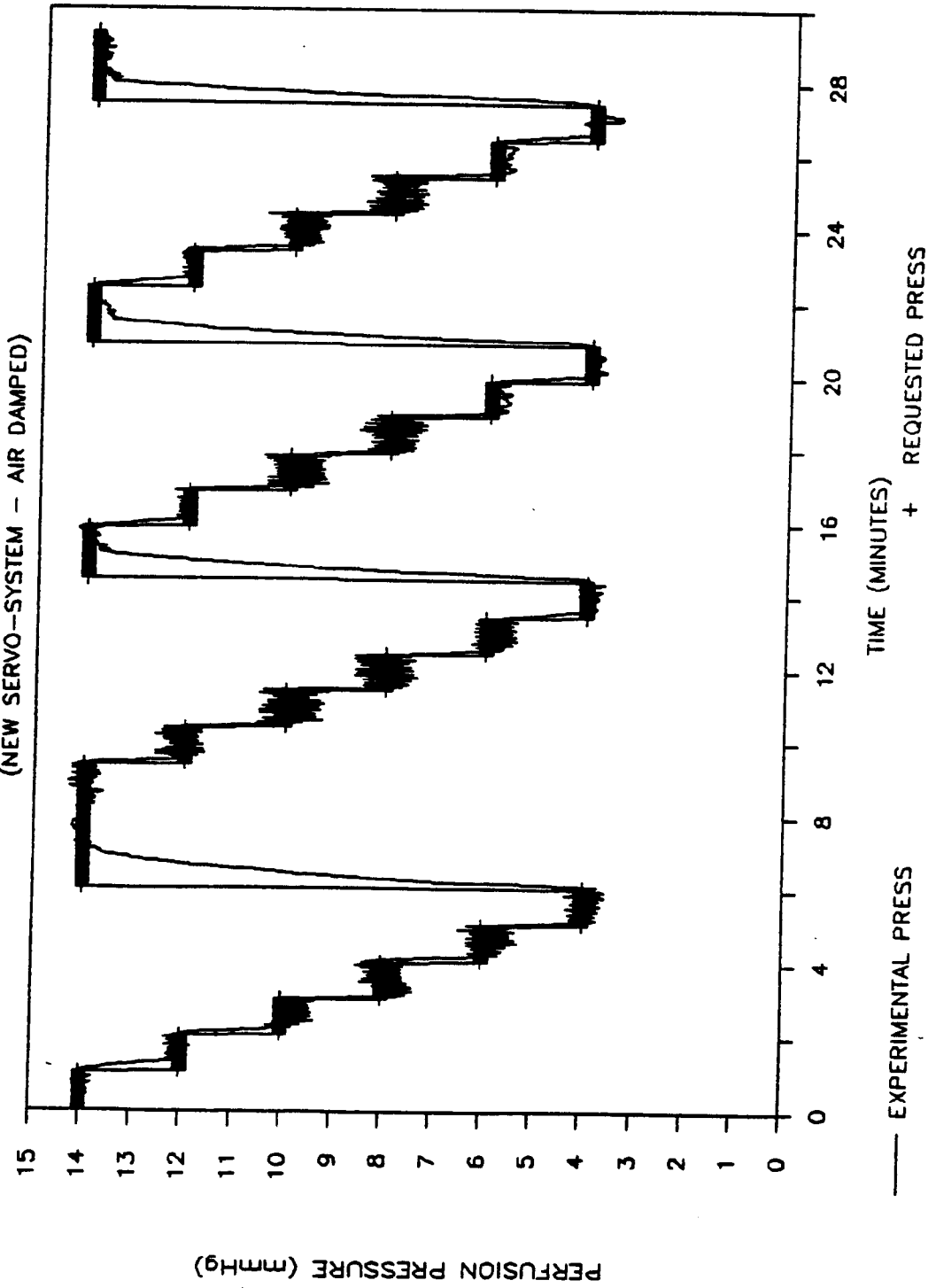
The electrical and mechanical damping in this system was determined empirically by optimizing the system's control over perfusion pressure in response to changes in 1) the RC filter, 2) the potentiometer setting, and 3) the amount of air in the balloon line. The optimization of these parameters resulted in values of .68  $\mu\text{F}$  for the capacitance of the RC filter, 11 ml of air for the balloon line, and approximately 200K ohms for the potentiometer. The new values for the damping parameters have resulted in a relatively quick system response while keeping the oscillations to approximately 0.5 mmHg or less (see Figure 6-8).

## FIGURE 6-8

## IN-VIVO TEST OF THE SERVO-BALLOON SYSTEM

After optimization of the system's damping parameters, control of perfusion pressure is relatively rapid while minimizing the oscillatory response to approximately 0.5 mmHg. Also, with the introduction of the new animal model, perfusion pressure can be controlled throughout the entire ischemic range.

# BILATERAL SUBCLAVIAN OCCLUSION (NEW SERVO-SYSTEM - AIR DAMPED)



— EXPERIMENTAL PRESS

+ REQUESTED PRESS

It should be mentioned that the original damping values were 2.0  $\mu\text{F}$  for the capacitance of the RC filter, 1.0 Megohms for the potentiometer, and 0.0 ml of air in the balloon line.

## **EEG MEASUREMENT**

EEG measurement in the animal is possible because electrodes are already implanted for hydrogen monitoring. Electrical activity is monitored between two electrodes. Because eight electrodes are implanted into the cerebrum, four different measurements of EEG can be made. The criterion for choosing the anatomical pairs between which electrical activity is to be monitored was distance. From the stereotaxic locations, the hippocampus-cortex and thalamus-substantia nigra distances are 3.6 mm. Any other pairing combination would yield a greater separation distance. Thus, the deeper nuclei and the more superficial nuclei are grouped together. This electrode grouping was chosen prior to the initiation of the experiments. Experimental results show (see Results section) that the pairing was justified as cortical-hippocampal flows are quite similar just as the flows for the thalamic-substantia nigral areas are quite similar.

The difference in electrical activity between each anatomical pair is fed into a Grass Wide Band A.C. EEG Pre-Amplifier. The output of the pre-amps are fed into the Grass D.C. Driver Amplifiers for further amplification. The driver amplifiers also clip the signal at 15 Hz to half strength before feeding the active EEG filter circuitry.

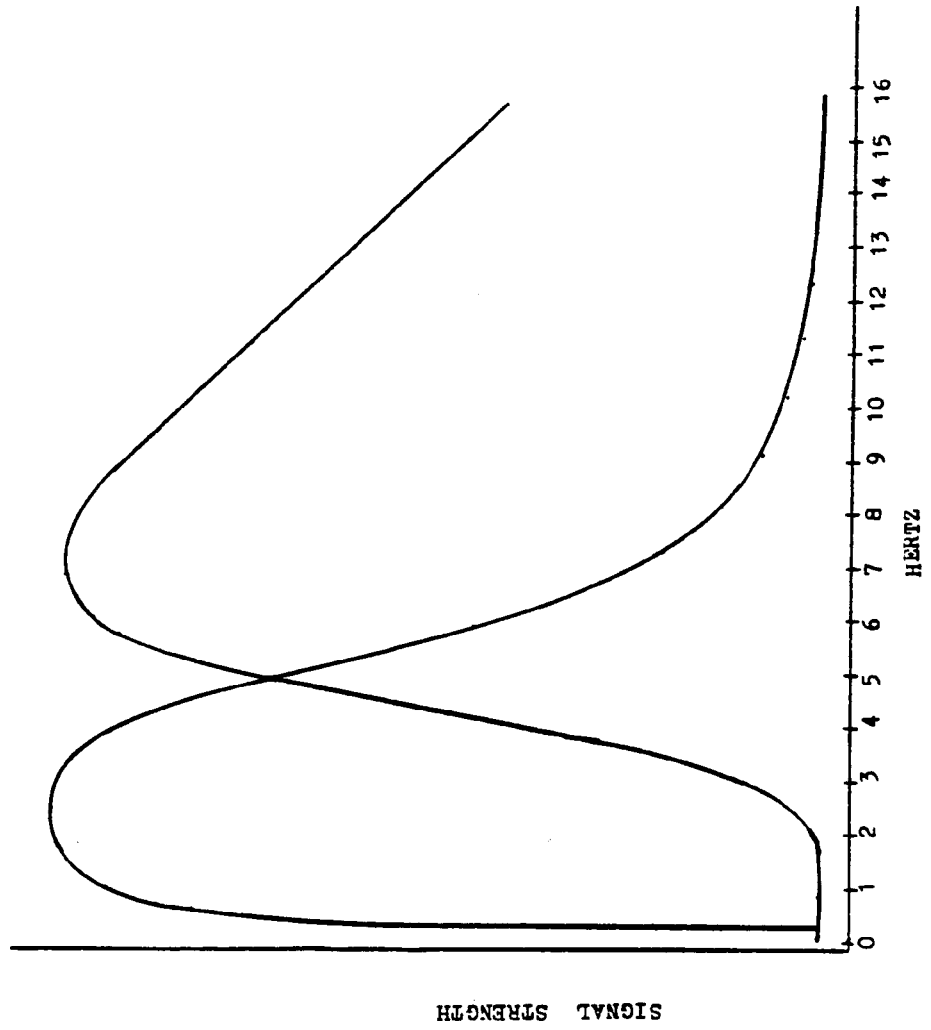
The electrical activity between each anatomical pair is broken down into fast and slow components in the active EEG filter. The frequency

response curve for the active EEG filter is shown in Figure 7-1. The low pass filter quantitates the signal component between frequencies of 0.3 to 5.6 Hz while the high pass filter processes the signal between 4.4 and 15 Hz. The high pass filter is limited to 15 Hz because of the signal clipping by the Grass Driver Amplifier. The maximum sensitivity for the high and low pass filters correspond to 7 Hz and 2 Hz, respectively. Thus, fast EEG refers to the output signal whose sensitivity is maximum at 7 Hz while slow EEG refers to the output signal whose sensitivity is maximum at 2 Hz.

The incoming signal to the EEG filter circuit must be periodically switched from the different driver amplifiers because there is only one active EEG filter circuit for four different anatomical pairs. The switching is under computer control via the ERB-24 as detailed for the hydrogen solenoid valve discussed in the Hydrogen Clearance Method section. The computer program provides the operator a means to 1) set the time over which the fast and slow EEG signal is to be averaged before switching to the next anatomical pair and 2) set the delay time between switching and the commencement of the actual signal averaging. A delay time must be incorporated to minimize signal artifacts due to the perturbation caused by the actual switching itself and to allow the active filter circuitry to clear the fast and slow signals from the previous anatomical pair. Currently, the delay time is approximately 30 seconds followed by a 35 second averaging period for both fast and slow EEG activity. Thus, this arrangement enables periodic monitoring of fast and slow EEG between four different anatomical pairs of electrodes.

**FIGURE 7-1**  
**FREQUENCY RESPONSE CURVES FOR THE ACTIVE EEG FILTER**

The active EEG filter circuitry breaks down the electrical activity between each anatomical pair into fast and slow components. The low and high pass filters quantitate the incoming wide band signal into two signals whose maximum sensitivities are 7 Hz and 2 Hz. The fast EEG activity corresponds to the 7 Hz signal and the slow EEG activity corresponds to the 2 Hz signal.



## **EXPERIMENTAL PROTOCOL**

The animals are commercially obtained male Sprague Dawley rats weighing between 220 and 400 grams and maintained on a standard laboratory diet (Purina Lab Chow). Food and water are provided ad libitum up until the study is performed.

### **Animal Preparation # 1 (electrode implantation)**

The Sprague Dawley rats are placed under general anesthesia (70% N<sub>2</sub>O, 30% O<sub>2</sub>, and 1% Halothane). Normothermia is maintained with a thermistor-driven negative feedback device. Following a dorsal sagittal incision, blunt dissection is performed to expose the cranial vault. One craniectomy (approximately 2 X 3 mm), is performed 1 mm from each side of the sagittal suture and 2 mm dorsal to the bregma (a total of two per animal). This is done with a high speed dental drill, taking care not to traumatize the dural surface of the brain. Two arrays containing four platinum electrodes each are stereotactically placed into the right and left hemispheres, such that the electrodes are placed in the cortex, hippocampus, thalamus, and substantia nigra bilaterally (Hudetz et al., 1985a). Dental acrylic cement is molded around the electrode holders forming in effect a methacrylate skull-cap (see Figure 8-1). Edges of the bony defects are also covered. The animals are then placed in their home-box for at least 24 hours allowing for recovery.

### **Animal Preparation # 2 (surgical preparation)**

**FIGURE 8-1****BILATERAL ELECTRODE ARRAY IMPLANT**

Two electrode arrays consisting of four platinum electrodes each are implanted bilaterally into the cerebrum of a rat. Implantation is performed stereotactically to provide CBF measurements at four different anatomical locations, bilaterally. This procedure takes approximately 35 minutes to perform.



Before the surgical preparation is started, a neurologic exam is performed on each animal to determine if the electrode implant procedure caused some gross damage in the cerebrum. If the animal appears to be grossly affected, then it is excluded from the study.

The animals are placed under general anesthesia (70% N<sub>2</sub>O, 29% O<sub>2</sub>, and 1% Halothane) and normothermia is maintained with a thermistor-driven negative feedback device. A midline incision is made from approximately 5 mm inferior to the mental protuberance of the mandible to the inferior level of the xyphoid process. The skin flaps are retracted back and the parotid, mandibular, and greater sublingual glands are removed via bipolar cautery taking care not to ligate the jugular vein. After resecting the muscles sternohyoideus, omohyoideus, and stylohyoideus, a tracheostomy is performed and the animal is ventilated by a small animal respirator (Harvard 683). An incision is made through the left portion of the muscles pectoralis superficialis, and pectoralis profundus at their partial origins at the manubrium, and sternebrae and the second sternebrae and xiphisternum, respectively. The first five ribs are detached from the left side of the sternum using sharp scissor dissection, taking care not to sever the left internal thoracic artery or vein. The left side of the thoracic cavity is approached because of easier accessibility to the left subclavian artery. After the thoracic cavity is exposed, the thymus is retracted such that three of the four major vessels (innominate, right and left common carotid arteries) of the aortic arch are exposed. The left superior vena cava is retracted in order to adequately expose the left subclavian artery. Bilateral subclavian artery ligation using micro-clipping devices is performed just prior to the initiation of partial occlusion of the left common carotid artery. The carotid arteries are isolated from the vagus nerves and internal jugular veins that accompany them. After

ligation of the right external carotid artery, two cannulas are inserted into the right common carotid artery, one anterograde for measurement of Circle of Willis pressure (CBP) and one retrograde for measurement of systemic blood pressure (SBP). A plastic cylinder and deflated balloon is placed around the left common carotid artery. Partial resection of the muscle sternomastoideus may also be necessary for balloon and cuff placement. The balloon is connected to the servo-syringe as described previously. The right jugular vein is cannulated for venous pressure monitoring. The cannulas for CBP, SBP, and VP are connected to their respective pressure transducers. The right femoral artery is cannulated for arterial blood gas determination and infusion delivery as needed.

#### Pre-experimental Setup

All animals are allowed to stabilize for at least 60 minutes after the surgery. During this time, the pressure transducers, EEG, and the hydrogen electrodes are zeroed and these values are input into the computer. Arterial blood gasses are determined. The animal's  $p_a\text{CO}_2$ ,  $p_a\text{O}_2$ , and pH are maintained within normal limits. If necessary, sodium bicarbonate is administered via the femoral artery to adjust pH, the ventilatory rate is changed to adjust  $p_a\text{CO}_2$ , and  $\%O_2$  is changed to adjust  $p_a\text{O}_2$ . At the end of the experiment, the animal's hematocrit is determined.

#### Specific Experimental Protocol

The experimental aims are to (1) show the model's versatility in reaching and maintaining different ischemic pressure levels, (2) to determine the hemodynamic and EEG characteristics at different anatomical locations with respect to time at different perfusion pressure levels, and (3) to evaluate hemispheric differences in flow or EEG.

Following the implantation and surgical preparation (described above), control flows are obtained while continuously monitoring CBP, VP, balloon pressure, perfusion pressure, and SBP. When resaturation is complete following the last control flow, the subclavian arteries are clipped using a microclipping device and the perfusion pressure is lowered to the desired level (12 mmHg or 7 mmHg) by balloon compression and maintained constant throughout the entire experiment. CBF and EEG information is then obtained from the different electrode sites.

## RESULTS

A total of 16 animals were studied. Two groups of seven animals were studied at perfusion pressures of 12 mmHg and 7 mmHg, and two animals were studied at 9 mmHg. Pre-ischemic measurements of blood gasses and pre-ischemic pressure data are given in Tables 9-1 and 9-2, respectively. The pH, pCO<sub>2</sub>, and pO<sub>2</sub> were obtained before the initiation of the partial occlusion while the hematocrit was determined just before the termination of the experiment. The pressure data in Table 9-2 is the average value during the 60 minute period preceding bilateral subclavian occlusion and partial occlusion of the left common carotid artery by balloon compression. No significant differences existed in pre-ischemic pH, pCO<sub>2</sub>, pO<sub>2</sub>, or hematocrit between the animals or animal groups. The pre-ischemic pressures for the 7 mmHg series are somewhat higher than the 12 mmHg series. This is probably due to the surgeon's increased proficiency in the surgical preparation resulting in shorter preparation times. The average CBF's for all anatomical locations during the 60 minute pre-ischemic period are presented in Table 9-3. Significant hemispheric differences exist in CBF for the thalamus and substantia nigra while the pre-occlusive CBF's for the cortex and hippocampus are essentially the same bilaterally. Even with these differences, it can be assumed that all animals in this study were healthy and had similar physiologic parameters at the beginning of the experiments.

TABLE 9-1

## BLOOD GASSES AND HEMATOCRIT FOR ALL ANIMALS IN THE STUDY

Animal Number	pH	pCO <sub>2</sub>	pO <sub>2</sub>	Hct
<i>Perfusion Pressure = 12 mmHg</i>				
624	7.52	35.0	127	48
626	7.39	36.5	200	48
625	7.31	38.0	150	47
628	7.44	36.4	187	47
629	7.31	40.4	193	48
631	7.35	35.5	144	51
633	7.39	35.6	167	49
Average	7.39	36.8	167	48
<i>Perfusion Pressure = 9 mmHg</i>				
634	7.47	35.3	154	41
646	7.39	38.0	112	50
Average	7.43	36.7	133	46
<i>Perfusion Pressure = 7 mmHg</i>				
636	7.38	34.3	183	52
637	7.41	38.0	172	47
639	7.42	38.8	183	50
640	7.41	37.8	177	49
641	7.40	40.0	120	47
642	7.48	37.0	205	48
643	7.37	38.5	201	50
Average	7.41	37.8	177	49
<i>Overall</i> Average	7.40	37.2	167	48

There is no significance between any group's pH, pCO<sub>2</sub>, pO<sub>2</sub>, or Hct or between any group's pH, pCO<sub>2</sub>, pO<sub>2</sub>, or Hct and the normal range.

TABLE 9-2  
PRE-ISCHEMIC PRESSURES

Animal Number	SBP	CBP	VP	PP
<i>Perfusion Pressure = 12 mmHg</i>				
624	92.1	53.8	9.7	44.2
626	82.0	44.4	10.6	33.8
625	97.6	55.2	6.9	48.3
628	90.9	39.3	6.2	33.1
629	79.8	52.9	11.7	41.2
631	97.2	63.9	7.2	56.8
633	92.6	56.8	14.9	41.2
<b>Average</b>	<b>92.1</b>	<b>53.8</b>	<b>9.7</b>	<b>44.2</b>
<i>Perfusion Pressure = 9 mmHg</i>				
634	88.1	61.3	6.0	55.3
646	104.2	59.1	7.0	52.1
<b>Average</b>	<b>97.7</b>	<b>60.0</b>	<b>6.5</b>	<b>53.4</b>
<i>Perfusion Pressure = 7 mmHg</i>				
636	108.3	59.7	6.6	53.1
637	94.8	49.1	6.8	42.3
639	91.7	56.9	10.0	47.0
640	110.7	61.1	9.1	52.0
641	106.8	53.0	8.4	44.6
642	87.2	41.2	8.8	32.4
643	104.4	58.3	5.7	52.5
<b>Average</b>	<b>100.5</b>	<b>54.5</b>	<b>7.9</b>	<b>46.6</b>
<b>Overall Average</b>	<b>96.8</b>	<b>56.1</b>	<b>8.1</b>	<b>48.1</b>

TABLE 9-3  
PRE-ISCHEMIC CBF LEVELS

Location	CBF (ml/100g/min)	
	Right Hemisphere	Left Hemisphere
Hippocampus	51.8 ± 16.5	58.1 ± 14.0
Thalamus	45.6 ± 12.1	70.3 ± 19.5
Substantia Nigra	59.6 ± 14.3	74.9 ± 15.9
Cortex	63.2 ± 20.1	69.4 ± 21.9

Figure 9-1 illustrates an atypical perfusion control experiment. The wide range of balloon pressures necessary to maintain the perfusion pressure at the desired level of 10 mmHg is clearly demonstrated in this pilot experiment. Unlike the animals within this study, SD622's systemic arterial blood pressure response to the reduction in perfusion pressure was highly irregular and the cause for this irregularity is unknown. However, this experiment demonstrates the relatively rapid response time of the servo-control system and the ability of this system to maintain perfusion pressure at a precisely controlled level despite wide fluctuations in systemic arterial pressure.

Figures 9-2 and 9-3 illustrate the system's ability to obtain and maintain desired perfusion pressures. Maintenance of perfusion pressure for 300 minutes or longer was not uncommon for the 12 mmHg series. The experimental time course for the 7 mmHg and 9 mmHg groups was limited to approximately 95 minutes to ensure that the animals survived the reperfusion period required to confirm hydrogen baselines. The standard deviation in the perfusion pressure for the 12 mmHg group is larger than for the 7 mmHg group because the original pressure transducers, which were replaced during the 12 mmHg series, exhibited a significant amount of drift throughout the

## FIGURE 9-1

## PERFUSION CONTROL EXPERIMENT

In this pilot experiment, the system was controlling to a desired perfusion pressure of 10 mmHg. Despite wide fluctuations in the animal's systemic arterial blood pressure, the servo-control system maintained the actual perfusion pressure at  $9.8 \pm 0.6$  mmHg throughout the experiment by changing the balloon pressure as shown in the illustration. The cause for the wide fluctuations in systemic arterial blood pressure after partial occlusion is unknown.

# PERFUSION PRESSURE CONTROL SD622

(EXP= 9.8 +/- .6 mmHg    REQ= 10 mmHg)

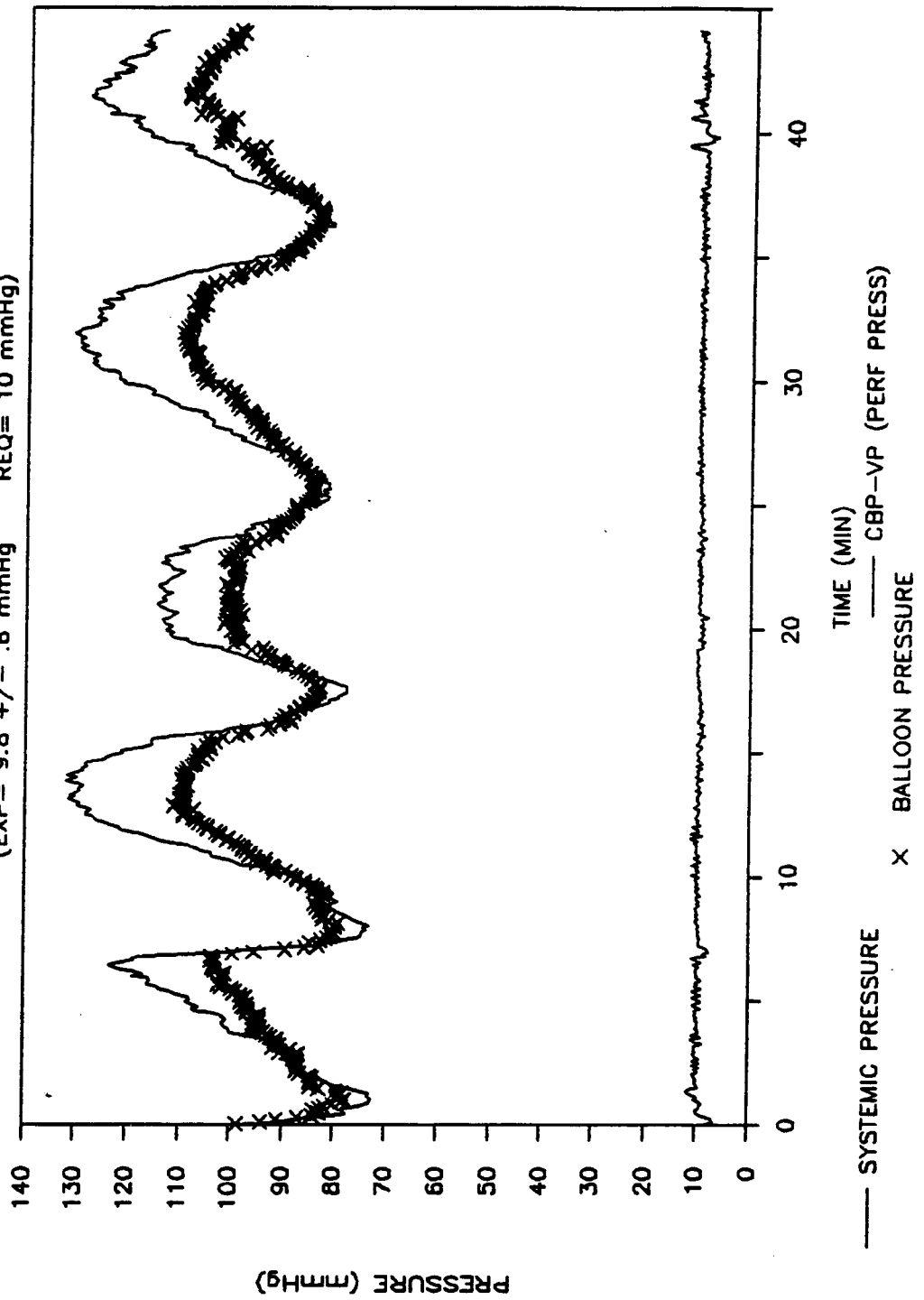


## FIGURE 9-2

## CONTROL OF PERFUSION PRESSURE AT 12 mmHg AND 7 mmHg

Perfusion pressure is plotted as a function of time for the 12 mmHg and 7 mmHg animal series. Partial occlusion of the left common carotid artery by the balloon was initiated at time zero. The mean control pressure with standard deviation for the seven animals in each group is provided on the illustration. The standard deviations are due to the baseline drift in the pressure transducers and the Grass Polygraph recorder and the servo error (see text). The standard deviation for the 7 mmHg group is much lower than for the 12 mmHg group because during the conduct of the 12 mmHg series the original pressure transducers were replaced with newer ones that exhibited a much smaller drift.

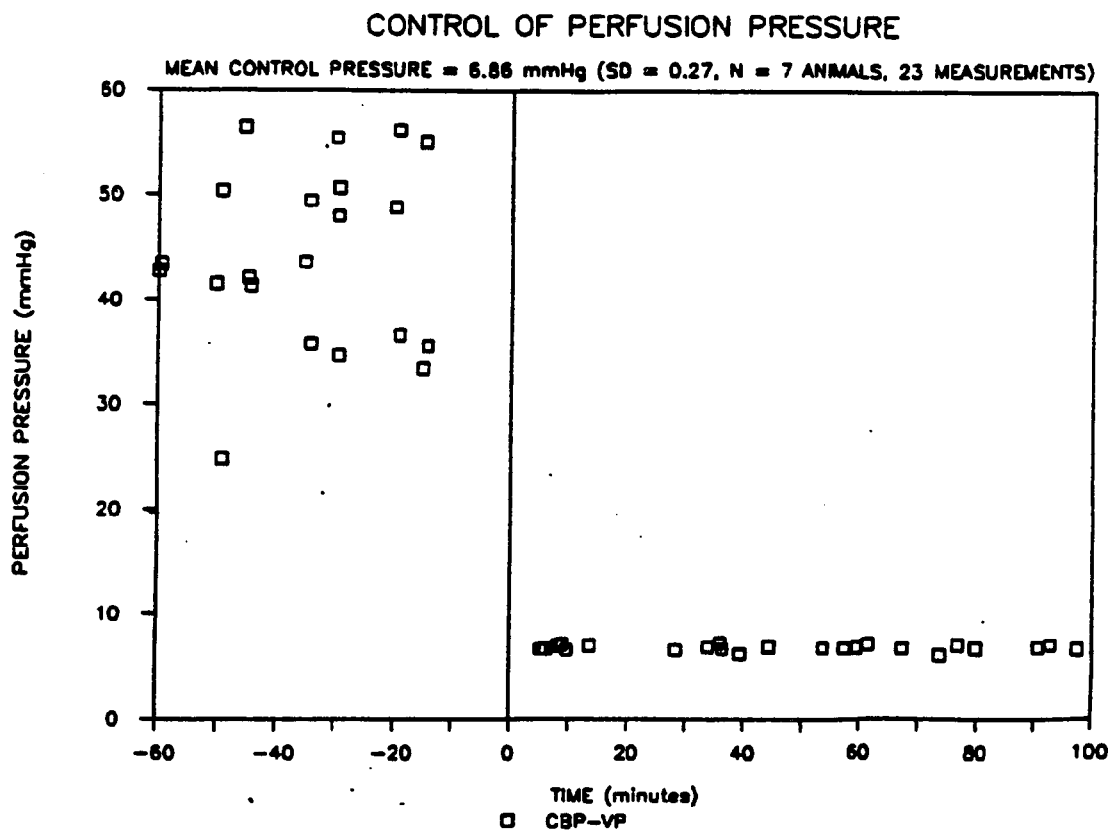
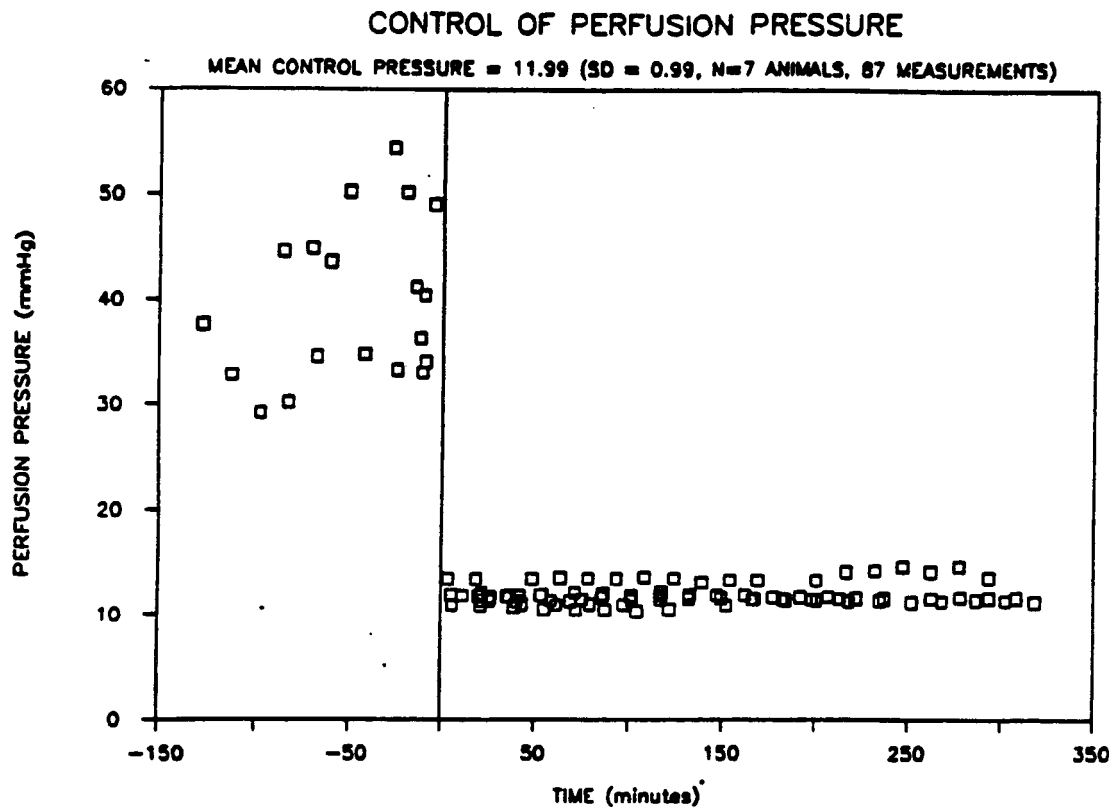
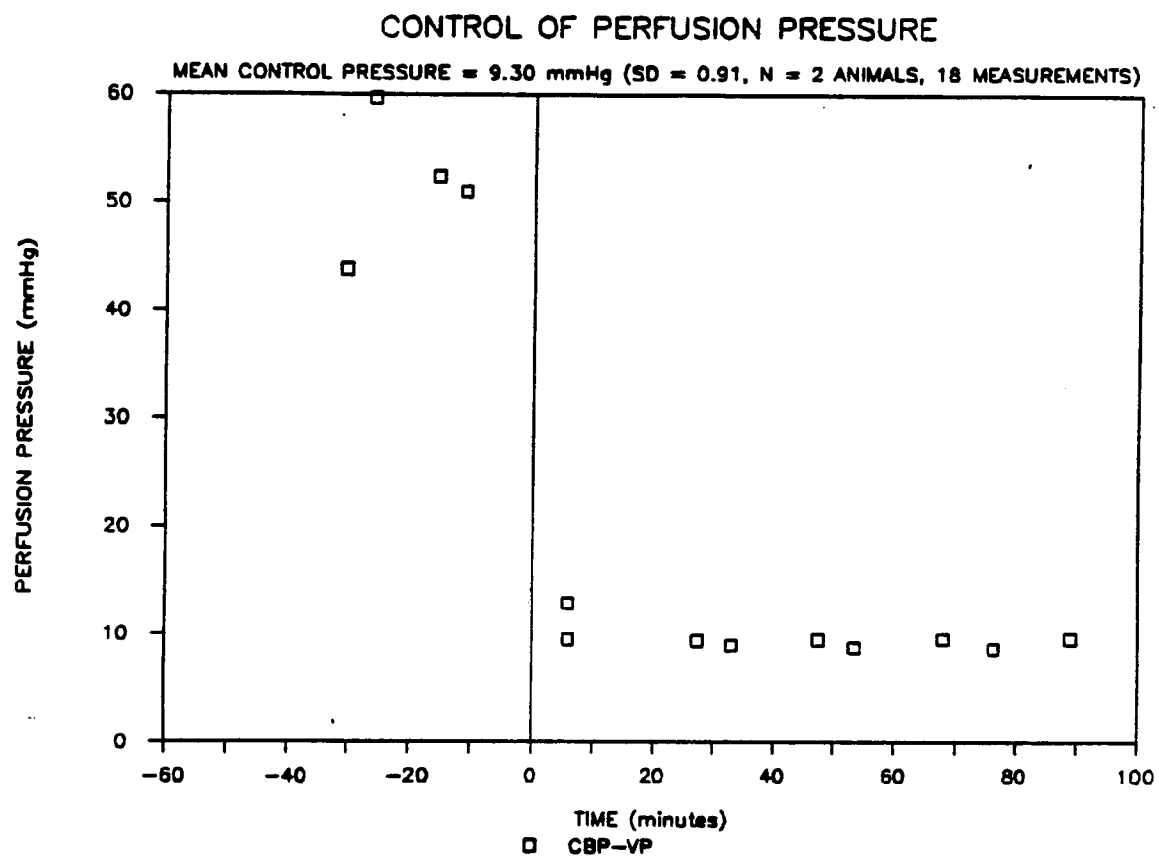


**FIGURE 9-3****CONTROL OF PERFUSION PRESSURE AT 9 mmHg**

Perfusion pressure is plotted as a function of time for the 9 mmHg animal series. Partial occlusion of the left common carotid artery by the balloon was initiated at time zero. The mean control pressure with standard deviation for the two animals in this group is provided on the illustration.



course of an individual experiment. Thus, the standard deviation of 0.27 mmHg for the 7 mmHg group more accurately reflects the current system's ability in maintaining perfusion pressure. The servo system reproducibility is approximately 0.5 mmHg on either side of the desired pressure level. These errors are not readily seen because the perfusion pressures corresponding to the CBF measurements are actually averaged values over the period that the hydrogen washout phase was occurring.

Table 9-4 depicts the average ischemic pressure levels during the partial occlusion period for all three groups of animals. Also shown is the average ratio of balloon pressure to SBP necessary to maintain perfusion pressure during the partial occlusion period. The ratios are significant ( $p < 0.001$ ) between pressure groups.

Each individual experiment yielded CBF and EEG activity (both fast and slow) as a function of time for each anatomical location. Figure 9-4 represents a compendium of the CBF versus time histories for the right and left substantia nigra for the combined 12 mmHg and 7 mmHg groups. Fast EEG activity as a function of time within the right and left thalamic-substantia nigral areas for the 12 mmHg and 7 mmHg series is presented in Figure 9-5. The initiation of partial compression of the left common carotid artery by the balloon occurs at time zero. Similar illustrations are found in Appendix D showing CBF, fast EEG activity, and slow EEG activity as a function of time for each anatomical location at each perfusion pressure.

The mean ischemic CBF's for each pressure group and anatomical location are presented in Table 9-5 and Figure 9-6. Table 9-5 clearly shows that as the perfusion pressure is lowered from 12 mmHg to 9 mmHg to 7 mmHg, CBF decreases within the same anatomical location. Figure 9-6 illustrates in all cases but one (cortex at 12 mmHg perfusion pressure), that

TABLE 9-4  
ISCHEMIC PRESSURES

Animal Number	BAL/SBP	SBP	CBP	VP	PP
<i>Perfusion Pressure = 12 mmHg</i>					
624	1.20	60.9	19.7	8.1	11.5
626	0.97	121.8	16.1	5.4	10.7
625	1.17	92.8	18.2	6.4	11.8
628	1.20	97.6	16.4	4.9	11.5
629	1.18	96.5	18.3	6.6	11.7
631	1.11	87.6	16.7	5.6	11.1
633	1.41	103.8	20.3	6.6	13.7
Average	1.21	92.2	18.6	6.6	12.0
<i>Perfusion Pressure = 9 mmHg</i>					
634	1.78	56.6	13.8	4.4	8.8
646	1.30	115.5	15.6	6.0	9.5
Average	1.58	81.4	14.6	5.3	9.3
<i>Perfusion Pressure = 7 mmHg</i>					
636	1.48	61.2	10.3	3.5	6.8
637	1.78	61.7	12.0	5.6	6.3
639	1.29	82.7	13.3	6.5	6.8
640	2.14	49.2	11.6	4.6	7.0
641	2.24	47.1	11.7	4.8	7.0
642	1.74	68.1	11.7	4.9	6.8
643	1.81	56.3	11.1	3.9	7.2
Average	1.79	61.3	11.8	4.9	6.9

## FIGURE 9-4

BILATERAL SUBSTANTIA NIGRAL CBF  
AT 12 mmHg AND 7 mmHg PERFUSION PRESSURE

This figure is shown here to provide the reader a better understanding of where the information contained within future combined CBF illustrations came from. Similar illustrations for each anatomical location are presented in Appendix D.

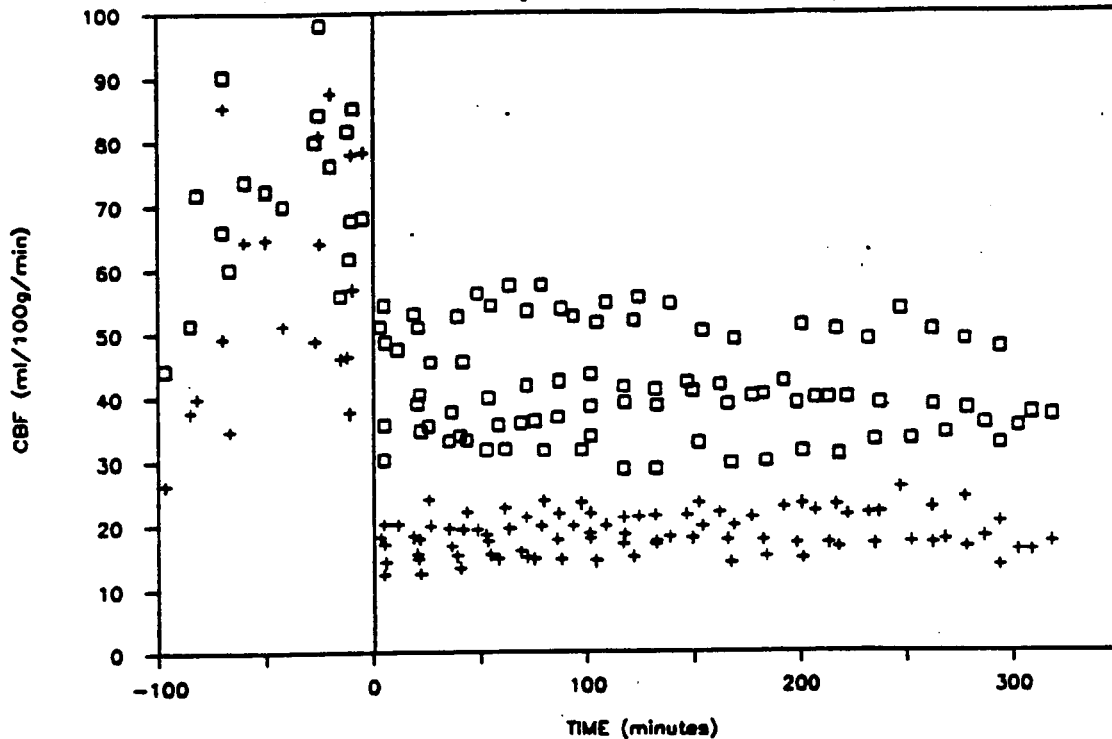
Cerebral blood flow is plotted as a function of time for both the right and left substantia nigra at perfusion pressures of 12 mmHg and 7 mmHg. Time zero is the time at which partial occlusion of the left common carotid artery by the balloon was initiated. Before partial occlusion, both the right and left substantia nigra in both series of animals had CBF's that were not significantly different from each another.

Figure 9-4a. At 12 mmHg perfusion pressure, the average CBF in the left substantia nigra ( $41.7 \pm 8.2$  ml/100g/min) is significantly higher than the average CBF in the right substantia nigra ( $18.5 \pm 3.1$  ml/100g/min ( $p < 0.001$ )).

Figure 9-4b. At 7 mmHg perfusion pressure, the left substantia nigral CBF is again significantly higher ( $p < 0.001$ ) with an average flow of  $17.1 \pm 6.0$  ml/100g/min as compared to  $4.5 \pm 2.6$  ml/100g/min for the right. Note that these values are one half to one third the values reported for 12 mmHg and that the flows decrease as a function of time after partial occlusion.

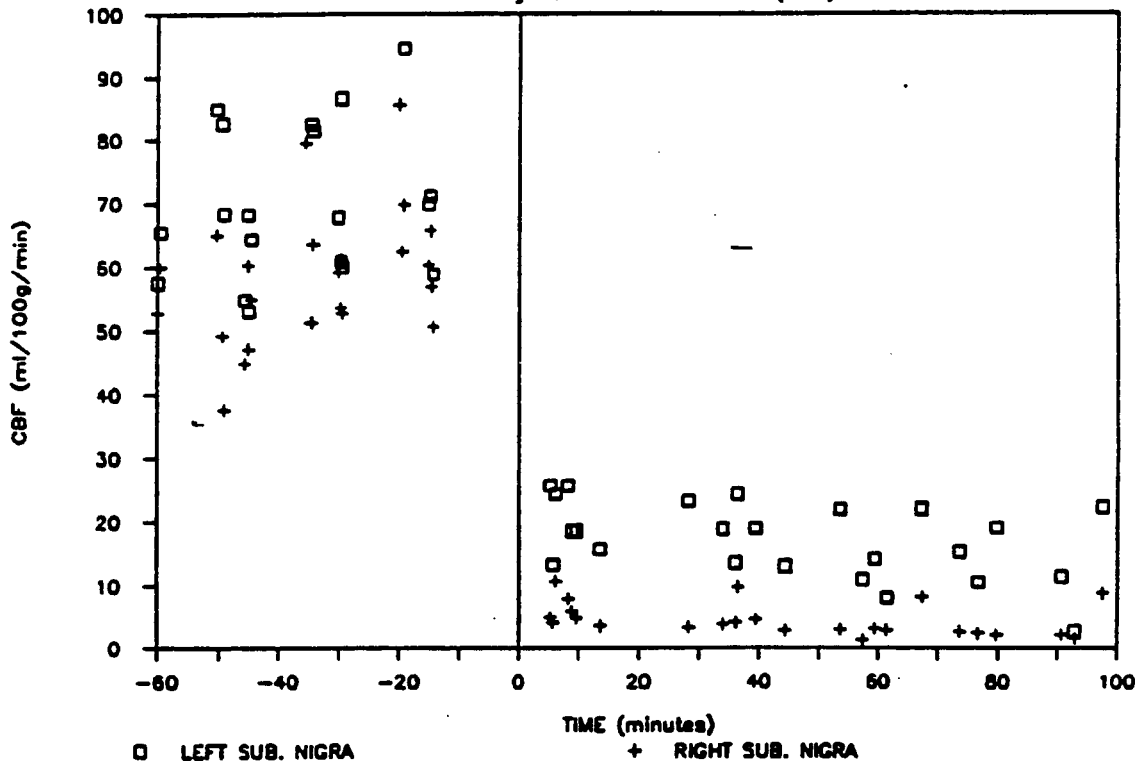
**SUBSTANTIA NIGRAL CBF**

12mmHg PERFUSION PRESSURE (N=7)



**SUBSTANTIA NIGRAL CBF**

7mmHg PERFUSION PRESSURE (N=7)



□ LEFT SUB. NIGRA

+ RIGHT SUB. NIGRA

## FIGURE 9-5

**BILATERAL THALAMIC-SUBSTANTIA NIGRAL FAST EEG  
AT 12 mmHg AND 7 mmHg PERFUSION PRESSURE**

This figure is shown here to provide the reader a better understanding of where the information contained within combined EEG illustrations came from. Similar illustrations for each anatomical location are presented in Appendix D.

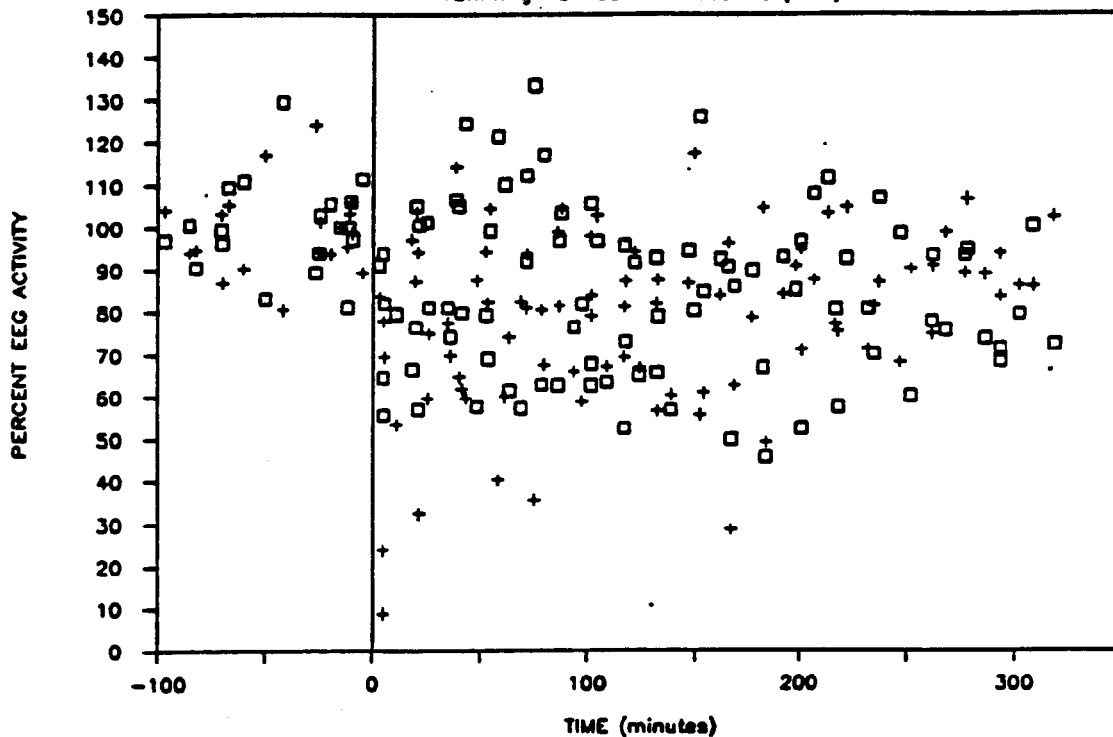
Percent fast EEG activity is plotted as a function of time for both the right and left thalamic-substantia nigral areas at perfusion pressures of 12 mmHg and 7 mmHg. Time zero is the time at which partial occlusion of the left common carotid artery by the balloon was initiated. The average activity in both the right and left thalamic-substantia nigral areas before partial occlusion represents the control value or 100% activity. All of the individual points throughout the experiment are then computed as a percentage of the control value.

Figure 9-5a. At 12 mmHg perfusion pressure, the average CBF in the left thalamus and substantia nigra is  $36.3 \pm 9.2$  ml/100g/min and  $41.7 \pm 8.2$  ml/100g/min, respectively. The relative EEG activity measured between the left thalamus and substantia nigra is  $83.8 \pm \pm 19.4\%$ . The average CBF in the right thalamus and substantia nigra is  $13.7 \pm \pm 8.7$  ml/100g/min and  $18.5 \pm 3.1$  ml/100g/min, respectively, and the relative EEG activity is  $78.6 \pm 20.4\%$  which is not significantly different than that reported on the contralateral side. Thus, a 22 ml/100g/min drop in flow in both the thalamus and substantia nigra did not result in a significant reduction in EEG activity.

Figure 9-5b. At 7 mmHg perfusion pressure, the average CBF in the left thalamus and substantia nigra is  $14.4 \pm 4.0$  ml/100g/min and  $17.1 \pm 6.0$  ml/100g/min, respectively. The relative EEG activity measured between the left thalamus and substantia nigra is  $63.6 \pm 43.8\%$ . The average CBF in the right thalamus and substantia nigra is  $2.3 \pm 1.4$  ml/100g/min and  $4.5 \pm 2.6$  ml/100g/min, respectively, and the relative EEG activity is  $36.1 \pm 38.0\%$  which is not significantly different than that reported on the contralateral side.

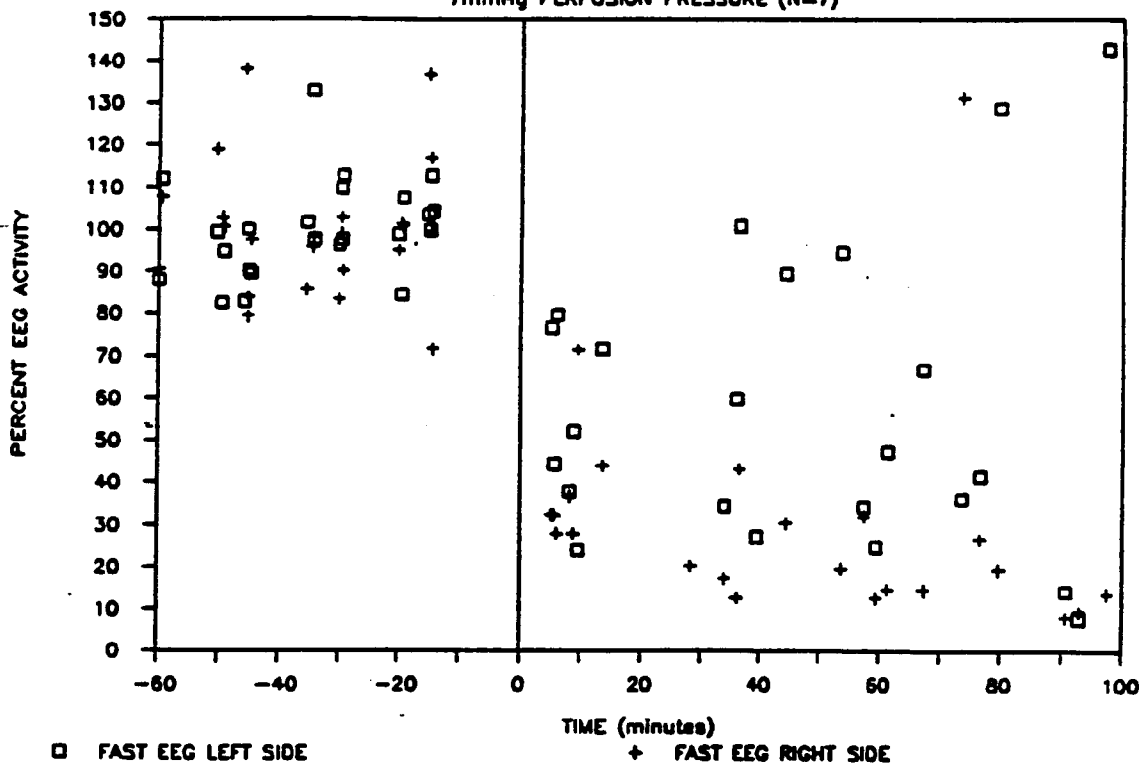
THALAMIC-SUBSTANTIA NIGRAL FAST EEG

12mmHg PERFUSION PRESSURE (N=7)



THALAMIC-SUBSTANTIA NIGRAL FAST EEG

7mmHg PERFUSION PRESSURE (N=7)



□ FAST EEG LEFT SIDE

+ FAST EEG RIGHT SIDE

**FIGURE 9-6****CBF COMPARISON BETWEEN RIGHT AND LEFT  
HEMISPHERES FOR ALL ANATOMICAL LOCATIONS  
AND PERFUSION PRESSURES**

The average CBF for each anatomical location at each perfusion pressure is calculated from the combined data found in Appendix D. The CBF's in the right hemispheric structures are significantly lower than the CBF's obtained for the left hemispheric structures in all locations at all perfusion pressures except for the cortical area at 12 mmHg perfusion pressure. \*\*\* =  $p < 0.001$ ; \*\* =  $p < 0.01$ ; \* =  $p < 0.05$ ; ns = not significant.

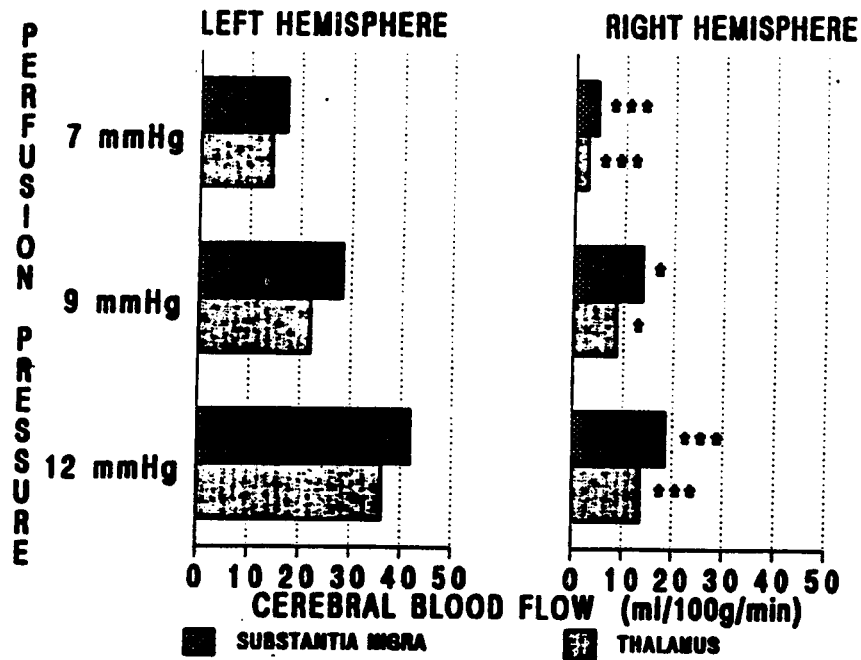
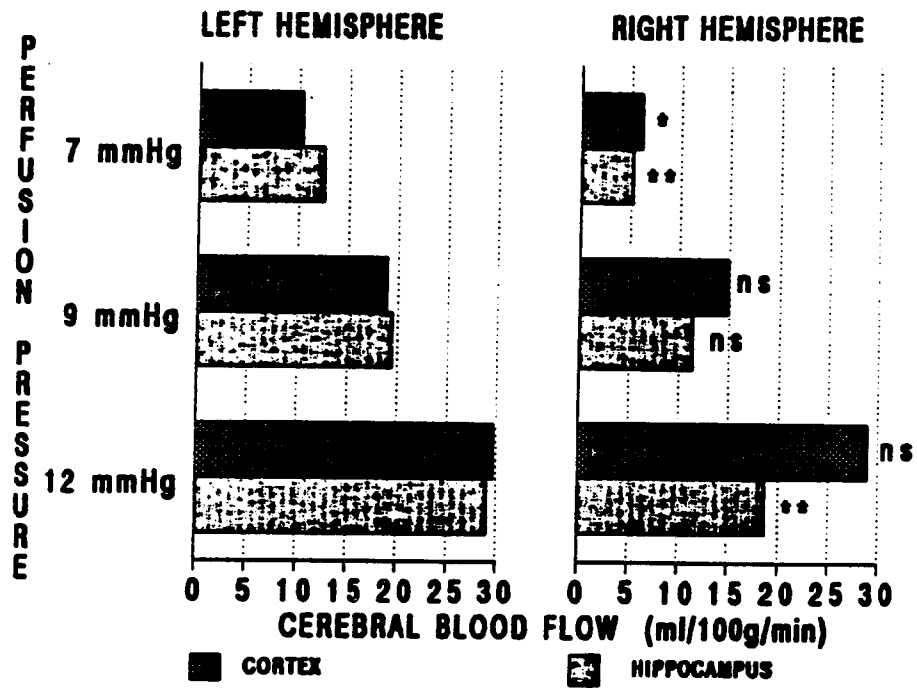


TABLE 9-5  
 AVERAGE CBF AS A FUNCTION OF PERFUSION PRESSURE  
 AND ANATOMICAL LOCATION AFTER  
 PARTIAL OCCLUSION WAS INITIATED

Perfusion Pressure (mmHg)	12 (N = 7)	9 (N = 2)	7 (N = 7)	
	(CBF in ml/100g/min)			
Location				Sig
L. Hippocampus	29.1 ± 6.1	19.5 ± 3.6	12.6 ± 4.0	a,c,f
L. Thalamus	36.3 ± 9.3	22.2 ± 4.9	14.4 ± 4.0	a,c,f
L. Substantia Nigra	41.7 ± 8.2	28.2 ± 5.5	17.1 ± 6.0	a,c,f
L. Cortex	29.8 ± 6.3	18.9 ± 5.5	10.4 ± 4.7	a,c,f
R. Hippocampus	18.7 ± 3.1	11.5 ± 2.2	5.2 ± 2.3	a,b,e
R. Thalamus	13.7 ± 2.9	8.7 ± 1.3	2.7 ± 1.4	a,b,d
R. Substantia Nigra	18.5 ± 3.1	13.8 ± 2.3	4.5 ± 2.6	a,c,e
R. Cortex	29.0 ± 9.1	14.9 ± 4.4	6.2 ± 3.7	a,b,f

a =  $p < 0.001$  for 12mmHg vs. 7mmHg

b =  $p < 0.01$  for 12mmHg vs. 9mmHg

c =  $p < 0.05$  for 12mmHg vs. 9mmHg

d =  $p < 0.001$  for 9 mmHg vs. 7mmHg

e =  $p < 0.01$  for 9 mmHg vs. 7mmHg

f =  $p < 0.05$  for 9 mmHg vs. 7mmHg

All statistics done by student's t-test.

the CBF within the right hemispheric anatomical structures is lower than the CBF within the identical structures on the contralateral side. Thus, the side contralateral to the balloon placement and ipsilateral to the perfusion pressure measurement is the side most severely affected.

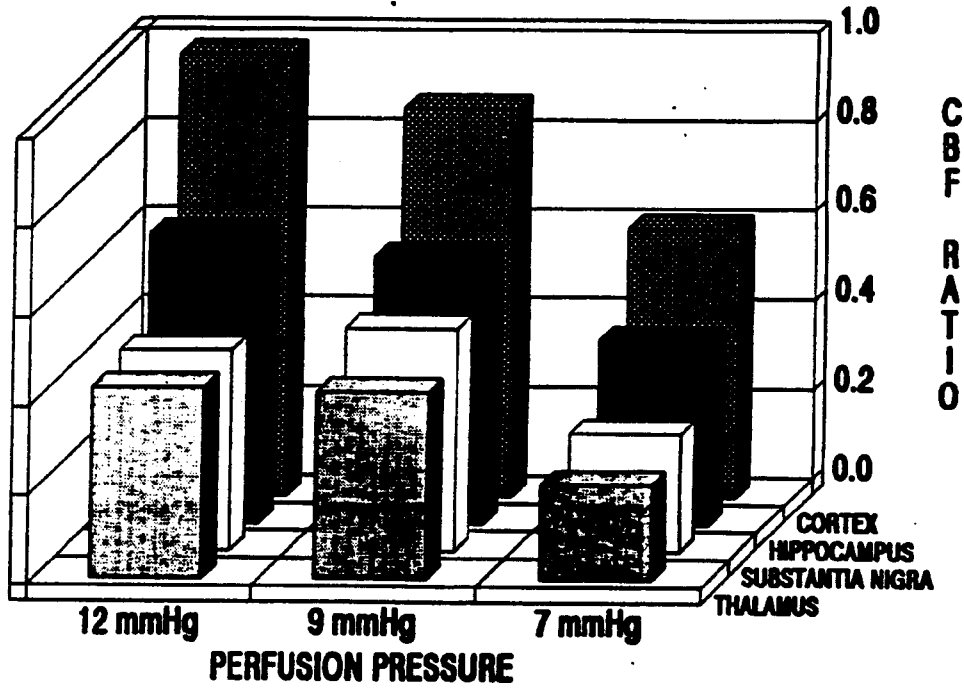
To further elucidate the patterns of CBF differences between right and left hemispheres, a right to left CBF ratio was determined for each anatomical location at each perfusion pressure and is presented in Figure 9-7a. As the perfusion pressure is decreased, the CBF ratio decreases at a given anatomic

**FIGURE 9-7****CBF RATIO FOR EACH ANATOMICAL LOCATION  
AT 12 mmHg, 9 mmHg, AND 7 mmHg PERFUSION PRESSURES**

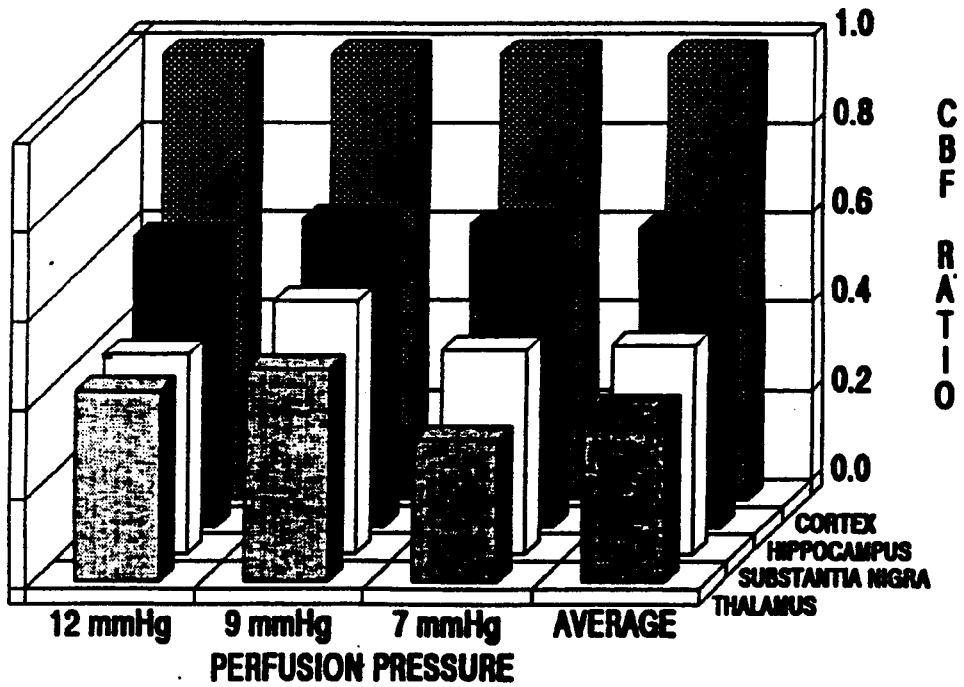
CBF ratio is determined by taking the ratio between the initial right and left hemispheric flows at time zero (time of initiation of partial occlusion) for an anatomical structure at a given perfusion pressure.

Figure 9-7a shows the relationship between CBF ratio and anatomic location as a function of perfusion pressure. Figure 9-7b shows the relationship of CBF ratio for each anatomical location as a function of perfusion pressure when the ratios are normalized to the cortical CBF ratio at a particular perfusion pressure. As expected, the anatomical order in which the CBF ratio decreases is the same as that in Figure 9-7a, but it is remarkable in that the fractional CBF ratios are consistent within the same anatomical location regardless of perfusion pressure. The weighted averages of the normalized CBF ratios are also included for comparison.

### RIGHT/LEFT HEMISPHERIC FLOW RATIOS



### NORMALIZED HEMISPHERIC FLOW RATIOS



location. This is not observed within the substantia nigra between perfusion pressures of 12 mmHg and 9 mmHg. However, there are only two animals in the 9 mmHg group. Comparison of the CBF ratios between 7 mmHg and 12 mmHg groups shows that the CBF ratio decreases by approximately 42% at each anatomical location for a corresponding 42% decrease in perfusion pressure. At each perfusion pressure, the anatomical order in which the CBF ratio decreases is cortex, hippocampus, substantia nigra, and thalamus. Figure 9-7b shows the different anatomical CBF ratios after they are normalized to the cortical CBF ratio for each perfusion pressure.

Unlike the 12 mmHg and 9 mmHg groups, the 7 mmHg group exhibited a decrease in CBF with time after initiation of partial occlusion in all anatomical locations. Figure 9-8a is a sample illustration showing the decrease in CBF with time at three anatomical locations in one animal. Similar regression lines representing the rate of change in CBF with time were obtained for all anatomical locations in all three series of animals. Every line was extrapolated back to time zero and this point represents the initial CBF or the CBF resulting from the partial occlusion at time zero. Figure 9-8b illustrates the relationship of initial CBF versus the rate of change in CBF for all three series of animals determined above. The information in Figure 9-8b is broken down into separate hemispheres in Figure 9-9. The linearity of the right hemispheric 7 mmHg group suggests that regardless of anatomical location, CBF will collapse to zero in  $137 \pm 43$  minutes (SE = 9.2 minutes) in the right hemisphere when the perfusion pressure is lowered to 7 mmHg (see Figure 9-9a). Animal SD639 was not included in the right hemispheric 7 mmHg regression because it was significantly different from the other six animals. SD639's different behavior may have resulted from controlling to a perfusion pressure higher than 7 mmHg due to a possible artifact in venous

**FIGURE 9-8A****RIGHT HEMISPHERIC CBF VERSUS TIME AT 7 mmHg PERFUSION PRESSURE**

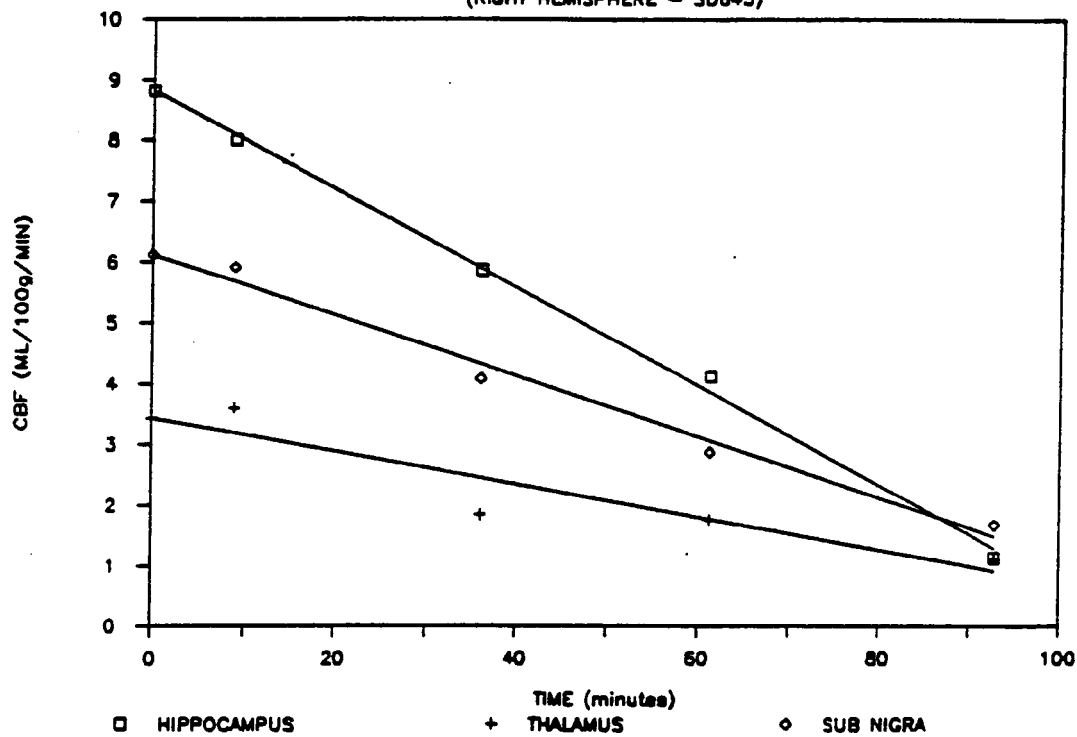
At 7 mmHg perfusion pressure, the CBF for each anatomical location was observed to decrease with time. Regression analysis was performed on each CBF versus time profile for all anatomical locations for all series of animals. This illustration shows a sample of three of these CBF versus time profiles for SD643. The initiation of partial occlusion of the left common carotid artery by the servo-controlled balloon occurs at time zero. Initial CBF values corresponding to time zero were determined by extrapolation. The lines were determined by the method of least squares.

**FIGURE 9-8B****INITIAL CBF VERSUS RATE OF CHANGE IN CBF**

The slopes of the regression lines and their respective initial CBF's determined for all animals above are plotted in Figure 9-8b.

## PLOT OF CBF VS TIME AT 7 mmHg

(RIGHT HEMISPHERE - SD643)



## PLOT OF INITIAL CBF VERSUS RATE OF CHANGE IN CBF

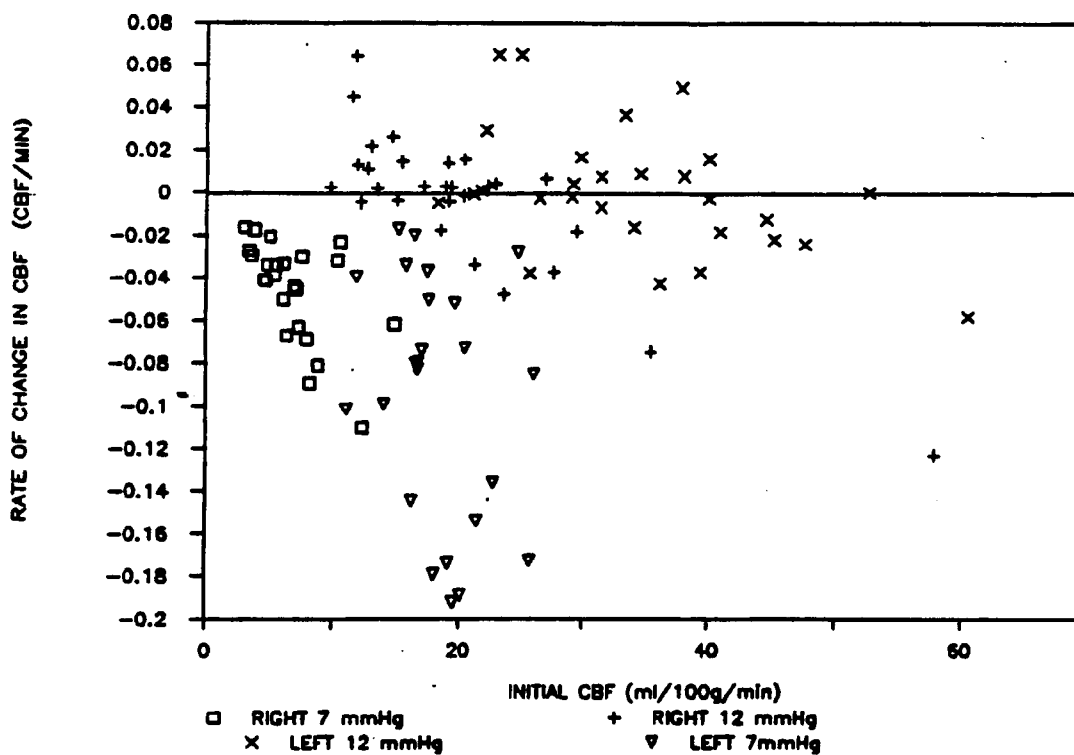
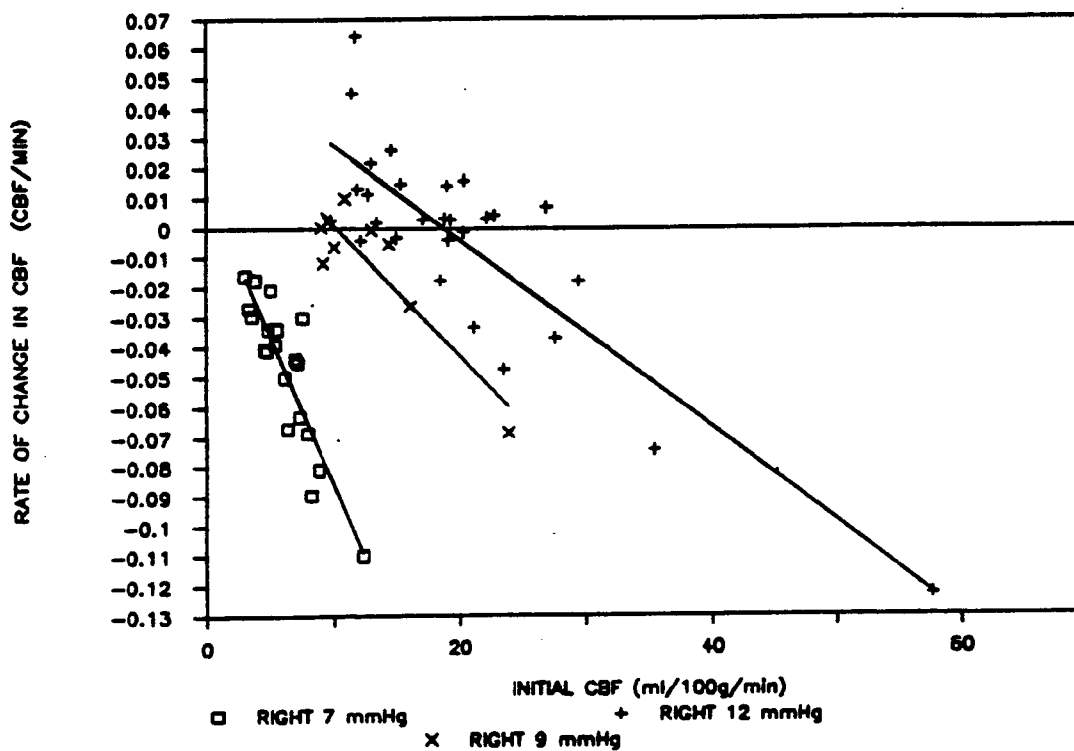


## FIGURE 9-9

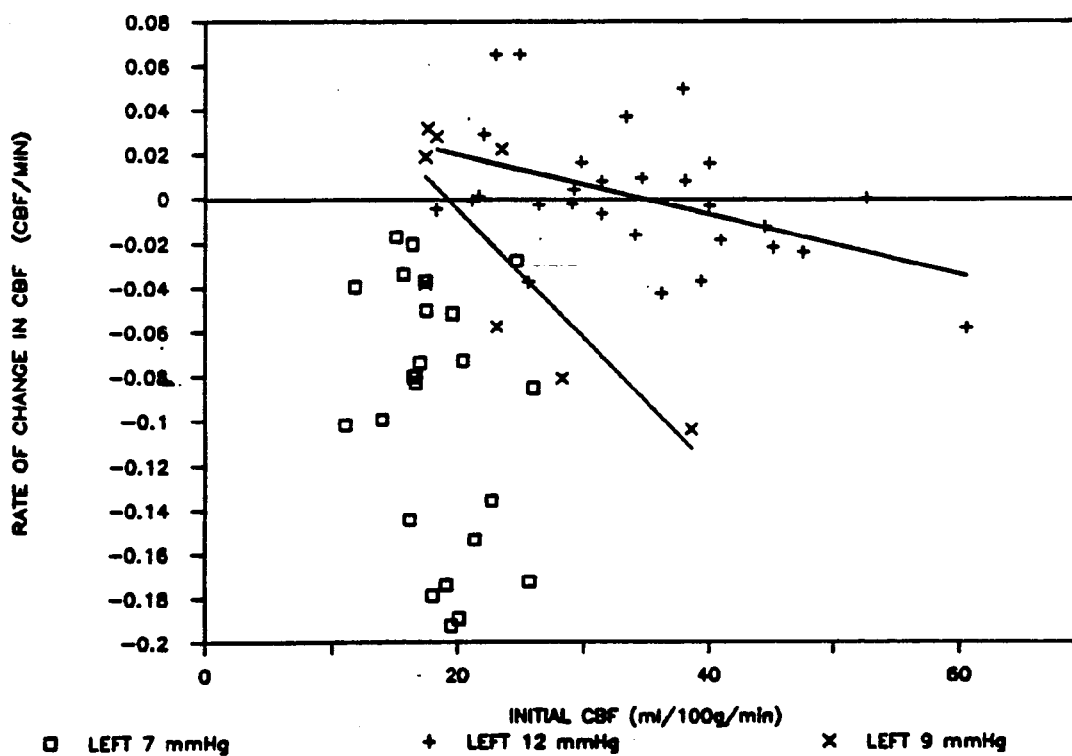
## INITIAL CBF VERSUS RATE OF CHANGE IN CBF

The data presented in Figure 9-8b is separated by hemisphere and illustrated here. Figure 9-9a shows the right hemispheric data and Figure 9-9b show the left hemispheric data. Because all flows collapsed at a perfusion pressure of 7 mmHg, the linearity of the 7 mmHg line suggests that flow will collapse at a constant time point in the right hemisphere. The 12 mmHg and 9 mmHg information shows that areas with higher initial flows exhibited subsequent reduction while the areas with marginal flow exhibited a partial recovery in flow. Unlike the 7 mmHg right hemisphere, the right hemispheres at 12 mmHg and 9 mmHg apparently had enough input of blood to prevent total collapse of the entire hemisphere.

## REGRESSION OF INITIAL CBF VERSUS RATE OF CHANGE IN CBF



## REGRESSION OF INITIAL CBF VERSUS RATE OF CHANGE IN CBF



pressure measurement (see Table 9-4). Right and left hemispheric regressions for the 12 mmHg and 9 mmHg series are also shown in Figure 9-9. At these two perfusion pressures the areas with the higher initial flows exhibit a subsequent reduction in flow while the areas with marginal initial flows exhibit a partial recovery in flow. A regression for the left hemispheric 7 mmHg relationship of initial CBF versus the rate of change in CBF was not presented due to the scatter (see Figure 9-9b) in the data.

The average fast and slow EEG activity was determined and is presented in Table 9-6 and Figure 9-10 as a function of perfusion pressure and anatomical location after partial occlusion was initiated. Right and left hemispheric comparisons of fast and slow EEG activity are presented in Figure 9-10. Fast EEG activity is lower in the right hemisphere in the cortical-hippocampal areas at all perfusion pressures. Slow EEG activity is lower in the right hemisphere only in the thalamic-substantia nigral areas at a 12 mmHg perfusion pressure. However, the standard deviations for the fast and slow EEG activities are large.

The relationship between CBF and EEG activity for all anatomical locations and perfusion pressures is illustrated in Figures 9-11 and 9-12. Figure 9-11 shows the CBF-EEG relationships within the cortical-hippocampal areas while Figure 9-12 shows the EEG-CBF relationship within the thalamic-substantia nigral areas. Lines determined by the method of least squares are drawn between zero CBF and a CBF of approximately 45 ml/100g/min. These lines are in turn intersected with lines representing a 100% EEG activity level. The breakpoint for fast and slow EEG activity within the thalamic-substantia nigral areas occurs at approximately 41 ml/100g/min while the breakpoint for fast and slow EEG activity within the cortical-hippocampal areas occurs between 32 and 38 ml/100g/min. The slopes of these lines are presented in

TABLE 9-6  
 AVERAGE EEG ACTIVITY AS A FUNCTION  
 OF PERFUSION PRESSURE AND ANATOMICAL LOCATION AFTER  
 PARTIAL OCCLUSION WAS INITIATED

Perfusion Pressure (mmHg)	12 (N = 7)	9 (N = 2)	7 (N = 7)	
<i>(Relative Fast EEG Activity in percent)</i>				
Location				Sig
L. Hippocampus/ L. Cortex	96.1 ± 15.6	67.0 ± 10.6	33.0 ± 26.4	a,d,h
L. Thalamus/ L. Substantia Nigra	83.8 ± 19.4	53.6 ± 16.9	63.6 ± 43.8	c,e,i
R. Hippocampus/ R. Cortex	74.7 ± 17.2	28.1 ± 13.9	12.9 ± 9.3	a,d,i
R. Thalamus/ R. Substantia Nigra	7 8.6 ± 20.4	58.2 ± 16.4	36.1 ± 38.0	b,f,i
<i>(Relative Slow EEG Activity in percent)</i>				
L. Hippocampus/ L. Cortex	79.2 ± 25.4	52.4 ± 7.8	19.3 ± 13.7	a,e,g
L. Thalamus/ L. Substantia Nigra	84.0 ± 19.6	43.2 ± 9.3	69.4 ± 57.6	c,d,i
R. Hippocampus/ R. Cortex	70.9 ± 27.0	25.3 ± 11.9	15.5 ± 10.0	a,d,i
R. Thalamus/ R. Substantia Nigra	65.1 ± 15.9	55.5 ± 14.8	37.8 ± 41.2	c,f,i

a =  $p < 0.001$  for 12 mmHg vs 7 mmHg  
 b =  $p < 0.05$  for 12 mmHg vs 7 mmHg  
 c = not significant for 12 mmHg vs 7 mmHg  
 d =  $p < 0.01$  for 12 mmHg vs 9 mmHg  
 e =  $p < 0.05$  for 12 mmHg vs 9 mmHg  
 f = not significant for 12 mmHg vs 9 mmHg  
 g =  $p < 0.01$  for 9 mmHg vs 7 mmHg  
 h =  $p < 0.05$  for 9 mmHg vs 7 mmHg  
 i = not significant for 9 mmHg vs 7 mmHg

All statistics done by student's t-test.

**FIGURE 9-10****PERCENT SLOW AND FAST EEG ACTIVITY  
AS A FUNCTION OF PERFUSION PRESSURE  
AND ANATOMICAL LOCATION FOR EACH HEMISPHERE**

Percent EEG activity is determined by comparing the average pre-ischemic activity to the activity obtained at each measurement after time zero. Figure 9a illustrates the average slow EEG activity in percent for each anatomic location at different perfusion pressure levels while Figure 9b illustrates the average fast activity in percent.

\* =  $p < 0.05$ ; ns = not significant.

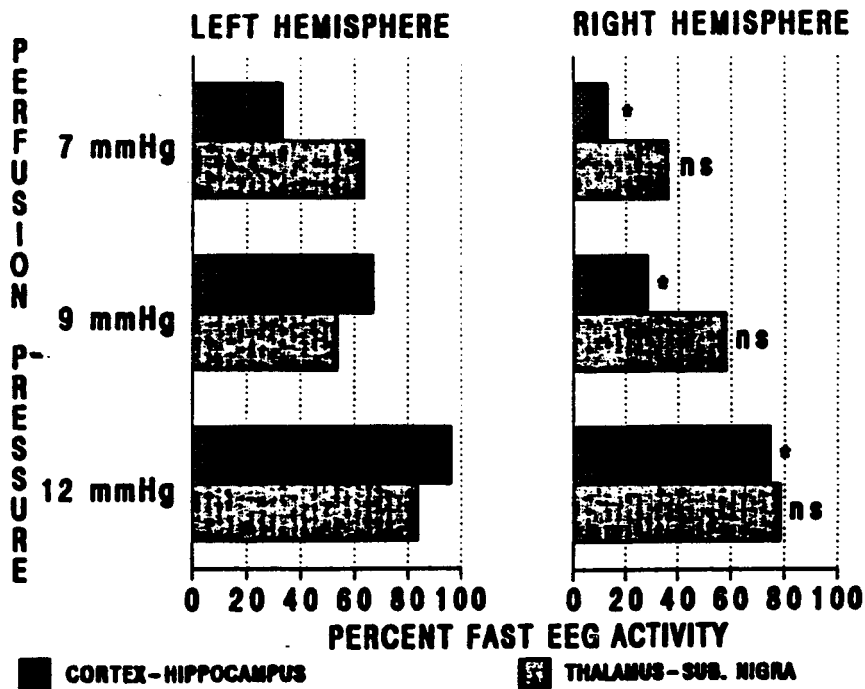
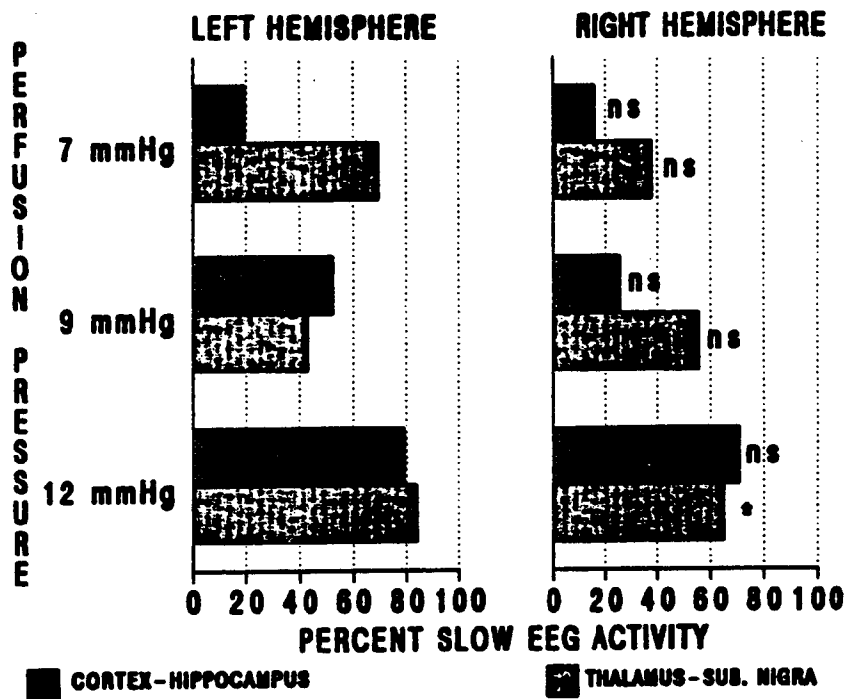
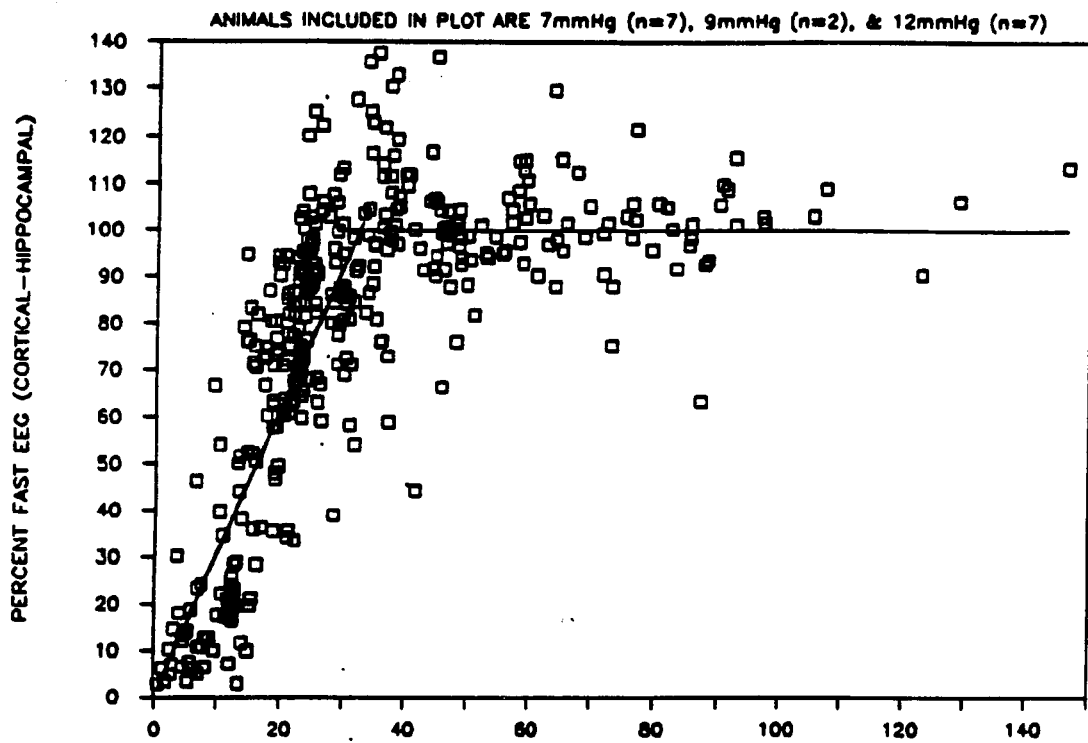


**FIGURE 9-11**

**COMBINED EEG-CBF RELATIONSHIP FOR  
THE CORTICAL-HIPPOCAMPAL AREAS**

The combined EEG and CBF data are compiled within this illustration from all three groups of animals for the cortical-hippocampal areas.

## RELATIONSHIP BETWEEN FLOW AND FAST EEG



## RELATIONSHIP BETWEEN FLOW AND SLOW EEG

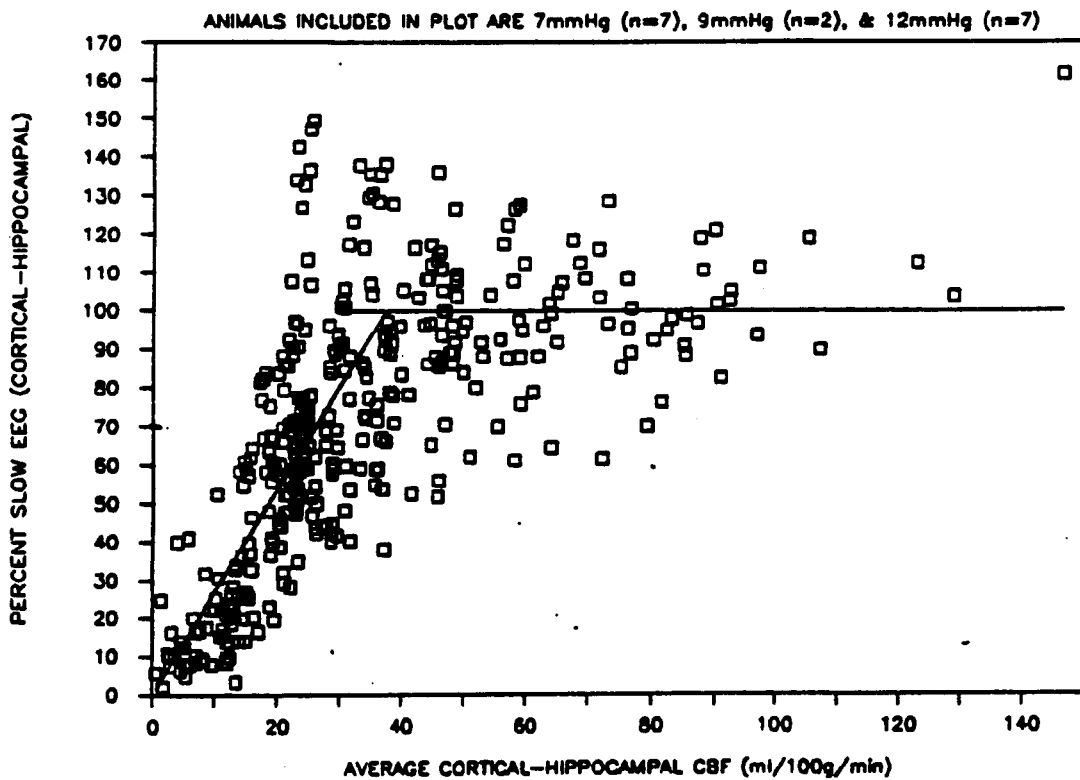


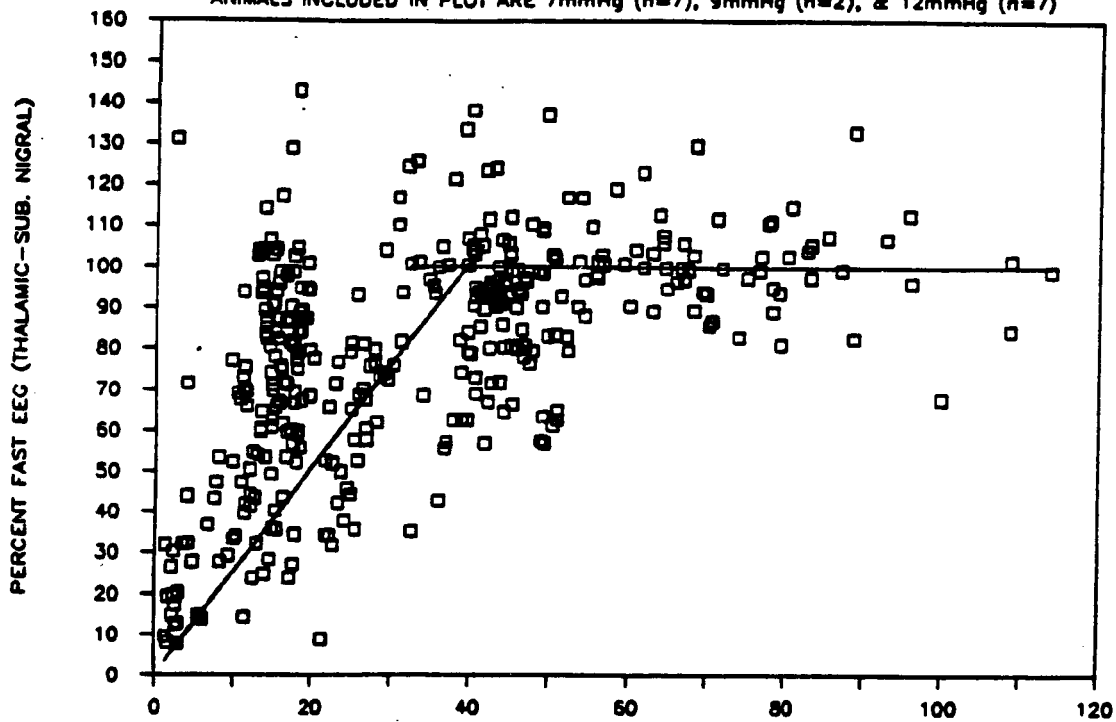
**FIGURE 9-12**

**COMBINED EEG-CBF RELATIONSHIP FOR  
THE THALAMIC-SUBSTANTIA NIGRAL AREAS**

**The combined EEG and CBF data are compiled within this illustration from all three groups of animals for the thalamic-substantia nigral areas.**

## RELATIONSHIP BETWEEN FLOW AND FAST EEG

ANIMALS INCLUDED IN PLOT ARE 7mmHg (n=7), 9mmHg (n=2), &amp; 12mmHg (n=7)



## RELATIONSHIP BETWEEN FLOW AND SLOW EEG

ANIMALS INCLUDED IN PLOT ARE 7mmHg (n=7), 9mmHg (n=2), &amp; 12mmHg (n=7)

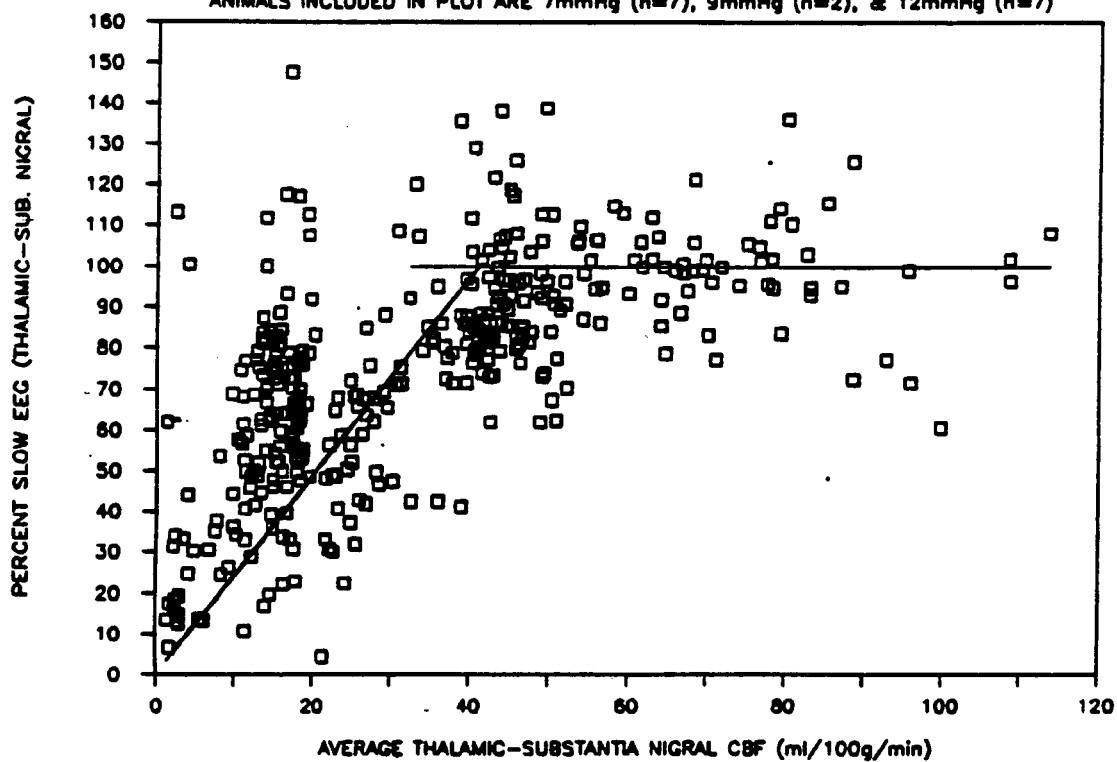


Table 9-7. The slopes indicate that below the breakpoint, there is approximately a decrease of 25 to 30% EEG activity in all areas for every 10 ml/100g/min decrease in CBF.

TABLE 9-7

## SLOPES FOR EEG REGRESSION LINES

	Fast EEG Activity
Location	Slope
Cortex/Hippocampus	3.08
Thalamus/Substantia nigra	2.53
	Slow EEG Activity
Cortex/Hippocampus	2.68
Thalamus/Substantia nigra	2.43

## DISCUSSION

Numerous ischemic models in the rat have been developed in the past. Most of these models can be classified as either global or regional. Global models are designed to produce ischemic damage by affecting the entire cerebral circulation while regional models affect the blood supply to a specific area within the brain. The MCA occlusion method used by many investigators (Tamura et al., 1981; Coyle, 1982; Hossmann, 1983; Chen et al., 1986) is an example of a regional model. This model requires a craniectomy with subdural manipulations which may result in traumatic damage to the cerebrum and it also does not allow for reperfusion in the infarcted area.

The evolution of global model development includes the method of Levine (1960) in which he used systemic anoxia and hemorrhagic hypotension to produce brain infarcts. Similarly, other investigators (Brown, 1968; Salford, 1973) used anoxia alone to produce brain infarcts. The systemic derangements caused by these models complicate the analysis of the information yielded by these models and therefore are limited.

Pulsinelli et al. (1979) greatly improved the global model by eliminating the need to employ systemic insults to produce infarcts by successively occluding the four major vascular inputs to the brain. However, the consistency of Pulsinelli's results have been challenged by others (Furlow, 1982). Menelow (1984) uses the method introduced by Pulsinelli et al. (1979),

but in conjunction with hemorrhagic hypotension. Kameyama et al. (1985) showed that in addition to bilateral carotid artery ligation he could obtain more consistent results than Pulsinelli et al. (1979) by occluding the basilar artery instead of occluding the vertebral arteries bilaterally. However, we have been unable to obtain consistent results with the basilar artery approach. Todd et al. (1986) obtains consistent results using a modified Pulsinelli approach in rats weighing between 200 grams and 300 grams, but we have been unable to reproduce these results in larger animals. Infarcts have been produced with these models, but the variations in the results and/or the contribution of the systemic derangements greatly complicates the analysis. Also, with the exception of the hemorrhagic method, none of these models can modulate the level of ischemia. They are limited in that they can reach only one level of ischemia and sometimes this level is not severe enough to produce infarcts.

The animal model described in the Animal Model section makes cerebral blood supply solely dependent on the input of an extracranial artery in animals weighing up to 450 grams without employing systemic insults (see Figure 3-3). It allows reperfusion in the infarcted area and does not require any subdural manipulations. Perfusion pressure modulation by the computer controlled servo system enables us to reproduce a range of partial ischemic states as demonstrated in Figures 9-2 and 9-3.

Control over the input of the left common carotid by the computer controlled servo-balloon technique allows for effective modulation of the perfusion pressure within the ischemic range. The servo-balloon technique is a modification of the servo system introduced by Hester et al. (1983). Better pressure control ( $SD = \pm 0.5$  mmHg compared to  $SD = \pm 2.0$ ) is provided by our balloon-servo system at the expense of a poorer rate response when

compared to Hester's servo system. Also, to minimize the animal's initial systemic blood pressure response to the induction of severe partial ischemia, a halothane level of approximately 1.0% has to be used in order to keep the animal's response within the rate response limit of our balloon-servo system.

The blood gasses and hematocrits contained in Table 9-1 compare well with other investigators as being in the normal range (Todd et al., 1986; Barry et al., 1982; Tamura et al., 1981). The hematocrits were normal at the experiment's end, thus ruling out the possibility of CBF changes due to hematocrit.

Pre-ischemic systemic pressure values in Table 9-2 are approximately 20% lower than that reported by Todd et al. (1986), Hoffmann et al. (1983), Tamura et al. (1981), Pulsinelli et al. (1979), and Chen et al. (1986) while they are approximately 25% higher than that reported by Hudetz et al. (1985) and Barry et al. (1982). These differences can be explained by the different anesthetic regimens used by the different investigators. Chen et al. (1986) and Hoffmann et al. (1983) use a ketamine regimen, Tamura et al. (1981) and Todd et al. (1986) use a 0.5% halothane regimen while Pulsinelli et al. (1979) did not use any anesthesia. Thus, these three regimens would certainly result in higher SBP's since our regimen consisted of using a 1.0% halothane level. Hudetz et al. (1985) induced anesthesia with 4.0% halothane and then used a maintenance dose of 1.5%. Thus, the higher level of halothane resulted in a lower SBP. Likewise, the explanation that our pre-ischemic CBP level is 25% higher than that reported by Hudetz et al. (1985) can be made on the anesthetic differences. Fujishima et al. (1976) report a relationship between CBP and SBP for normotensive rats before and after common carotid artery occlusion with one common carotid artery already being occluded. These relationships are as follows:

$$\text{CBP} = 0.66(\text{SBP}) - 14.32 \quad (\text{before occlusion}), \text{ and}$$

$$\text{CBP} = 0.43(\text{SBP}) - 3.00 \quad (\text{after occlusion})$$

Substituting our overall average SBP value of 96.8 mmHg into their relationships yield CBP's of 49.9 mmHg and 38.6 mmHg for the pre and post occlusive values, respectively. The 49.9 mmHg CBP value obtained from their relationship compares well to our overall average CBP value of 56.1 mmHg with one common carotid artery occluded.

The pre-ischemic CBF's in Table 9-3 compare favorably with other investigators results. The cortical values from our system are approximately 20% lower than that reported by Todd et al. (1986) which is  $91 \pm 7$  ml/100g/min. This 20% reduction in pre-ischemic cortical flow corresponds to the 20% decrease in SBP due to the relative increase in halothane level used within our system. Also, our cortical flow values are 25% higher than that reported by Hudetz et al. (1985) which corresponds to the 25% increase in SBP and CBP due to the relative decrease in halothane level used within our system. However, there are some inconsistencies when comparing our pre-ischemic flow values to other investigators. Barry et al. (1982) reports a average pre-ischemic cortical flow of  $87 \pm 12$  ml/100g/min which is 20% higher than our cortical flows while using a similar halothane level. This difference may be due to the difference in the methods of calculating CBF from a hydrogen washout curve. While we use a significant portion of the hydrogen washout curve in determining CBF, Barry et al. (1982) uses the initial slope method. Hudetz et al. reports pre-ischemic CBF's within the hippocampus, thalamus, and substantia nigra that are very similar to the values in Table 9-3 even though he uses a much higher level of halothane. The reason for the similarity in these flows is unknown. Also, Table 9-3 shows that hemispheric differences in CBF exists for the thalamus and the substantia

nigra. Because the right common carotid artery is occluded for CBP and SBP monitoring, the thalamus and substantia nigra must normally receive a significant portion of their blood supply from the carotid inputs to exhibit this hemispheric difference.

The stability of the animal preparation before initiating partial occlusion is demonstrated by the CBF's and EEG's being constant during the 60 minute pre-ischemic period. However, there was a slight tendency for CBF to increase with time in the substantia nigra with a corresponding increase in slow EEG activity from 94% to 105% ( $p < 0.05$ ).

The ischemic cortical CBF of  $5.9 \pm 0.6$  ml/100g/min reported by Todd et al. (1986) compares very well to the right cortical CBF of  $6.2 \pm 3.7$  ml/100g/min that we obtained at 7 mmHg perfusion pressure. This suggests that the perfusion pressure in the four vessel occlusion model that Todd et al. (1986) uses in his 200-300 gram animals is approximately 7 mmHg when all four vessels are occluded. The ischemic CBF values that Hudetz et al. (1985) report for the hippocampus, thalamus, substantia nigra, and the cortex at a perfusion pressure of approximately 12 mmHg are very different from the values presented in Table 9-4. The possible explanation for the differences may lie in the different methodologies employed in obtaining these two sets of data. Hudetz et al. (1985) use the hemorrhagic technique in conjunction with the four vessel occlusion model three days after bilateral vertebral artery monopolar cauterization. Thus, the only input to the cerebrum in Hudetz's method comes from the collateral circulation of the vertebro-basilar system while the majority of the input in our system comes from the carotid system. Also, there may have been hematocrit influences on the CBF results from using the hemorrhagic technique that were not identified within his system.

The hemispheric differences in CBF for the different anatomical locations suggest a pressure gradient from the left hemisphere to the right hemisphere. Also, if it is assumed that the vascular resistance within all anatomical structures is equal when the initiation of partial carotid artery occlusion begins, then a pressure gradient exists between different anatomical structures on the same side.

At the 7 mmHg perfusion pressure level, CBF's were observed to decrease significantly with time at all anatomical locations, especially in the right hemisphere. Because all flows are collapsing, the linearity of the 7 mmHg curve in Figure 9-9a suggests a hemispheric collapse in flow such that all CBF's within the right hemisphere will collapse to zero at the same time. This behavior is not observed in the left hemisphere because the perfusion pressure is most likely higher than that being measured on the right side. The cause for the hemispheric collapse in flow could be due to edema formation from the ischemic insult as suggested by Crockard et al. (1980) and Iannotti et al. (1985). The results presented by Crockard et al. (1980) show a relationship of edema formation versus CBF. From his study, edema formation begins at approximately 20 ml/100g/min and continues to increase to a CBF of 7 ml/100g/min below which edema decreases. Thus, this implies a critical flow level in the vicinity of 15 to 20 ml/100g/min. Our results do not support a critical flow level. In Figure 9-9a, flows in the 8 to 12 ml/100g/min range were observed to collapse for the 7 mmHg series while they were observed to recover for the 9 and 12 mmHg series. Hence, this implies that the perfusion pressure level will dictate whether or not a marginal CBF in the 8 to 12 ml/100g/min range will subsequently collapse and not the absolute flow level.

In the 9 mmHg and 12 mmHg series, the anatomical areas with high initial CBF's had large negative rates of change of flow while the anatomical areas with marginal initial flows had positive rates indicating recovery. We do not feel that edema was forming in the higher flow areas but that a redistribution of the blood supply to the more severely affected areas was occurring. Because specific gravity measurements were not performed on the tissue we are unable to determine if edema formation was occurring in the areas with marginal flow at 9 mmHg or 12 mmHg perfusion pressure. However, if edema formation was present in these marginal areas, the positive recovery rate in CBF indicates that an adaptational process of greater magnitude than the edema formation was occurring. Also, this adaptational process could be occurring at a faster rate in the marginal areas than in the higher flow areas thus causing a steal phenomenon resulting in this redistribution of flows with time.

The combined fast and slow EEG activity versus CBF relationships presented in Figures 9-11 and 9-12 do not agree with the results obtained by Branston et al. (1974), Heiss et al. (1976), Sundt et al. (1974), or Trojaborg et al. (1973). These investigators report that flattening of the EEG occurs when hemispheric or local flow falls below 15 to 18 ml/100g/min irrespective of species differences and varying modes of anesthesia. Our results show a linear relationship between EEG and CBF down to zero flow. The differences in the results can be attributed to the different methodologies used to measure EEG levels. Branston et al. (1974), Heiss et al. (1976), Sundt et al. (1974), and Trojaborg et al. (1973) measure EEG in the cortex alone while our EEG measurements are made between different anatomical structures that are approximately 2 mm distant from one another. Thus, while we certainly do not have electrical silence in the deeper anatomical structures at 15

ml/100g/min, we may have electrical silence in the cortex. However, this is unlikely.

The reproducibility of this system is demonstrated by the consistent values in CBF for all the anatomical locations at a constant perfusion pressure. By automating the hydrogen clearance flow method and maintaining the perfusion pressure constant via computer control throughout flow determinations as well as for the entire experiment, the human element has virtually been eliminated from the data acquisition and flow determining phases of the experiment. Thus, by reproducing the same conditions for data acquisition and perfusion pressure regulation between different animals via computer automation, the results have been remarkably consistent from animal to animal within a given perfusion pressure group.

Finally, by performing morphological evaluations on the brain tissue, correlations to the hemodynamic data obtained can be made to further describe our system. Also, future experiments will employ CBP measurements on the contralateral side via the right external carotid artery. This will provide information on the difference in perfusion pressure between the two hemispheres. Thus, a better understanding of the hemodynamic events in the left hemisphere can be obtained.

## APPENDIX A

### THEORETICAL CONSIDERATIONS FOR THE CLEARANCE AND POLAROGRAPHIC EQUATIONS OF THE HYDROGEN CLEARANCE METHOD

The theoretical considerations regarding the hydrogen clearance and the hydrogen polarographic equations are discussed below.

Hydrogen is an inert gas which is defined as "one which dissolves in the blood and tissues in a manner that can be described by Henry's Law, which suffers no change in chemical identity during its passage through the organism, and which is therefore quantitatively recoverable from the organism at any time" (Kety, 1951). On the basis of Zuntz's fundamental assumptions (Zuntz, 1897) a general expression for the exchange of an inert gas with a single tissue can be obtained using the Fick principle (Hoff and Scott, 1948; Kety, 1951). The Fick principle can be stated for an inert gas such as follows: the amount of inert gas taken up by the tissue per unit time is equal to the amount of gas brought to the tissue per unit time by the arterial blood flow minus the amount of gas taken away per unit time by the venous blood flow. This is represented mathematically as:

$$dQ_i = F_i(C_a - C_v)dt \quad (1)$$

where,

$dQ_i$  = the amount of inert gas taken in or given off by the tissue,

$C_a$  = the arterial concentration of the inert gas,

$C_v$  = the venous concentration of the inert gas,

$F_i$  = the blood flow of the tissue, and

$dt$  = the time over which this process occurs.

Since the concentration of an inert gas is equal to the amount of inert gas contained within a volume ( $dC = dQ/V$ ), where  $V$  is volume, equation (1) becomes

$$WdC_i = F_i(C_a - C_v)dt \quad (2)$$

where,

$W$  = the specific volume, and

$dC_i$  = the change in tissue concentration of the inert gas.

Since the concentration of the inert gas in the tissue is in equilibrium with that in the veins (Kety, 1951),  $C_v = C_i/\lambda$ , where  $\lambda$  is the blood-brain partition coefficient for the inert gas.

$$WdC_i = F_i(C_a - C_i/\lambda)dt \quad (3)$$

The water gas partition coefficient of hydrogen is very low at 0.018 (Lawrence, 1946). If hydrogen is administered by inhalation then arterial concentration of the inert gas quickly falls to zero upon cessation of the hydrogen gas inhalation (Kety, 1951). Thus, when  $C_a = 0$

$$WdC_i = -C_i F_i/\lambda dt \quad (4)$$

or,

$$dC_i/C_i = -F_i/\lambda W dt \quad (5)$$

and integration yields the simple exponential equation

$$C_i = C_{i0}e^{-kt} \quad k = F/\lambda W \quad (6)$$

where,

$C_i$  = the hydrogen concentration in tissue at time  $t$ ,

$C_{i0}$  = the hydrogen concentration in tissue at the beginning of desaturation,

$k$  = the blood flow per tissue volume divided by the

blood:tissue partition coefficient in ml/min/ml (or min<sup>-1</sup>),

$\lambda$  = the blood:tissue partition coefficient,

$W$  = a defined tissue volume, and

$t$  = time after desaturation begins (minutes).

Assuming that hydrogen gas is in instantaneous diffusion equilibrium between the tissue and venous blood, and the arterial concentration of the hydrogen gas is zero when desaturation begins, and a homogeneously perfused tissue bed, the above equation can be stated as follows: The concentration of an inert gas approaches equilibrium during desaturation as a single exponential function based on the blood flow through the tissue and the tissue's capacity for the gas.

Rearranging the terms and taking the natural logarithm yields

$$\ln(C_i/C_{i0}) = -(F/\lambda W)t. \quad (7)$$

Since the partition coefficient,  $\lambda$ , for hydrogen has been found to be unity both for the brain (Fieschi et al., 1965) and for the kidney (Aukland et al., 1964) and if  $T_{1/2}$ , the half-life, is substituted for  $t$ , equation (7) will read:

$$\ln(2)/T_{1/2} = F/W = f \quad (8)$$

where  $f$  is the blood flow per volume in ml/g/min. The  $T_{1/2}$  is readily determined from the curve obtained from the fall of hydrogen voltage (measure of hydrogen concentration) with respect to time after hydrogen gas inhalation is terminated. The value of  $f$  is usually multiplied by 100 in order to yield  $f$  in units of ml/100g/min which is the normal convention for reporting local cerebral blood flow (LCBF).

The substitution of  $T_{1/2}$  for  $t$  allows the relative hydrogen concentrations to fall out of the derivation. This is an important feature of the hydrogen clearance method because it eliminates the need to calibrate the electrodes to absolute levels of hydrogen concentration. Therefore, the

tissue concentration of hydrogen does not influence the blood flow measurement. Only the rate of change of hydrogen concentration from some initial value to half that value measures the local blood flow. Because hydrogen is an inert gas, its transport properties to and from a tissue bed depend only upon its diffusion (discussed below) and the blood flow.

The basic principle of hydrogen polarography is that hydrogen can be oxidized to form 2 hydrogen ions and 2 electrons ( $H_2 \rightarrow 2H^+ + 2e^-$ ) (Will, 1963). When a substance such as platinum is placed within the vicinity of this reaction electrons will flow towards the acceptor surface, thus generating current flow. If the platinum electrode is positively polarized with respect to the reference electrode (Silver electrode in this case), and inserted into some medium containing hydrogen ( $H_2$ ), the hydrogen molecules closest to the platinum electrode will dissociate first causing more hydrogen molecules from the bulk area to diffuse toward the electrode. Thus, a concentration gradient is established between the bulk medium and the electrode surface. As the polarization potential is increased, the above reaction is in effect intensified (Adams, 1969) causing more and more hydrogen molecules to be dissociated at the electrode surface per time and thereby increasing the current generated. However, there will come a point at which any further increase in polarization potential will cause the depletion of hydrogen molecules at the electrode surface to exceed the rate of migration of hydrogen molecules from the bulk medium. At this point, the current generated at the electrode surface is limited by the diffusion coefficient of hydrogen in the medium and therefore, can be described by Fick's Law:

$$J = D(dC/dx) \quad (9)$$

where,

$J$  = the one dimensional flow of hydrogen towards the electrode in moles,

$D$  = the diffusion coefficient of hydrogen in the medium, and

$dC/dx$  = the concentration change over distance  $dx$  from the electrode.

The term  $J$  can be converted into a current term using Faraday's Law:

$$i_e = nFD(dC/dx) \quad (10)$$

where,

$i_e$  = the current density per unit area at the electrode surface,

$n$  = the number of charges being transferred by each  $H_2$  molecule, and

$F$  = Faraday's number.

If the concentration gradient is assumed to be linear from the bulk medium to the electrode surface, then equation (10) becomes

$$i_e = nFD((C_b - C_e)/L_d) \quad (11)$$

where,

$C_b$  = the concentration of hydrogen in the bulk medium,

$C_e$  = the concentration of hydrogen at the electrode surface, and

$L_d$  = the one dimensional diffusion length of the hydrogen.

If the oxidation of hydrogen at the electrode is such that any further increase in polarization potential results in a current plateau, then the rate at which hydrogen is being oxidized results in a hydrogen concentration of nearly zero at the electrode surface. With this consideration equation (11) becomes

$$i_e = nFD(C_b/L_d) \quad (12)$$

Equation (12) shows that the current generated at the electrode surface is linearly related to the hydrogen concentration in the bulk medium. Thus, the principles used in deriving equations (6) and (12) can be used to determine blood flow at the electrode site according to equation (7). An illustrative example is given in Figure 1 in the Hydrogen Clearance Method section.

## **APPENDIX B**

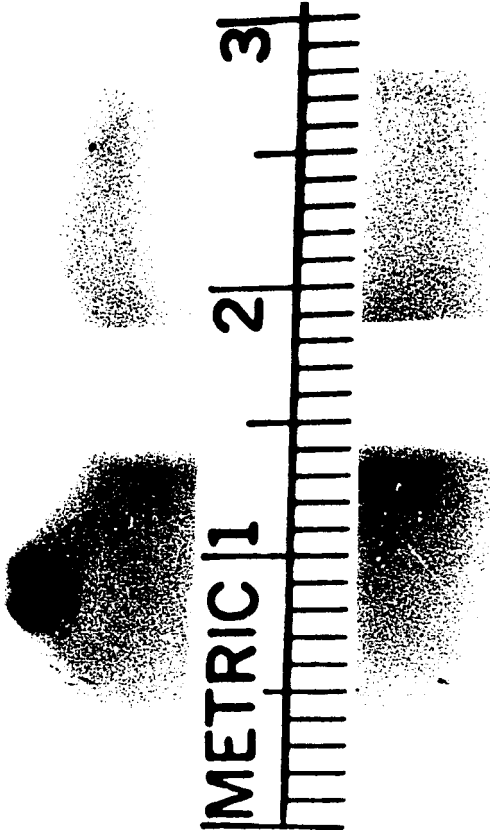
### **PLATINUM ELECTRODE ARRAY CONSTRUCTION**

With a 20 gauge needle, four holes are made in the apical end of a Number 52190 EFFA flat embedding mold (Ernest F. Fullam Co.) that correspond to the X and Y stereotaxic coordinate distance between each electrode. The mold was chosen because the flat apical end is 2 mm wide which corresponds to the Y distance between electrodes 1 and 4, 2 and 3, 5 and 8, and 6 and 7. Four 20 gauge needles are cut and beveled in lengths of about 1/3 inch each and are inserted into the four holes made above (see Figure B-1a). AMPHENOL series 221 multipurpose narrow width strip connectors (Pioneer-Standard, Huntsville, AL) are cut into sections of four socket holes. AMPHENOL socket contacts (#220-S02-100 Kierulff Electronics Inc., St. Petersburg, FL) are inserted into the strip connectors with the short barrelled end facing out and filled with solder. Hand drawn 90% platinum 10% iridium wire 0.005 inches (127 microns) in diameter (Englehard Industries) is cut into 1.5 inch lengths and soldered into the short barrelled end of the four socket contacts in the strip connector. The four platinum wire ends are gently passed through the four 20 gauge needle barrels lying within the embedding mold. The 20 gauge needle barrels are removed and then the strip connector is placed on the bottom of the mold. Devcon 5 minute epoxy is placed in the mold containing the connector and the four contacts each

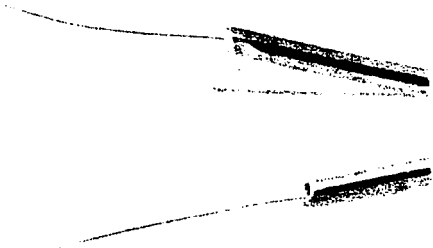
**FIGURE B-1****PLATINUM ELECTRODE CONSTRUCTION**

Figure B1a shows the spatial relationship of the four 1/3 inch 20 gauge needles within the apical end of the flat embedding mold. The apical end of the embedding mold is 2 mm wide to give the X distance between electrodes 1 and 4, 2 and 3, 5 and 8, and 6 and 7. Thus, the only measurement required to be made is the Y distance between the electrodes. Figure B1b shows the electrode array in the mold after the epoxy has been added to secure all the pieces together. Normally the 20 gauge needles would be removed before the epoxy is added but in this case they were left in to better show how the platinum wires traverse through the mold.

**a**



**b**

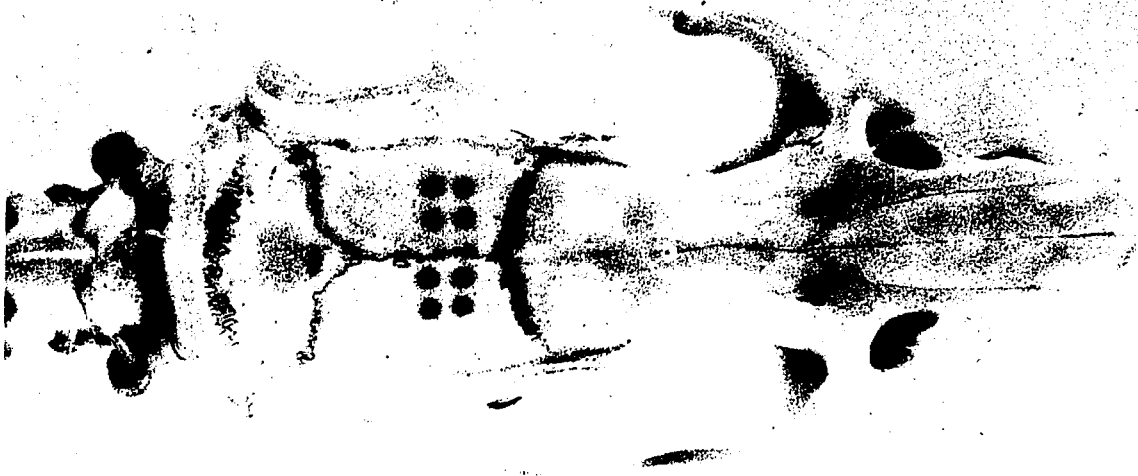


holding a soldered platinum wire taking care to ensure that the platinum wire is not close to the epoxy-mold interface except at the apical surface to prevent the platinum wire from coming out of the epoxy mold during stretching (see Figure B-1b). The entire structure is removed from the mold by pulling the platinum wire through the holes and the excess epoxy surrounding the four platinum wires is removed from the apical surface. Based on the Z coordinates of the desired anatomical locations, the exposed platinum wire lengths for each electrode are 6.0 mm, 8.0 mm, 11.0 mm, and 3.0 mm for electrodes 1 and 5, 2 and 6, 3 and 7, and 4 and 8, respectively. With this known, each wire on the mold is straightened and cut to the appropriate length with a blade leaving a pointed tip. With a thin glass applicator, each electrode wire is coated with epoxylite over its entire length leaving the last 1 mm at the tip bare. To prevent microbubbles from forming within the epoxylite, the array is degassed in the oven for 30 minutes at 200 degrees F and then baked at 300 degrees F for 45 minutes to set the epoxylite. Construction is complete when another coat of epoxylite is applied to the array and the baking sequence is repeated again (see Figure B-2).

To connect each electrode to its appropriate circuitry an adapter is constructed by soldering four copper wires to four AMPHENOL 220-P02-100 pins mounted in a strip connector modified as described above and epoxying the connector-copper wire junction. The free end of each copper wire is then connected to the appropriate circuitry. Because blood flow measurements are being carried on at eight different electrodes, there are eight identical circuits employed in this system.

**FIGURE B-2****PLATINUM ELECTRODE ARRAY**

The completed platinum electrode array is shown next to a rat skull with the desired X and Y coordinate markings on it. Two arrays are required for each experiment. The gold pin in the strip connector portion of the array represents where one of the four AMPHENOL 220-PO2-100 pins are inserted to connect the each electrode to its appropriate circuitry.



## **APPENDIX C**

### **LATEX BALLOON MANUFACTURE**

Balloons must be prepared within four days of the experimental procedure. Longer storage may result in possible balloon malfunction. The method for balloon manufacture consists of forming a stainless steel plug on a metal lathe to obtain an oval shape measuring 2 mm X 3 mm (minor & major axis) with a 1 mm neck. The stainless steel mold is then smoothed and polished with fine emory cloth. When a satisfactory mold has been constructed, balloons are manufactured as follows: the mold is first cleaned with acetone. The mold is dipped in latex and allowed to air dry until the latex appears clear (this takes approx. 15 min). Dipping and air drying is repeated. The mold is again dipped in latex but is immediately transferred to a 100 degrees C oven and cooked for 15 minutes. After cooking and cool-down (the mold and balloon is placed in the freezer for 10 min), about two drops of silicon oil is placed on the mold and the balloon is then gently removed from the mold.

Latex for balloon manufacture is obtained from:

Killian Latex Inc.  
2064 Killian Road  
Akron, OH 44312

## **APPENDIX D**

### **COMBINED EXPERIMENTAL RESULTS**

This appendix serves as a compendium of the results obtained from each series of animals performed in this study. Figures D-1 and D-10 show the system's ability in maintaining the desired perfusion pressure throughout the experiments. Figures D-2 through D-5 and Figures D-11 and D-12 show the CBF profiles for the different anatomical locations at perfusion pressures of 12 mm Hg, 9 mm Hg, and 7 mmHg. Finally, Figures D-6 through D-9 and Figures D-13 and D-14 show the relative fast and slow EEG activity profiles for the different anatomical locations at the different perfusion pressures. The legends provide a detailed description of all the data within this appendix.

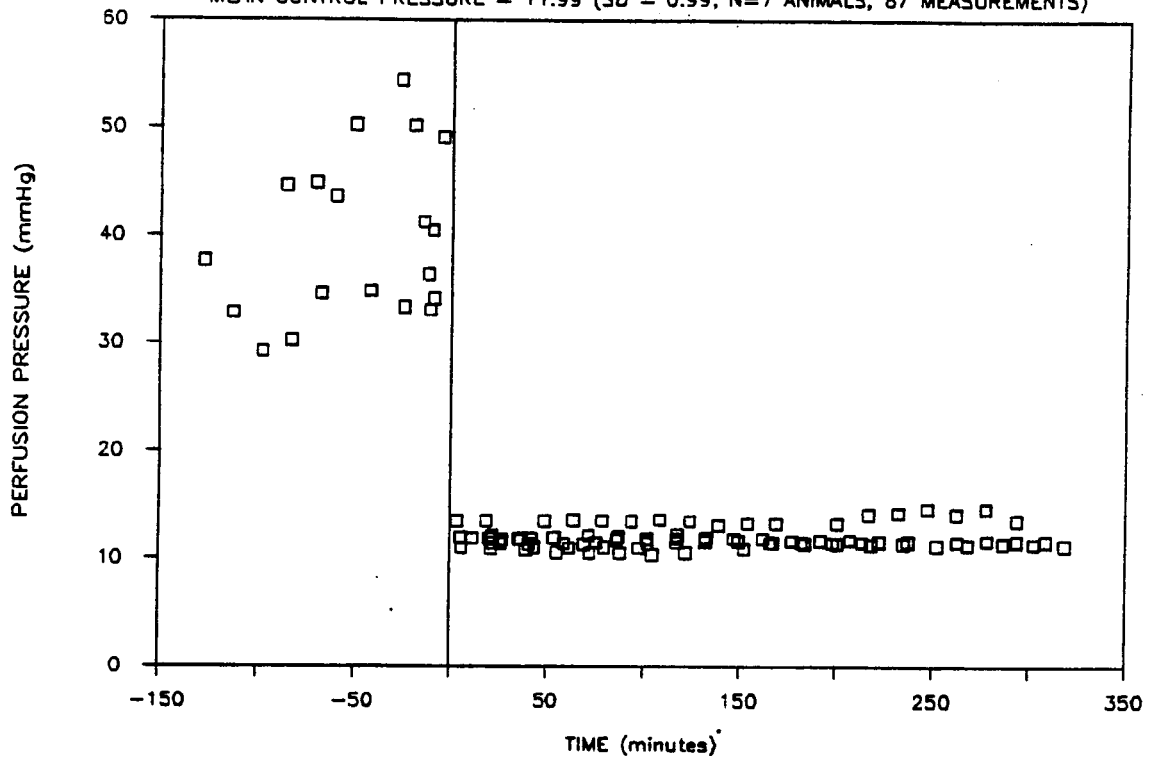
## FIGURE D-1

**CONTROL OF PERFUSION PRESSURE  
AT 12 mmHg AND 7 mmHg**

Perfusion pressure is plotted as a function of time for the 12 mmHg and 7 mmHg animal series. Partial occlusion of the left common carotid artery by the balloon was initiated at time zero. The mean control pressure with standard deviation for the seven animals in each group is provided on the illustration. The standard deviations are due to the baseline drift in the pressure transducers and the Grass Polygraph recorder and the servo error (see Results section). The standard deviation for the 7 mmHg group is much lower than for the 12 mmHg group because during the conduct of the 12 mmHg series the original pressure transducers were replaced with newer ones that exhibited a much smaller drift.

### CONTROL OF PERFUSION PRESSURE

- MEAN CONTROL PRESSURE = 11.99 (SD = 0.99, N=7 ANIMALS, 87 MEASUREMENTS)



### CONTROL OF PERFUSION PRESSURE

MEAN CONTROL PRESSURE = 6.86 mmHg (SD = 0.27, N = 7 ANIMALS, 23 MEASUREMENTS)

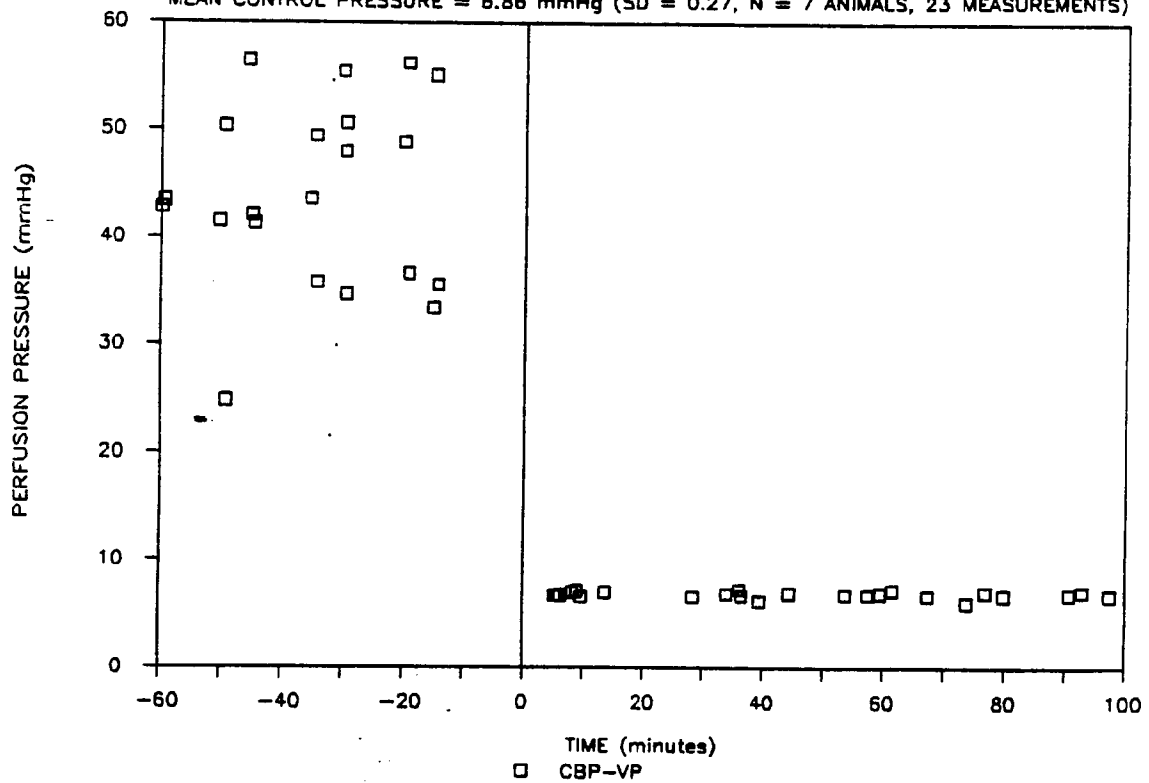


## FIGURE D-2

BILATERAL HIPPOCAMPAL CBF  
AT 12 mmHg AND 7 mmHg PERFUSION PRESSURE

Cerebral blood flow is plotted as a function of time for both the right and left hippocampus at perfusion pressures of 12 mmHg and 7 mmHg. Partial occlusion of the left common carotid artery was initiated at time zero. Before partial occlusion, both the right and left hippocampal CBF's in both series of animals were not significantly different from each another.

Figure D-2a. At 12 mmHg perfusion pressure, the CBF in the left hippocampus ( $29.1 \pm 6.1$  ml/100g/min) is significantly higher than the CBF in the right hippocampus ( $18.7 \pm 3.1$  ml/100g/min ( $p < 0.01$ )).

Figure D-2b. At 7 mmHg perfusion pressure, the left hippocampal CBF is again significantly higher ( $p < 0.01$ ) with an average flow of  $12.6 \pm 4.0$  ml/100g/min as compared to  $5.2 \pm 2.3$  ml/100g/min for the right. However, note that the flow levels are approximately one third to one fourth the levels reported at 12 mmHg and that the flow level decreases with time at 7 mmHg.

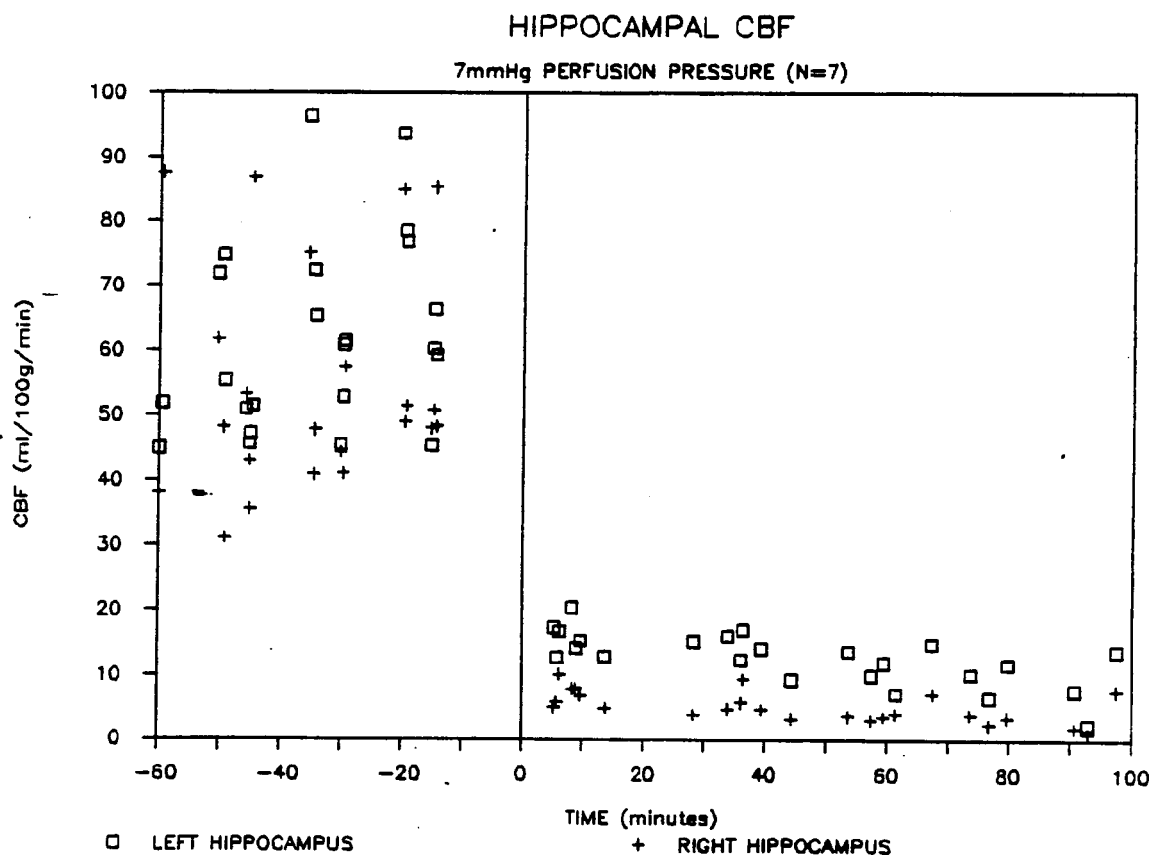
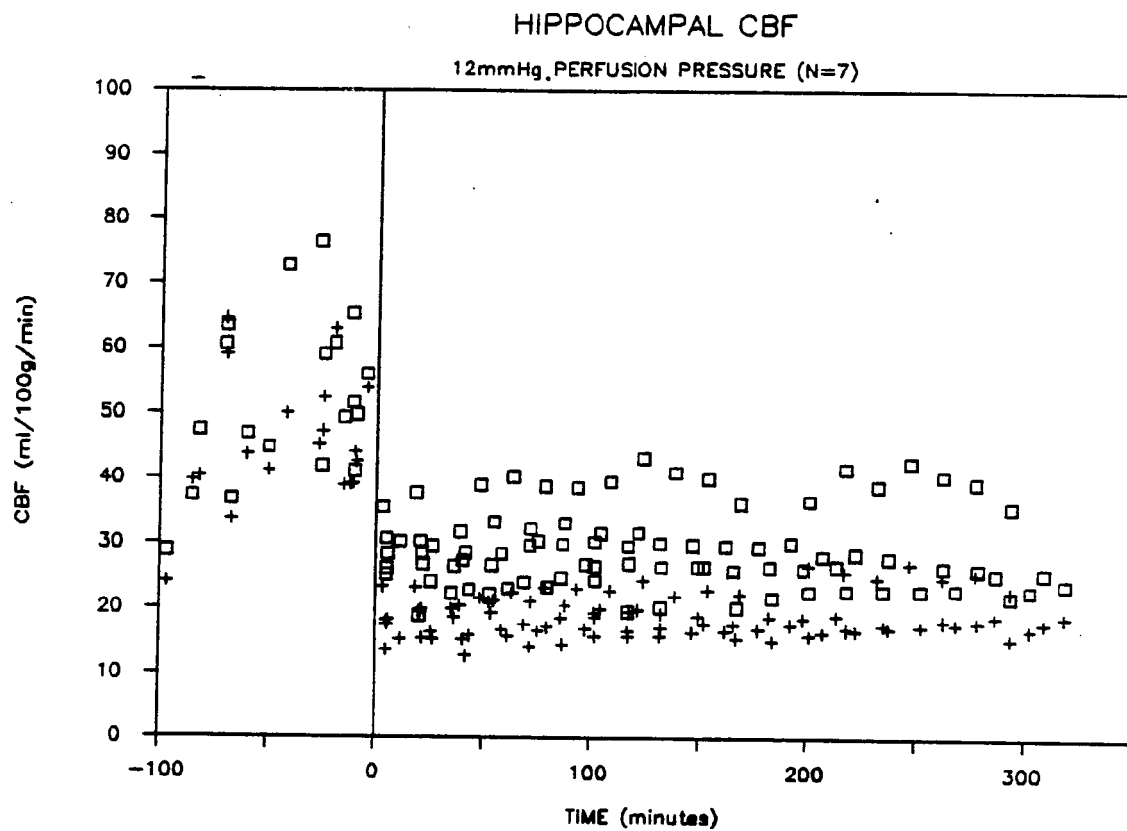


## FIGURE D-3

BILATERAL THALAMIC CBF  
AT 12 mmHg AND 7 mmHg PERFUSION PRESSURE

Cerebral blood flow is plotted as a function of time for both the right and left thalamus at perfusion pressures of 12 mmHg and 7 mmHg. Partial occlusion of the left common carotid artery was initiated at time zero. Before partial occlusion, both the right and left thalamic CBF's in both series of animals were significantly different from each another (see Table 9-3).

Figure D-3a. At 12 mmHg perfusion pressure, the CBF in the left thalamus ( $36.3 \pm 9.2$  ml/100g/min) is significantly higher than the CBF in the right thalamus ( $13.7 \pm 8.7$  ml/100g/min ( $p < 0.001$ )).

Figure D-3b. At 7 mmHg perfusion pressure, the left thalamic CBF is again significantly higher ( $p < 0.001$ ) with an average flow of  $14.4 \pm 4.0$  ml/100g/min as compared to  $2.3 \pm 1.4$  ml/100g/min for the right. However, note that the flow levels are approximately one third to one fourth the levels reported at 12 mmHg and that the flow level decreases with time at 7 mmHg.

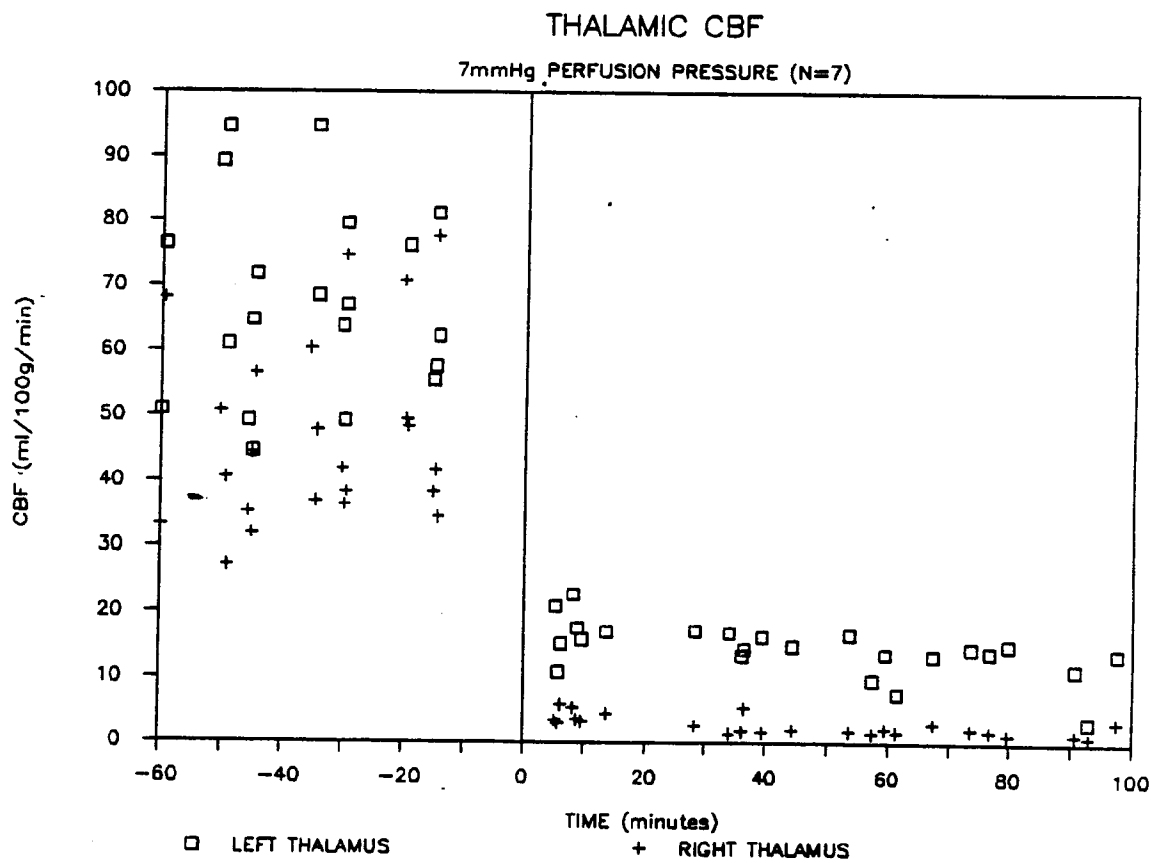
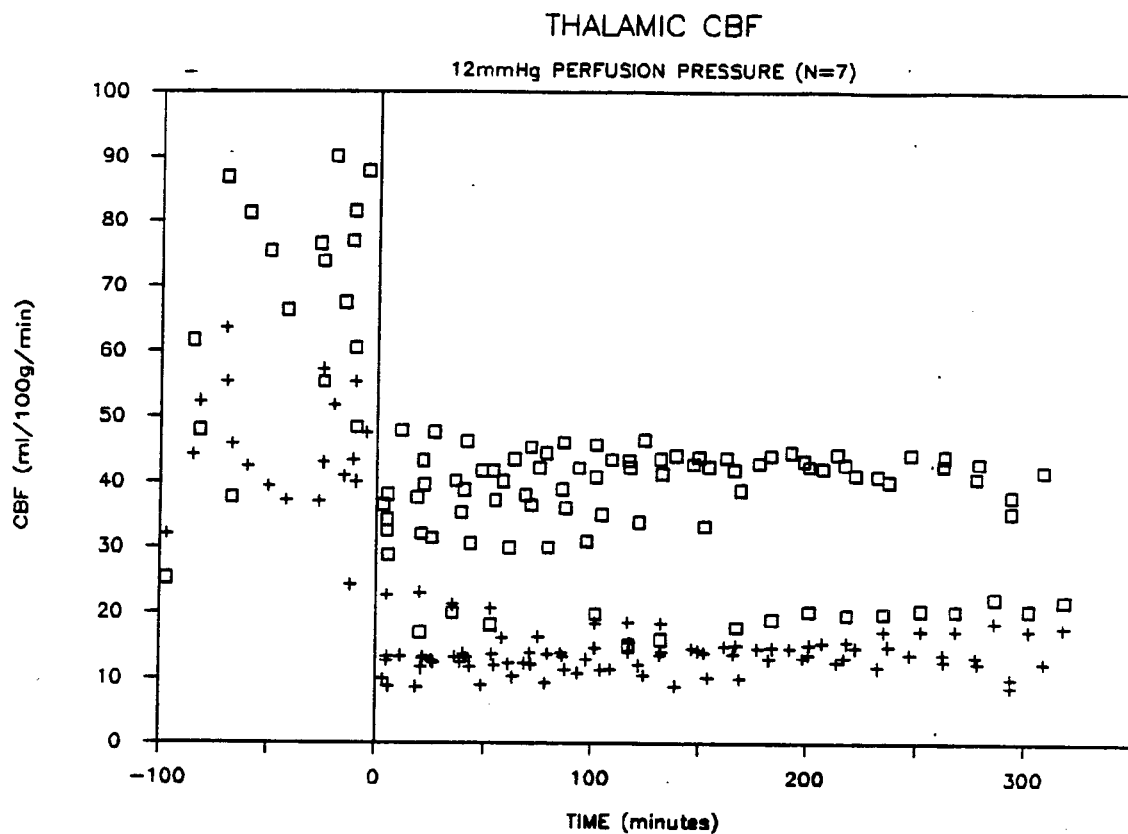


## FIGURE D-4

BILATERAL SUBSTANTIA NIGRAL CBF  
AT 12 mmHg AND 7 mmHg PERFUSION PRESSURE

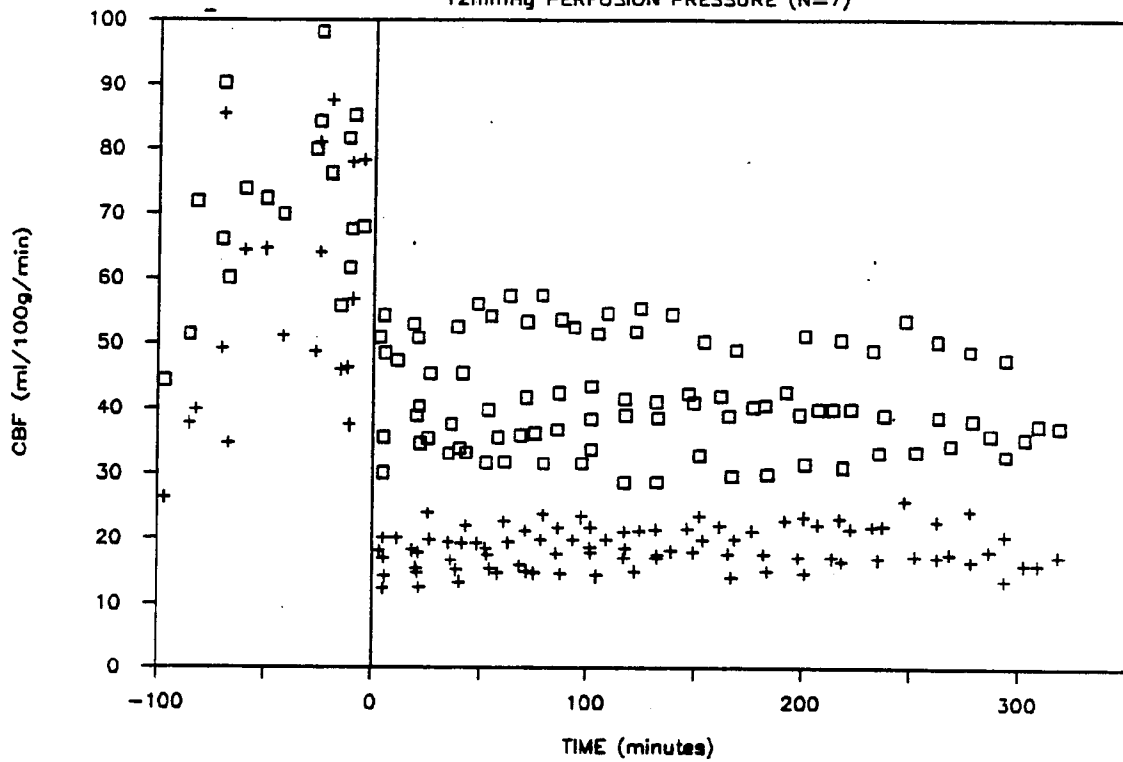
Cerebral blood flow is plotted as a function of time for both the right and left substantia nigra at perfusion pressures of 12 mmHg and 7 mmHg. Partial occlusion of the left common carotid artery by the balloon was initiated at time zero. Before partial occlusion, both the right and left substantia nigral CBF's in both series of animals were significantly different from each another (see Table 9-3).

Figure D-4a. At 12 mmHg perfusion pressure, the average CBF in the left substantia nigra ( $41.7 \pm 8.2$  ml/100g/min) is significantly higher than the average CBF in the right substantia nigra ( $18.5 \pm 3.1$  ml/100g/min ( $p < 0.001$ )).

Figure D-4b. At 7 mmHg perfusion pressure, the left substantia nigral CBF is again significantly higher ( $p < 0.001$ ) with an average flow of  $17.1 \pm 6.0$  ml/100g/min as compared to  $4.5 \pm 2.6$  ml/100g/min for the right. Note that these values are one half to one third the values reported for 12 mmHg and that the flows decrease as a function of time after partial occlusion.

SUBSTANTIA NIGRAL CBF

12mmHg PERFUSION PRESSURE (N=7)



SUBSTANTIA NIGRAL CBF

7mmHg PERFUSION PRESSURE (N=7)

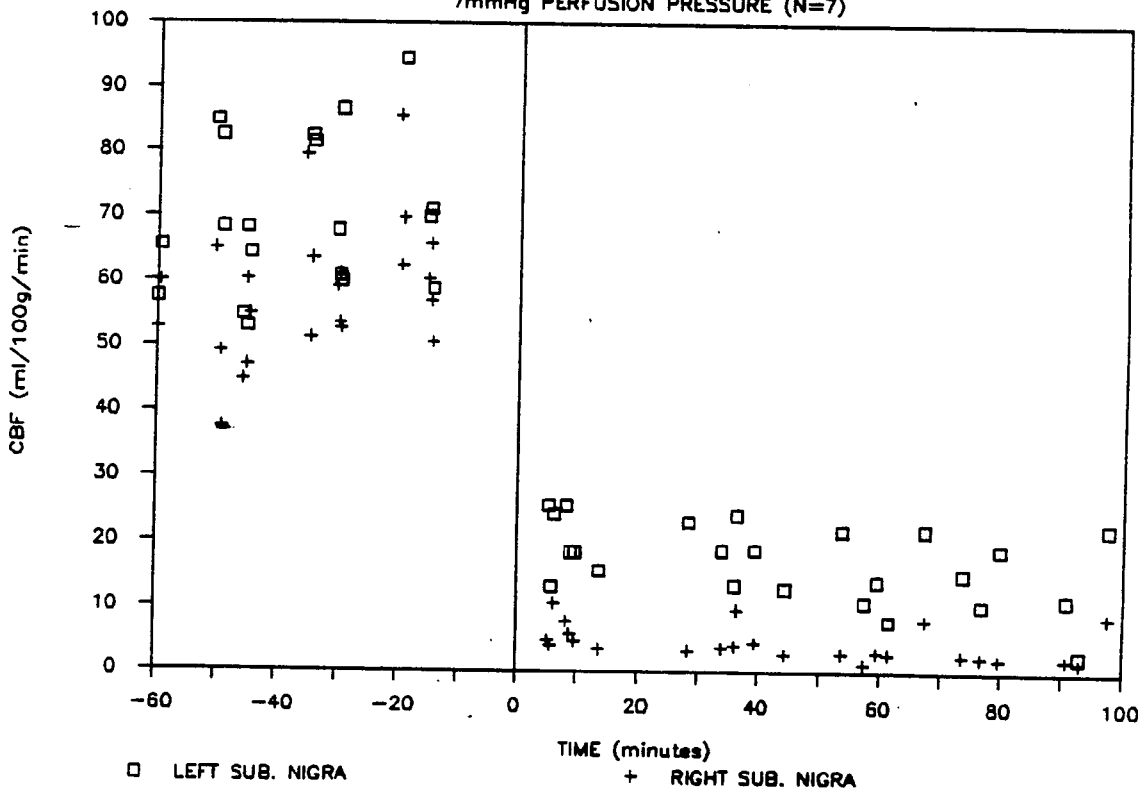


## FIGURE D-5

BILATERAL CORTICAL CBF  
AT 12 mmHg AND 7 mmHg PERFUSION PRESSURE

Cerebral blood flow is plotted as a function of time for both the right and left cortex at perfusion pressures of 12 mmHg and partial occlusion of the left common carotid artery was initiated at time zero. Before partial occlusion, both the right and left cortical CBF's in both series of animals were not significantly different from each another.

Figure D-5a. At 12 mmHg perfusion pressure, the left and right cortex had equivalent flow levels of  $29.8 \pm 6.3$  ml/100g/min and  $29.0 \pm 7.8$  ml/100g/min, respectively.

Figure D-5b. At 7 mmHg perfusion pressure, the left cortical CBF is significantly higher ( $p < 0.05$ ) with an average flow of  $10.4 \pm 4.7$  ml/100g/min as compared to  $6.2 \pm 3.7$  ml/100g/min for the right. With a decrease in perfusion pressure of only 5 mmHg, cortical flows decrease substantially from a relatively innocuous level to flow levels that have been reported by others (Pulsinelli et al., 1979; Furlow 1982) to result in ischemic damage. Also, unlike the 12 mmHg animals, the cortical CBF decreases bilaterally with respect to time after partial occlusion at 7 mmHg.

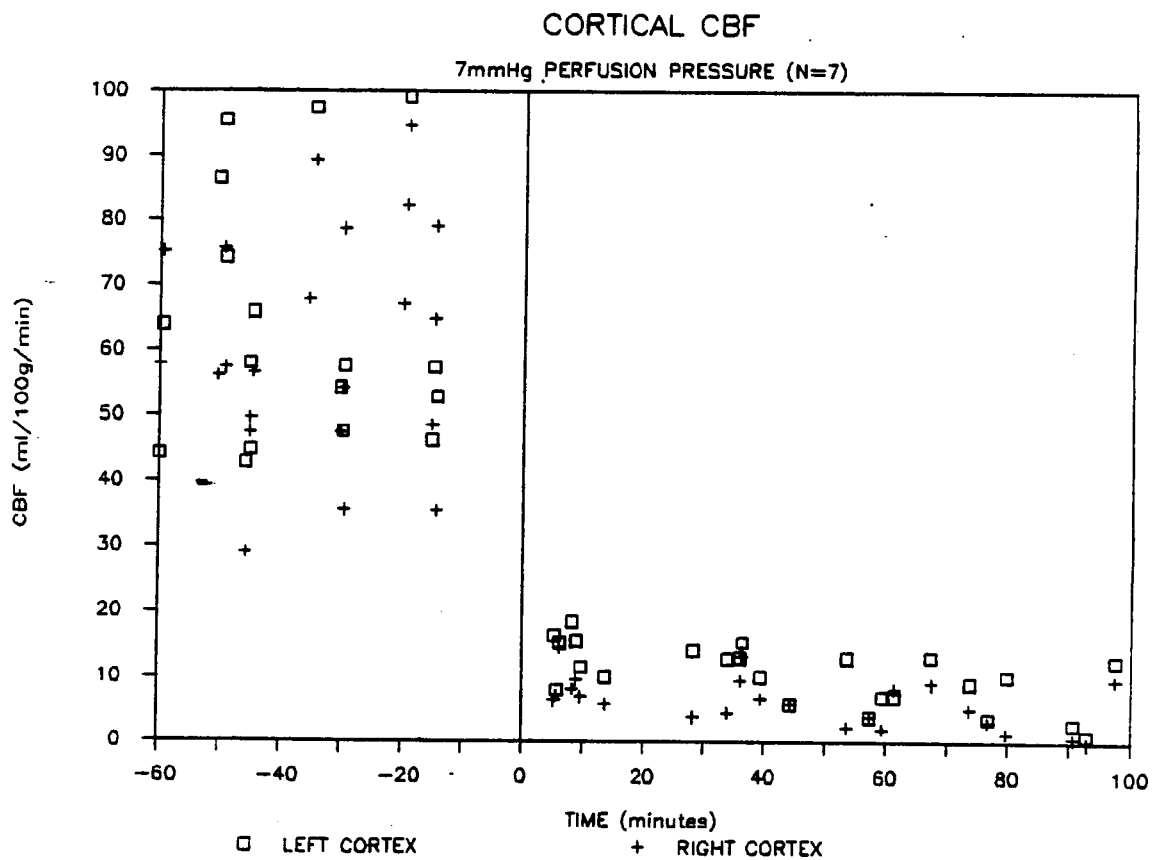
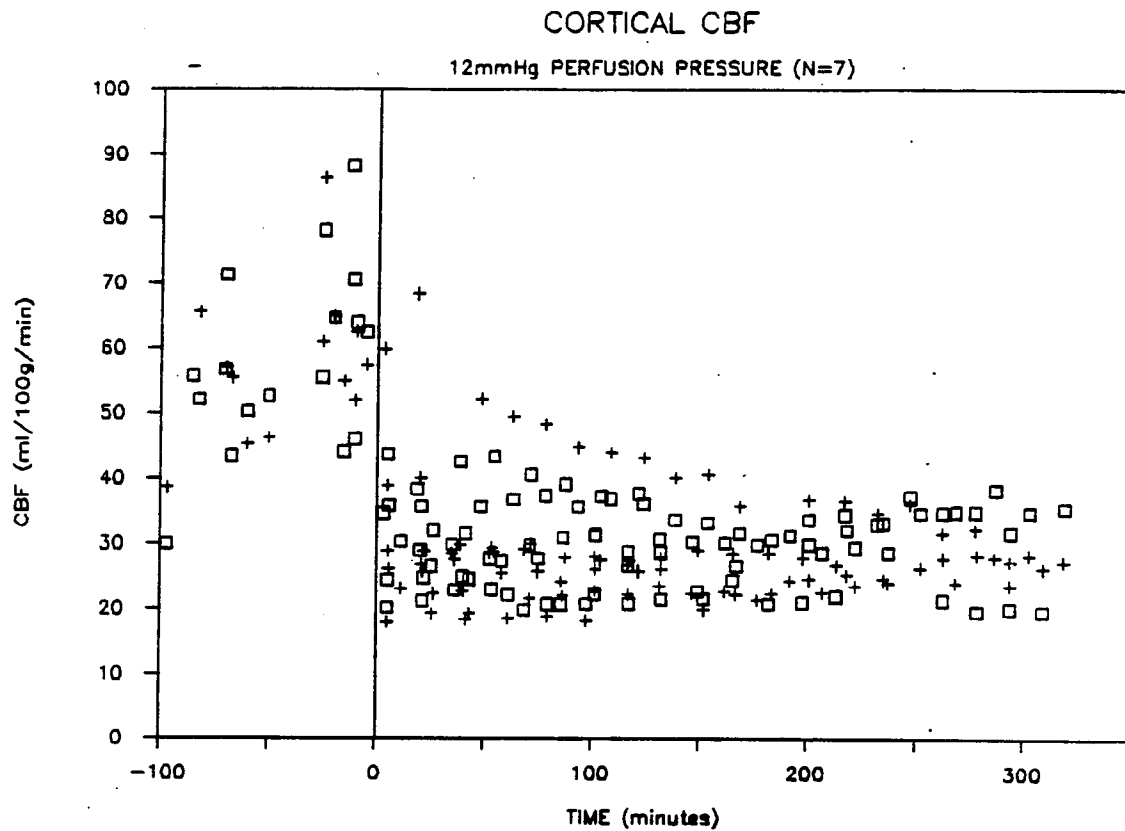


## FIGURE D-6

BILATERAL CORTICAL-HIPPOCAMPAL FAST EEG  
AT 12 mmHg AND 7 mmHg PERFUSION PRESSURE

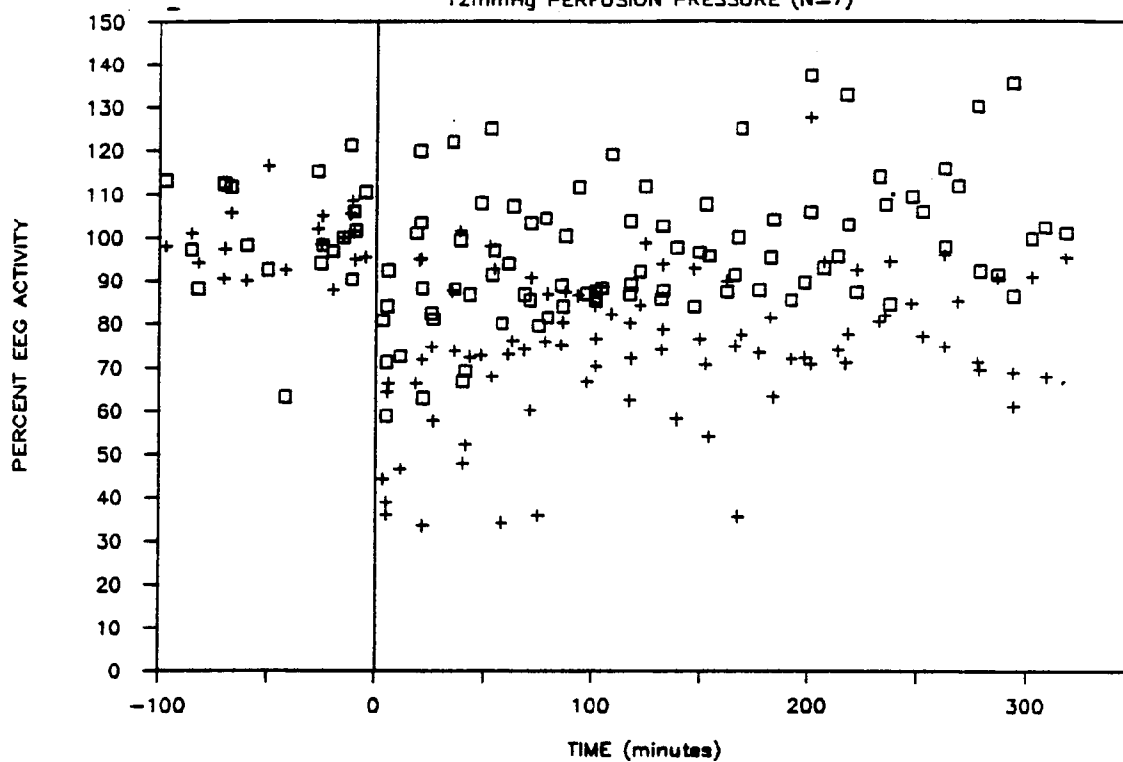
Percent fast EEG activity is plotted as a function of time for both the right and left cortical-hippocampal areas at perfusion pressures of 12 mmHg and 7 mmHg. Partial occlusion of the left common carotid artery by the balloon was initiated at time zero. The average activity in both the right and left cortical-hippocampal areas before partial occlusion represents the control value or 100% activity. All of the individual points throughout the experiment are then computed as a percentage of the control value.

Figure D-6a. At 12 mmHg perfusion pressure, the average CBF in the left cortex and hippocampus is  $29.8 \pm 6.3$  ml/100g/min and  $29.1 \pm 6.1$  ml/100g/min, respectively. The relative EEG activity measured between the left cortex and hippocampus is  $96.1 \pm 15.6\%$  which compares closely to the control value. The average CBF in the right cortex and hippocampus is  $29.0 \pm 7.8$  ml/100g/min and  $18.7 \pm 3.1$  ml/100g/min, respectively, and the relative EEG activity is  $74.7 \pm 17.1\%$  which is significantly lower ( $p < 0.05$ ) than that reported on the contralateral side. Since the CBF in the cortex is essentially the same on both sides, the reduction in EEG activity on the right side is probably due to the reduced activity in the right hippocampus. Thus, a 11 ml/100g/min drop in flow in the hippocampus without changing cortical flow resulted in a reduction in EEG activity by approximately 25%.

Figure D-6b. At 7 mmHg perfusion pressure, the average CBF in the left cortex and hippocampus is  $10.4 \pm 4.7$  ml/100g/min and  $12.6 \pm 4.0$  ml/100g/min, respectively. The relative EEG activity measured between the left cortex and hippocampus is  $33.0 \pm 26.4\%$ . The average CBF in the right cortex and hippocampus is  $6.2 \pm 3.7$  ml/100g/min and  $5.2 \pm 2.3$  ml/100g/min, respectively, and the relative EEG activity is  $12.9 \pm 9.3\%$  which is significantly lower ( $p < 0.05$ ) than that reported on the contralateral side. Thus, a further reduction in perfusion pressure of 5 mmHg to 7 mmHg resulted in a decrease in relative EEG activity of approximately 62% bilaterally..

## CORTICAL-HIPPOCAMPAL FAST EEG

12mmHg PERFUSION PRESSURE (N=7)



## CORTICAL-HIPPOCAMPAL FAST EEG

7mmHg PERFUSION PRESSURE (N=7)

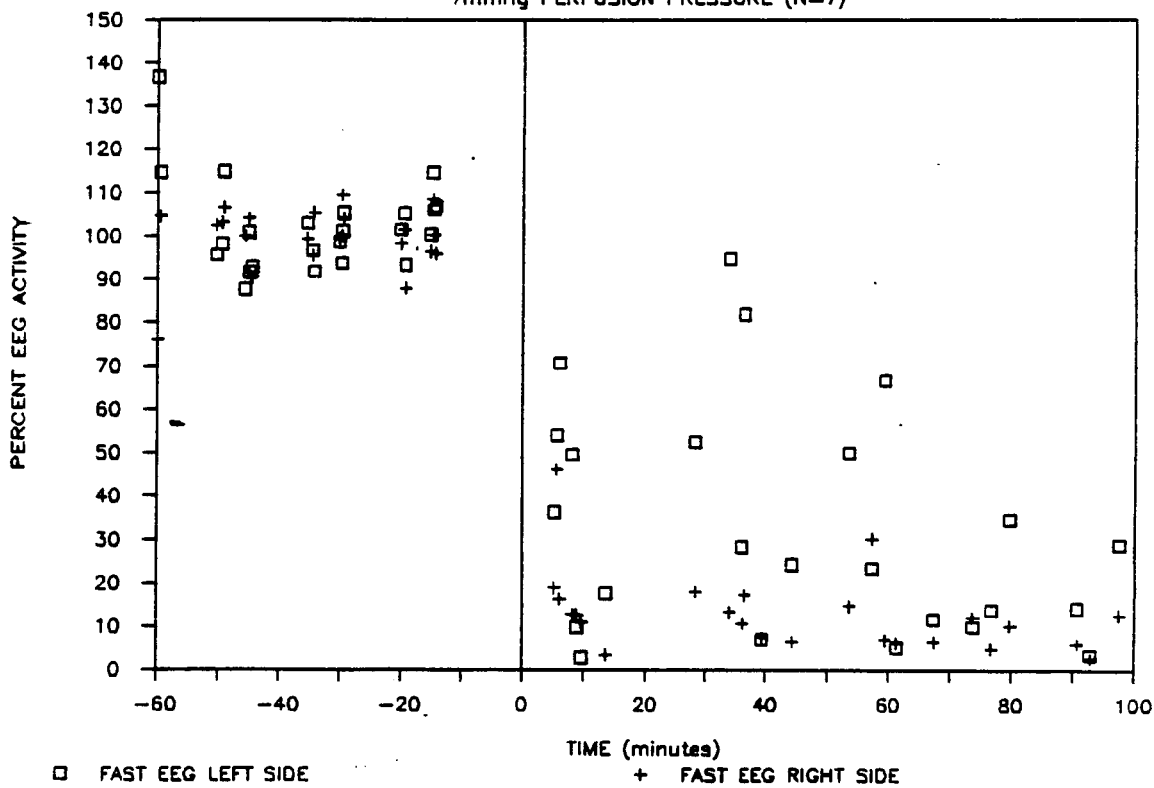


## FIGURE D-7

BILATERAL THALAMIC-SUBSTANTIA NIGRAL FAST EEG  
AT 12 mmHg AND 7 mmHg PERFUSION PRESSURE

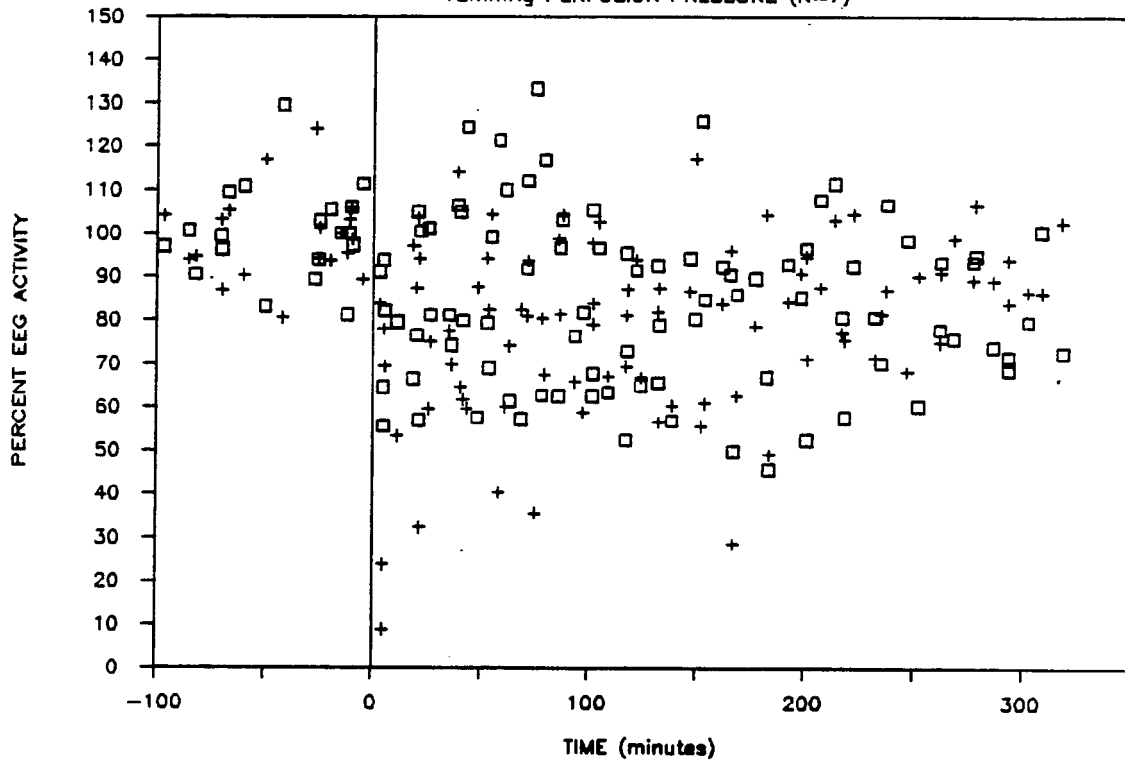
Percent fast EEG activity is plotted as a function of time for both the right and left thalamic-substantia nigral areas at perfusion pressures of 12 mmHg and 7 mmHg. Partial occlusion of the left common carotid artery by the balloon was initiated at time zero. The average activity in both the right and left thalamic-substantia nigral areas before partial occlusion represents the control value or 100% activity. All of the individual points throughout the experiment are then computed as a percentage of the pre-ischemic value.

Figure D-7a. At 12 mmHg perfusion pressure, the average CBF in the left thalamus and substantia nigra is  $36.3 \pm 9.2$  ml/100g/min and  $41.7 \pm 8.2$  ml/100g/min, respectively. The relative EEG activity measured between the left thalamus and substantia nigra is  $83.8 \pm 19.4\%$ . The average CBF in the right thalamus and substantia nigra is  $13.7 \pm 8.7$  ml/100g/min and  $18.5 \pm 3.1$  ml/100g/min, respectively, and the relative EEG activity is  $78.6 \pm 20.4\%$  which is not significantly different than that reported on the contralateral side. Thus, a 22 ml/100g/min drop in flow in both the thalamus and substantia nigra did not result in a significant differential reduction in EEG activity.

Figure D-7b. At 7 mmHg perfusion pressure, the average CBF in the left thalamus and substantia nigra is  $14.4 \pm 4.0$  ml/100g/min and  $17.1 \pm 6.0$  ml/100g/min, respectively. The relative EEG activity measured between the left thalamus and substantia nigra is  $63.6 \pm 43.8\%$ . The average CBF in the right thalamus and substantia nigra is  $2.31.4$  ml/100g/min and  $4.5 \pm 2.6$  ml/100g/min, respectively, and the relative EEG activity is  $36.1 \pm 38.0\%$  which is not significantly different than that reported on the contralateral side.

## THALAMIC-SUBSTANTIA NIGRAL FAST EEG

12mmHg PERFUSION PRESSURE (N=7)



## THALAMIC-SUBSTANTIA NIGRAL FAST EEG

7mmHg PERFUSION PRESSURE (N=7)

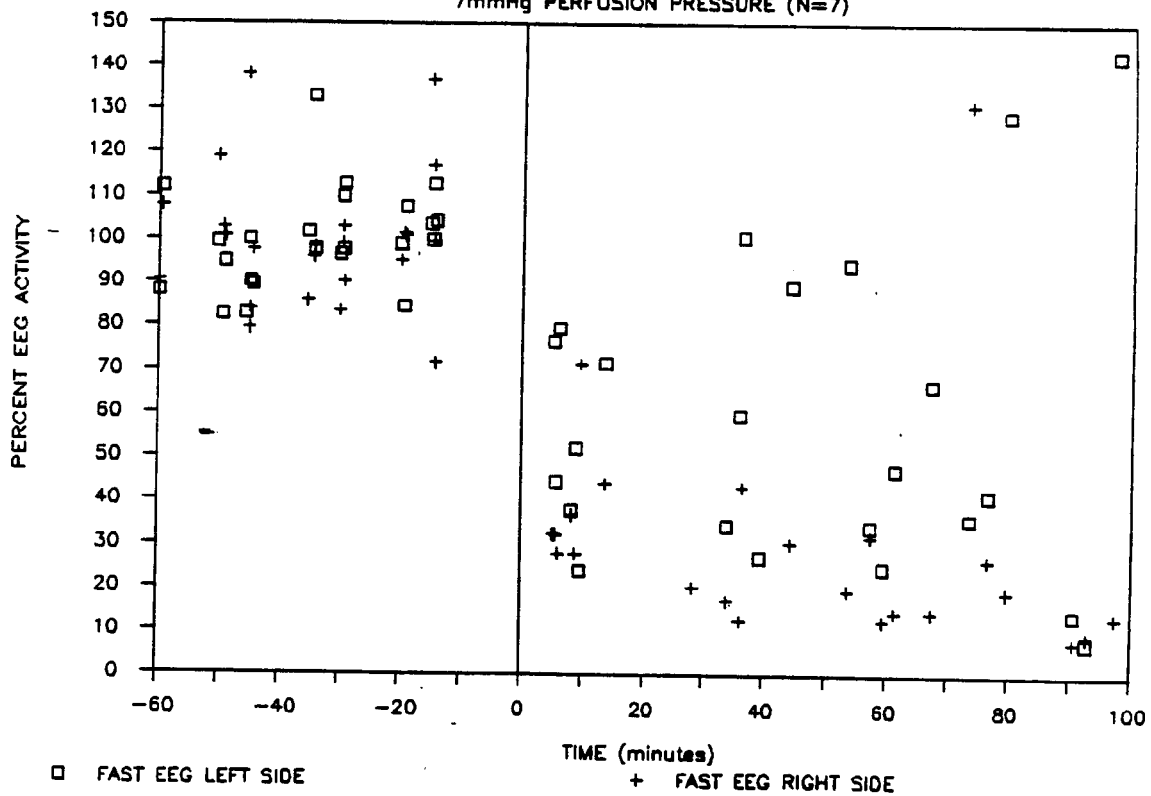


## FIGURE D-8

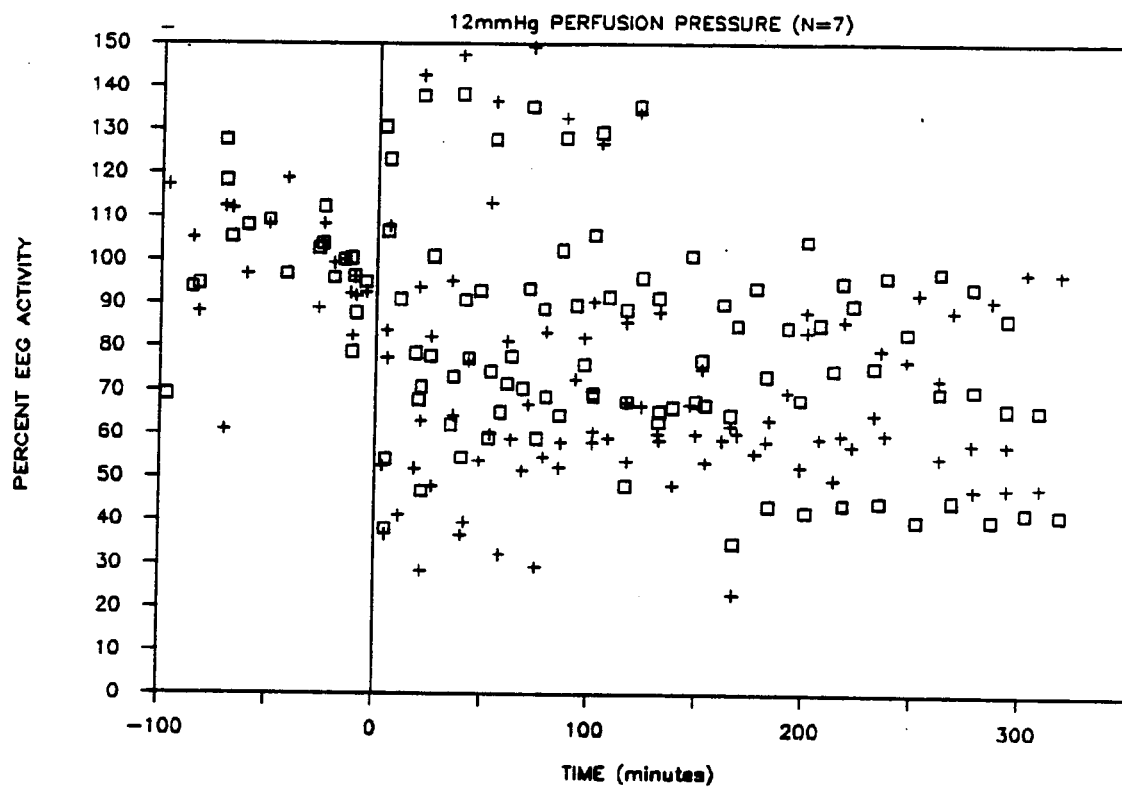
**BILATERAL CORTICAL-HIPPOCAMPAL SLOW EEG  
AT 12 mmHg AND 7 mmHg PERFUSION PRESSURE**

Percent slow EEG activity is plotted as a function of time for both the right and left cortical-hippocampal areas at perfusion pressures of 12 mmHg and 7 mmHg. Partial occlusion of the left common carotid artery by the balloon was initiated at time zero. The average activity in both the right and left cortical-hippocampal areas before partial occlusion represents the control value or 100% activity. All of the individual points throughout the experiment are then computed as a percentage of the pre-ischemic value.

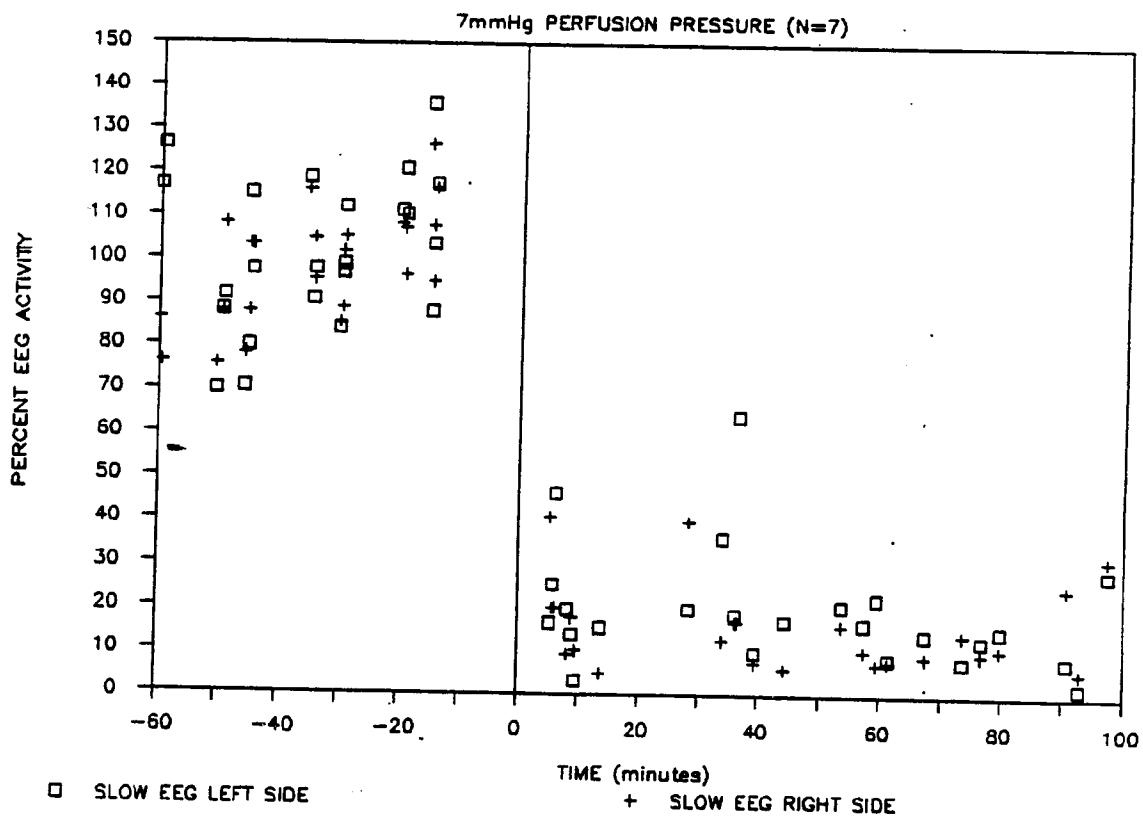
Figure D-8a. At 12 mmHg perfusion pressure, the average CBF in the left cortex and hippocampus is  $29.8 \pm 6.3$  ml/100g/min and  $29.1 \pm 6.1$  ml/100g/min, respectively. The relative slow EEG activity measured between the left cortex and hippocampus is  $79.2 \pm 25.4\%$ . The average CBF in the right cortex and hippocampus is  $29.0 \pm 7.8$  ml/100g/min and  $18.7 \pm 3.1$  ml/100g/min, respectively, and the relative slow EEG activity is  $70.9 \pm 27.0\%$  which is not significantly different than that reported on the contralateral side.

Figure D-8b. At 7 mmHg perfusion pressure, the average CBF in the left cortex and hippocampus is  $10.4 \pm 4.7$  ml/100g/min and  $12.6 \pm 4.0$  ml/100g/min, respectively. The relative EEG activity measured between the left cortex and hippocampus is  $19.3 \pm 13.7\%$ . The average CBF in the right cortex and hippocampus is  $6.2 \pm 3.7$  ml/100g/min and  $5.2 \pm 2.3$  ml/100g/min, respectively, and the relative EEG activity is  $15.5 \pm 10.0\%$  which is not significantly different than that reported on the contralateral side. Thus, a further reduction in perfusion pressure of 5 mmHg to 7 mmHg resulted in a decrease in relative slow EEG activity of approximately 60% bilaterally..

## CORTICAL-HIPPOCAMPAL SLOW EEG



## CORTICAL-HIPPOCAMPAL SLOW EEG



## FIGURE D-9

BILATERAL THALAMIC-SUBSTANTIA NIGRAL SLOW EEG  
AT 12 mmHg AND 7 mmHg PERFUSION PRESSURE

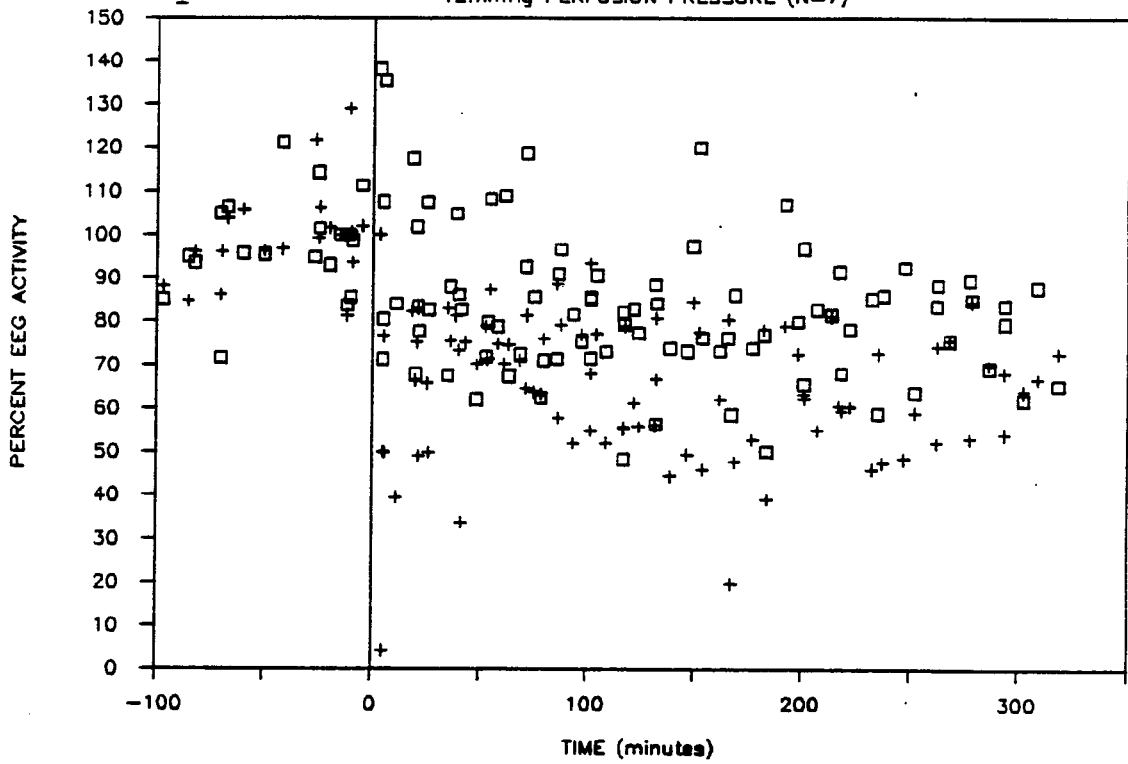
Percent slow EEG activity is plotted as a function of time for both the right and left thalamic-substantia nigral areas at perfusion pressures of 12 mmHg and 7 mmHg. Partial occlusion of the left common carotid artery by the balloon was initiated at time zero. The average activity in both the right and left thalamic-substantia nigral areas before partial occlusion represents the control value or 100% activity. All of the individual points throughout the experiment are then computed as a percentage of the pre-ischemic value.

Figure D-9a. At 12 mmHg perfusion pressure, the average CBF in the left thalamus and substantia nigra is  $36.3 \pm 9.2$  ml/100g/min and  $41.7 \pm 8.2$  ml/100g/min, respectively. The relative slow EEG activity measured between the left thalamus and substantia nigra is  $84.0 \pm 19.6\%$ . The average CBF in the right thalamus and substantia nigra is  $13.7 \pm 8.7$  ml/100g/min and  $18.5 \pm 3.1$  ml/100g/min, respectively, and the relative slow EEG activity is  $65.1 \pm 15.9\%$  which is significantly lower ( $p < .05$ ) than that reported on the contralateral side. Thus, a 22 ml/100g/min drop in flow in both the thalamus and substantia nigra resulted in a significant reduction in slow EEG activity by approximately 20%.

Figure D-9b. At 7 mmHg perfusion pressure, the average CBF in the left thalamus and substantia nigra is  $14.4 \pm 4.0$  ml/100g/min and  $17.1 \pm 6.0$  ml/100g/min, respectively. The relative slow EEG activity measured between the left thalamus and substantia nigra is  $69.4 \pm 57.6\%$ . The average CBF in the right thalamus and substantia nigra is  $2.3 \pm 1.4$  ml/100g/min and  $4.5 \pm 2.6$  ml/100g/min, respectively, and the relative slow EEG activity is  $37.8 \pm 41.2\%$  which is not significantly different than that reported on the contralateral side.

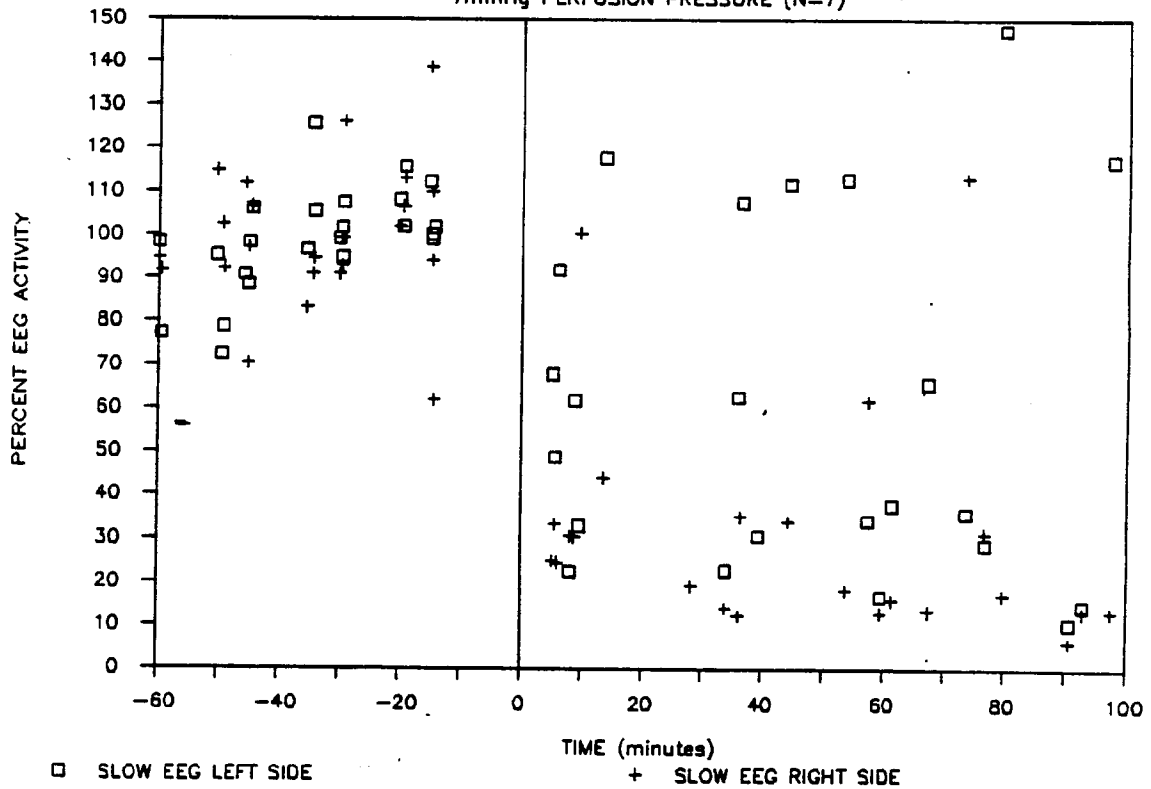
THALAMIC-SUBSTANTIA NIGRAL SLOW EEG

12mmHg PERFUSION PRESSURE (N=7)



THALAMIC-SUBSTANTIA NIGRAL SLOW EEG

7mmHg PERFUSION PRESSURE (N=7)



□ SLOW EEG LEFT SIDE

+ SLOW EEG RIGHT SIDE

**FIGURE D-10**  
**CONTROL OF PERFUSION PRESSURE**  
**AT 9 mmHg**

Perfusion pressure is plotted as a function of time for the 9 mmHg animal series. Partial occlusion of the left common carotid artery by the balloon was initiated at time zero. The mean control pressure with standard deviation for the seven animals in each group is provided on the illustration.

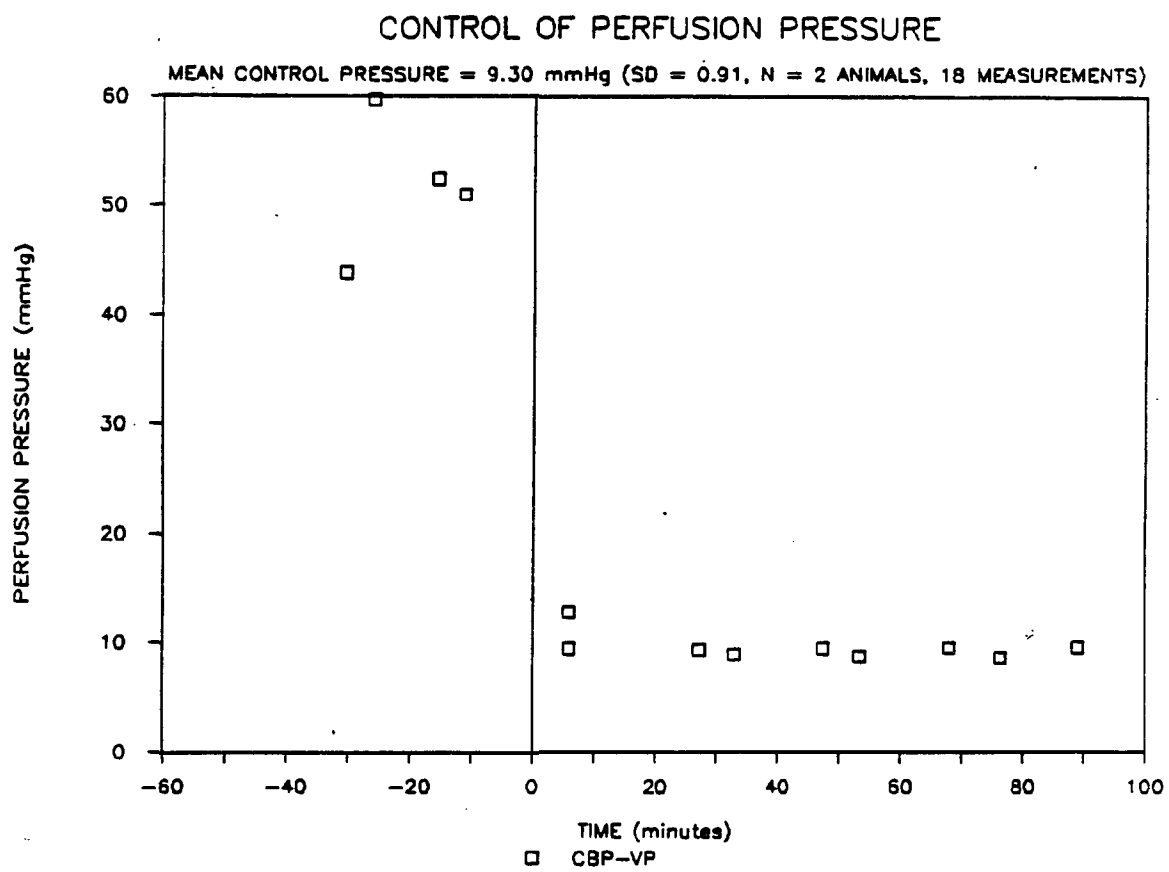


## FIGURE D-11

**BILATERAL CORTICAL AND HIPPOCAMPAL CBF  
AT 9 mmHg PERFUSION PRESSURE**

Cerebral blood flow is plotted as a function of time for both the right and left cortex and hippocampus at a perfusion pressure of 9 mmHg. Time zero represents the time at which partial occlusion of the left common carotid artery was initiated.

In Figure D-11a, both the right and left cortical CBF's in this series of animals were not significantly different from each another before or after time zero.

In Figure D-11b, both the right and left hippocampal CBF's in this series of animals were also not significantly different from each another before or after time zero.

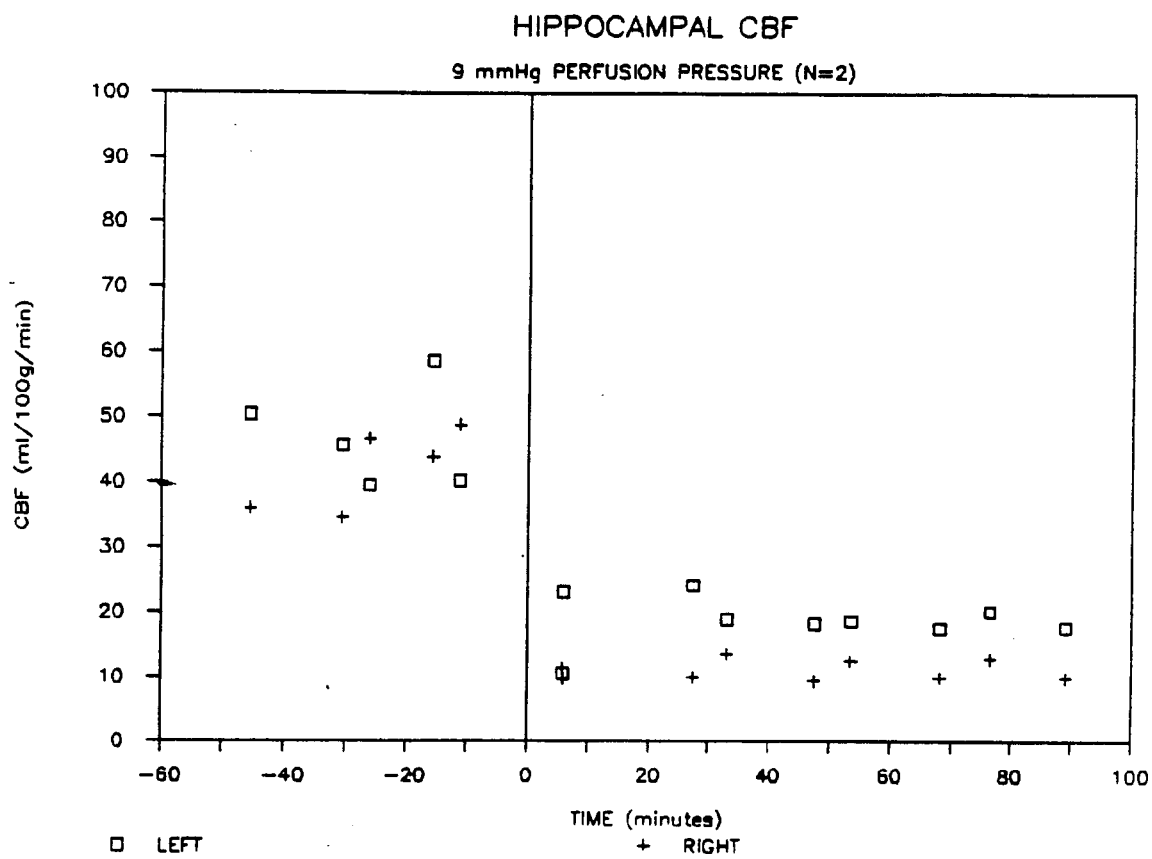
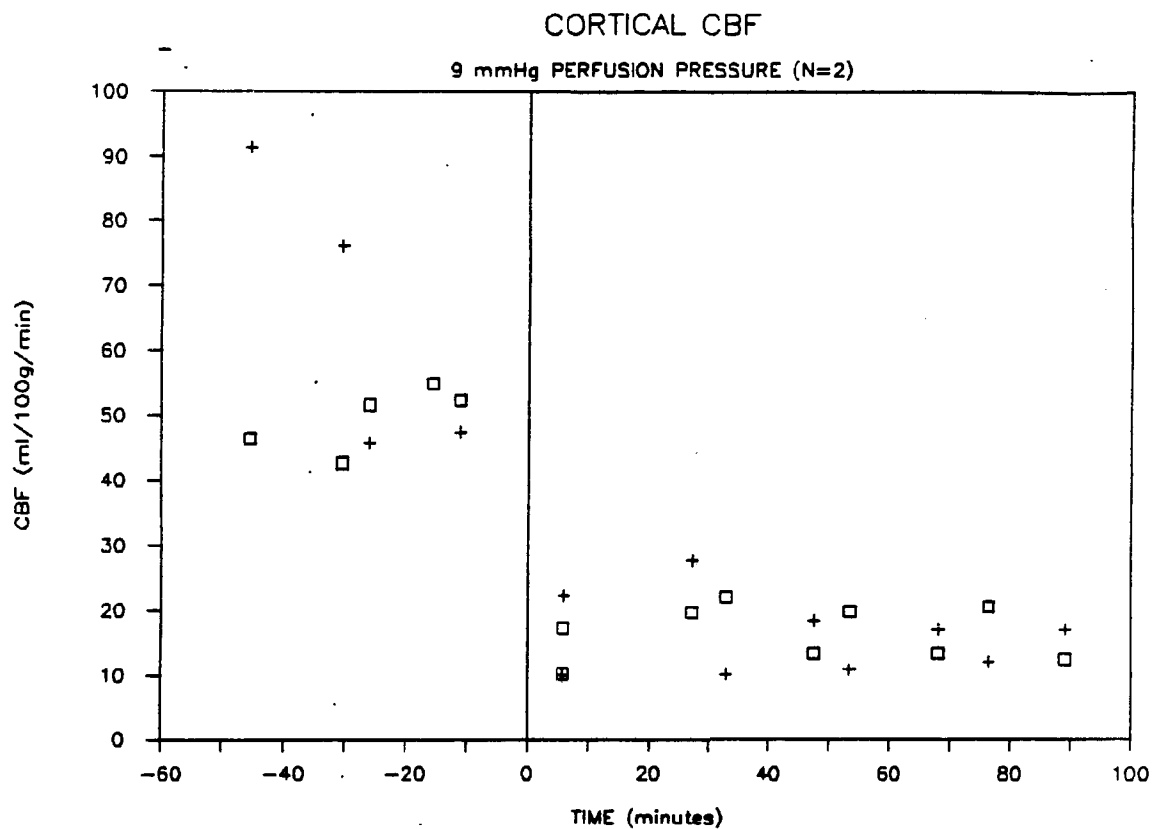


## FIGURE D-12

**BILATERAL THALAMIC AND SUBSTANTIA NIGRAL CBF  
AT 9 mmHg PERFUSION PRESSURE**

Cerebral blood flow is plotted as a function of time for both the right and left thalamus and substantia nigra at a perfusion pressure of 9 mmHg. Partial occlusion of the left common carotid artery was initiated at time zero.

In Figure D-12a, left thalamic CBF is significantly greater ( $p < 0.05$ ) than right thalamic CBF by being  $22.2 \pm 4.9$  ml/100g/min as compared to  $8.7 \pm 1.3$  ml/100g/min, respectively.

In Figure D-12b, left substantia nigral CBF is significantly greater ( $p < 0.05$ ) than right substantia nigral CBF by being  $28.2 \pm 5.5$  ml/100g/min as compared to  $13.8 \pm 2.3$  ml/100g/min, respectively.

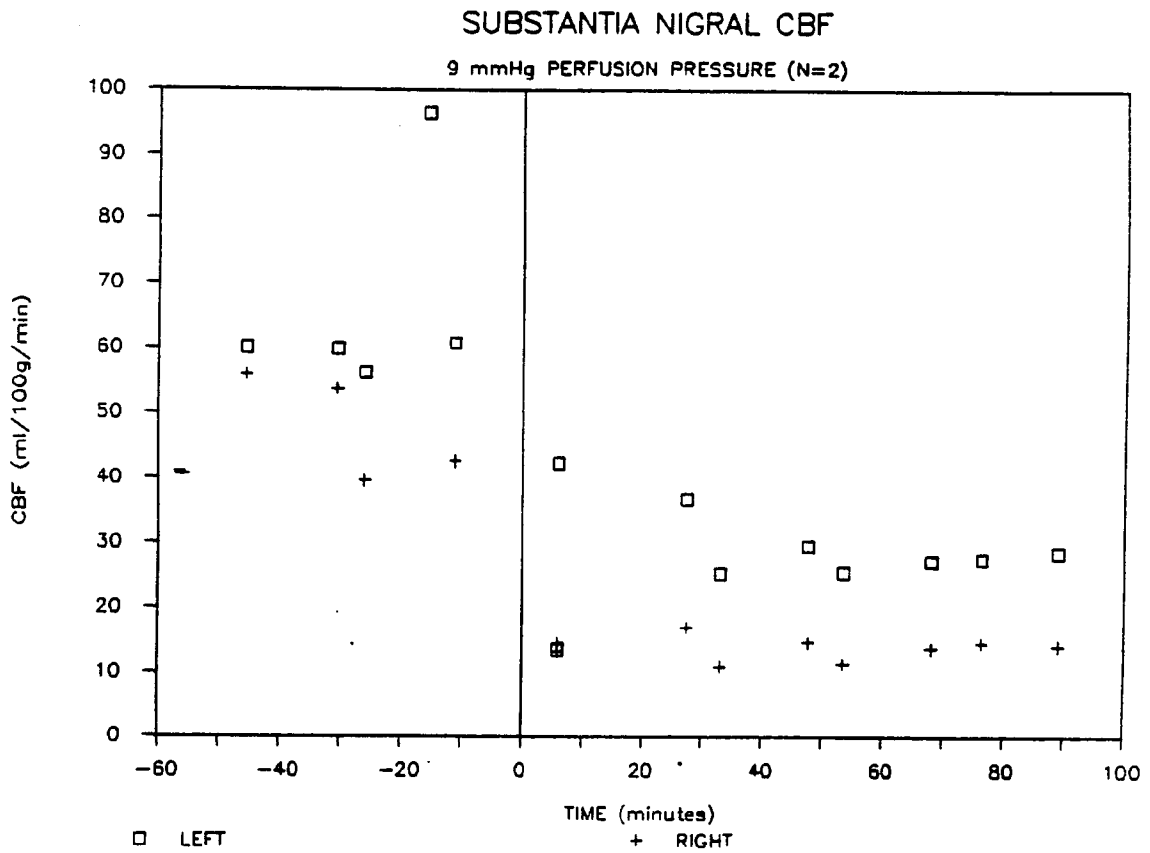
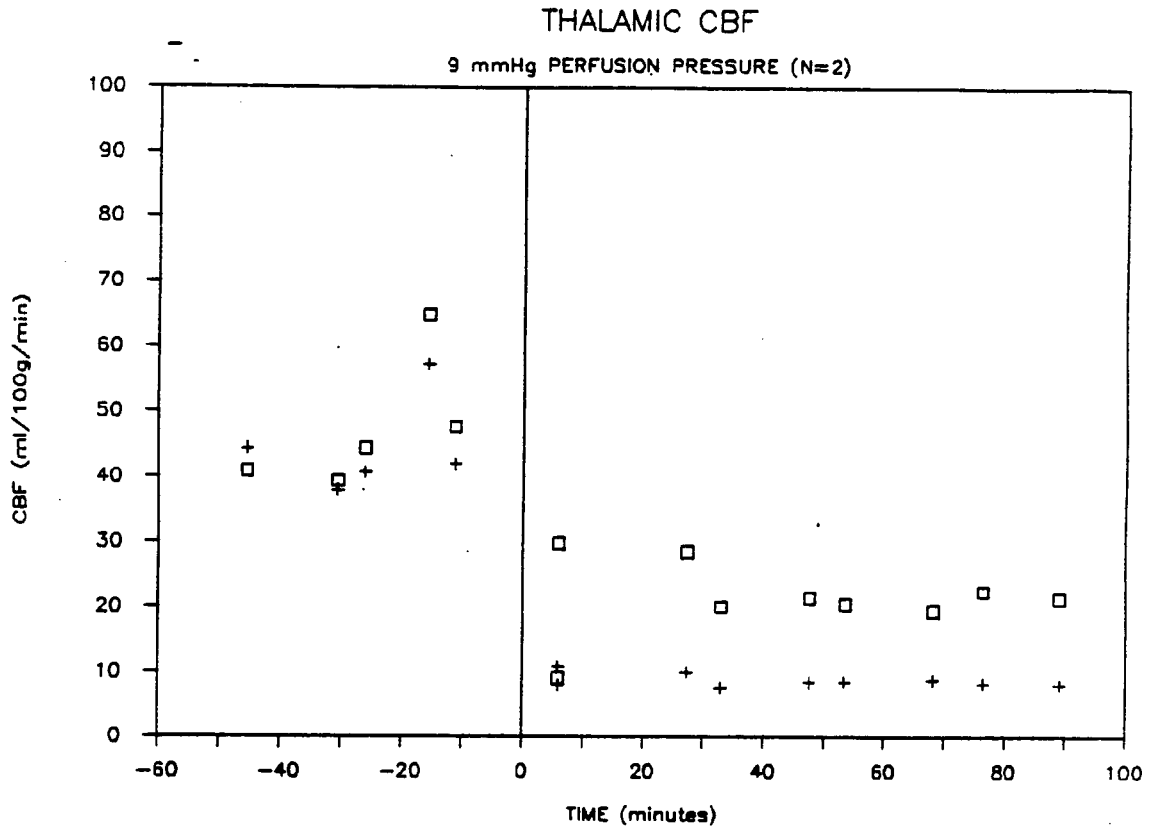


## FIGURE D-13

BILATERAL CORTICAL-HIPPOCAMPAL FAST AND SLOW EEG  
AT 9 mmHg PERFUSION PRESSURE

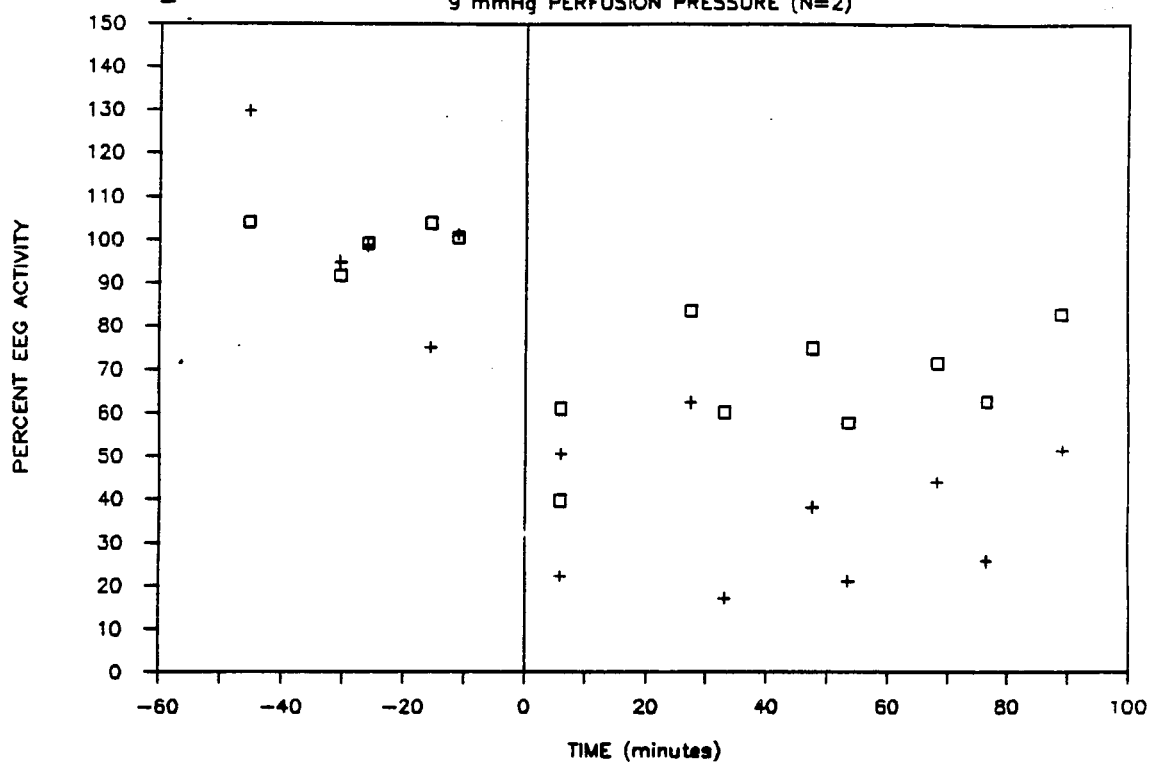
Percent fast and slow EEG activity is plotted as a function of time for both the right and left cortical-hippocampal areas at a perfusion pressure of 9 mmHg. Partial occlusion of the left common carotid artery by the balloon was initiated at time zero. The average activity in both the right and left cortical-hippocampal areas before partial occlusion represents the control value or 100% activity. All of the individual points throughout the experiment are then computed as a percentage of the pre-ischemic value. At 9 mmHg perfusion pressure, the average CBF in the left cortex and hippocampus is  $18.9 \pm 5.5$  ml/100g/min and  $19.5 \pm 3.6$  ml/100g/min, respectively, while the average CBF in the right cortex and hippocampus is  $14.9 \pm 4.4$  ml/100g/min and  $11.5 \pm 2.2$  ml/100g/min, respectively.

In Figure D-13a, the relative fast EEG activity measured between the left cortex and hippocampus is  $67.0 \pm 10.6\%$  which is significantly higher ( $p < 0.05$ ) than that reported on the contralateral side which is  $28.1 \pm 13.9\%$ . Thus, a 4 to 7 ml/100g/min drop in CBF resulted in a differential reduction in fast EEG activity by approximately 40%.

In Figure D-13b, the relative slow EEG activity measured between the left cortex and hippocampus is  $52.4 \pm 7.8\%$  which is not significantly different than that reported on the contralateral side which is  $25.3 \pm 11.9\%$ .

## CORTICAL-HIPPOCAMPAL FAST EEG

9 mmHg PERFUSION PRESSURE (N=2)



## CORTICAL-HIPPOCAMPAL SLOW EEG

9 mmHg PERFUSION PRESSURE (N=2)

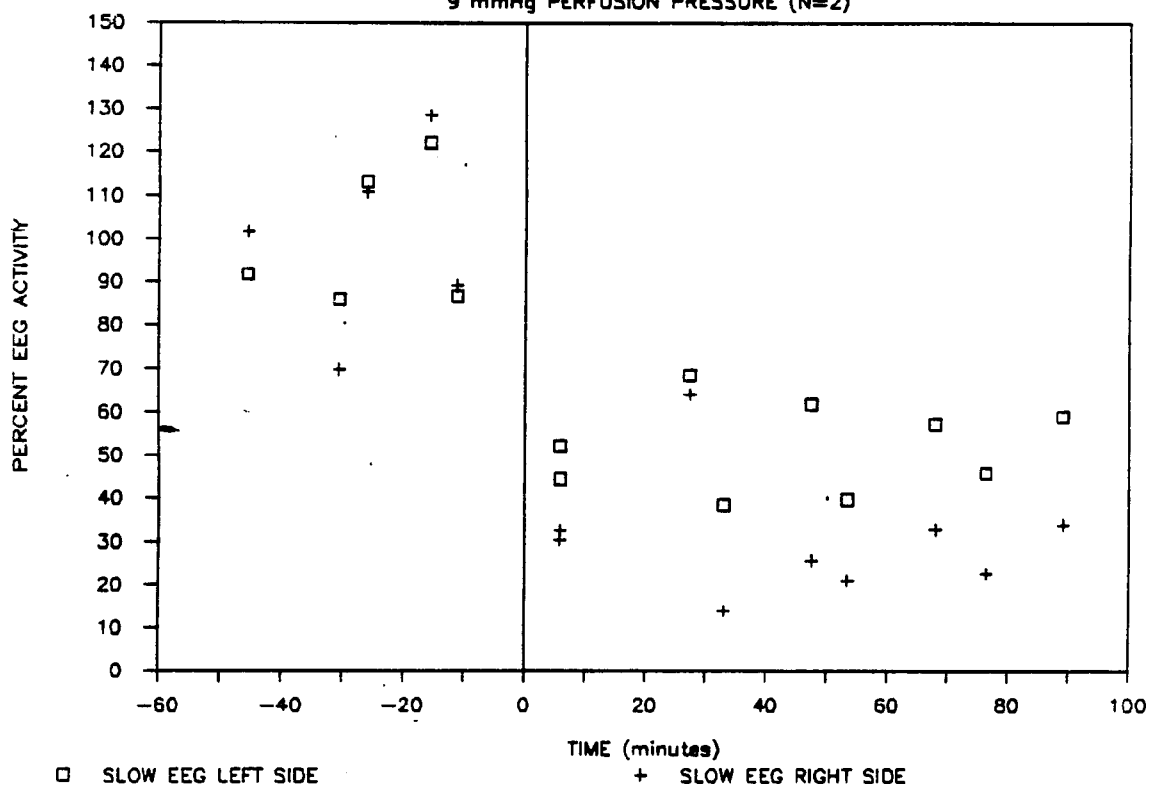


## FIGURE D-14

BILATERAL THALAMIC-SUBSTANTIA NIGRAL FAST AND SLOW EEG  
AT 9 mmHg PERFUSION PRESSURE

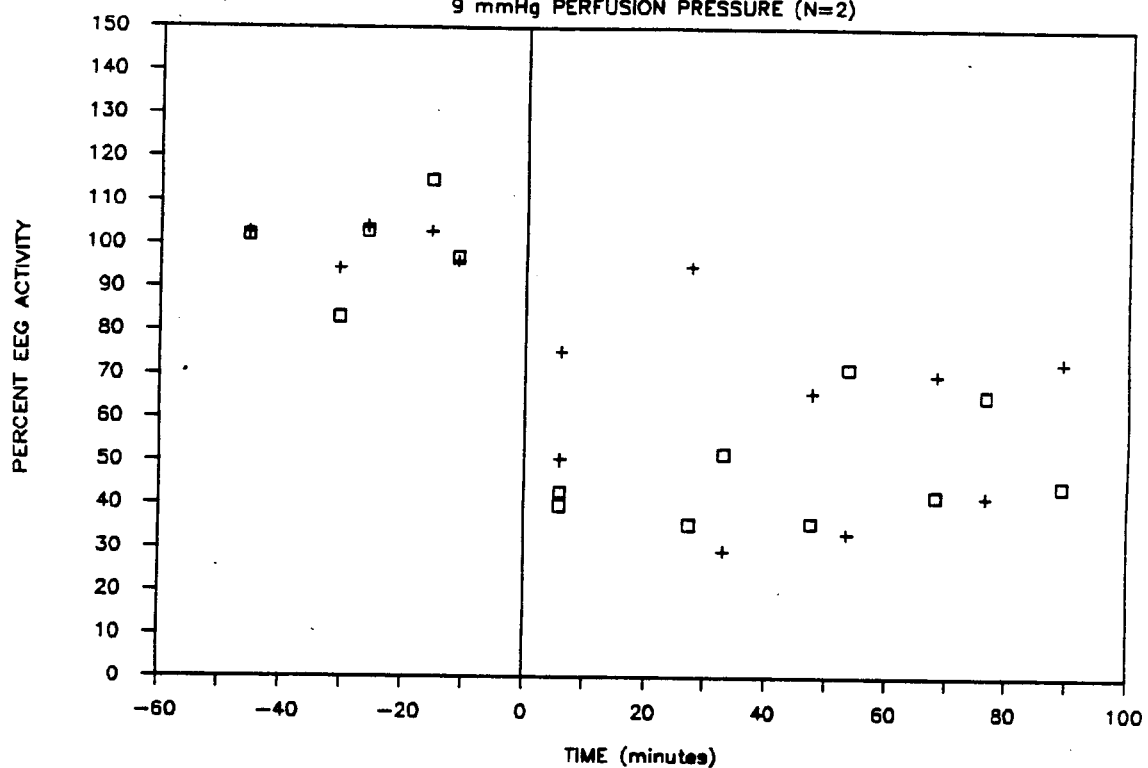
Percent fast and slow EEG activity is plotted as a function of time for both the right and left thalamic-substantia nigral areas at a perfusion pressure of 9 mmHg. Partial occlusion of the left common carotid artery by the balloon was initiated at time zero. The average activity in both the right and left thalamic-substantia nigral areas before partial occlusion represents the control value or 100% activity. All of the individual points throughout the experiment are then computed as a percentage of the pre-ischemic value. At 9 mmHg perfusion pressure, the average CBF in the left thalamus and substantia nigra is  $22.2 \pm 4.9$  ml/100g/min and  $28.2 \pm 5.5$  ml/100g/min, respectively, while the average CBF in the right thalamus and substantia nigra is  $8.7 \pm 1.3$  ml/100g/min and  $13.8 \pm 2.3$  ml/100g/min, respectively.

In Figure D-14a, the relative fast EEG activity measured between the left thalamus and substantia nigra is  $53.6 \pm 16.9\%$  which is not significantly different than that reported on the contralateral side which is  $58.2 \pm 16.4\%$ . Thus, a 13 to 14 ml/100g/min drop in CBF in both areas resulted in no significant differential reduction in fast EEG activity.

In Figure D-14b, the relative slow EEG activity measured between the left thalamus and substantia nigra is  $43.2 \pm 9.3\%$  which is not significantly different than that reported on the contralateral side which is  $55.5 \pm 14.8\%$ .

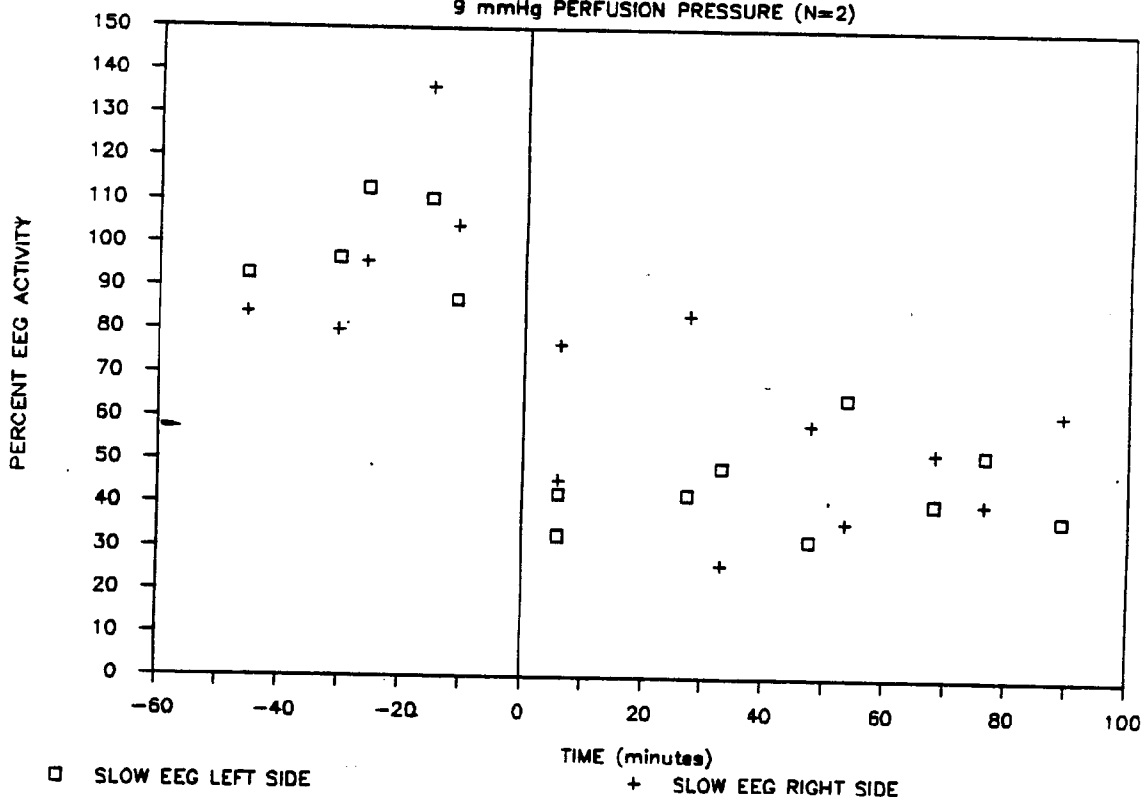
THALAMIC-SUBSTANTIA NIGRAL FAST EEG

9 mmHg PERFUSION PRESSURE (N=2)



THALAMIC-SUBSTANTIA NIGRAL SLOW EEG

9 mmHg PERFUSION PRESSURE (N=2)



□ SLOW EEG LEFT SIDE

+ SLOW EEG RIGHT SIDE

## REFERENCES

- Adams RN. *Electrochemistry at Solid Electrodes*. New York, Marcel Dekker Inc., 1969.
- Astrup J, Siesjo BK, Symon L. Thresholds of cerebral ischemia. The Ischemic Penumbra. *Stroke* 12:723-725, 1981.
- Aukland K, Bower BF, Berliner RW. Measurement of local blood flow with hydrogen gas. *Circ Res* 14:164, 1964.
- Aukland K, Kiil F, Kjekshus J, et al. Local myocardial blood flow measured by hydrogen polarography: Distribution and effect of hypoxia. *Acta Physiol. Scand.* 70: 99-111, 1967.
- Ball EG. Studies on oxidation-reduction. XXIII. Ascorbic acid. *J. Biol. Chem.* 118:219-239, 1937.
- Barry DI, Strandgaard S, Graham DI, Braendstrup O, Svendsen UG, Vorstrup S, Hemmingsen R, Bolwig TG: Cerebral blood flow in rats with renal and spontaneous hypertension: Resetting of the lower limit of auto-regulation. *J Cereb Blood Flow & Metab* 2:347-353, 1982.
- Branston NM, Strong AJ, Symon L. Extracellular potassium activity, evoked potential and tissue blood flow: relationship during progressive ischemia in baboon cerebral cortex. *J Neurol Sci* 32:305, 1977.
- Branston NM, Symon L, Crockard HA, Pasztor E. Relationship between the structures of the brain measured in acute cat experiments by means of a new beta-sensitive semiconductor needle detector. *Exp. Brain Res.* 4:126-137, 1967.
- Brock M, Ingvar DH, Sem Jacobsen CW. Regional blood flow in deep cortical evoked potential and local cortical blood flow following acute middle cerebral artery occlusion in the baboon. *Exp Neurol* 45:195, 1974.
- Brown AW, Brierly JB. The nature, distribution, and earliest stages of anoxic-ischemic nerve cell damage in the rat brain as defined by the optical microscope. *Br. J. Exp. Pathol.* 49:87-106, 1968.
- Brown K, Cooper SJ. *Chemical Influences on Behavior*. London, Academic Press, 1979.

- Chen ST, Hsu CY, Hogan EL, Maricq H, Balentine JD. A model of focal ischemic stroke in the rat: Reproducible extensive cortical infarction. *Stroke* 17:738-743, 1986.
- Clark LC Jr, Barger LM. Left to right shunt detection by an intravascular electrode with hydrogen as an indicator. *Science* 130:709-710, 1959.
- Clark LC Jr, Barger LM. Detection and direct recording of right to left shunts with a hydrogen electrode catheter. *Surgery* 46:797-804, 1959.
- Coyle P, Jokelainen PT. Dorsal cerebral arterial collaterals of the rat. *Anat Rec* 203:397-404, 1982.
- Crockard A, Iannotti F, Hunstock AT, Smith RD, Harris RJ, Symon L. Cerebral blood flow and edema following carotid occlusion in the gerbil. *Stroke* 11:494-498, 1980.
- Dorland WA. *Dorland's Illustrated Medical Dictionary*, Twenty-sixth ed. Philadelphia: WB Saunders Co, 1984.
- Fazekas P, Zosch E, and Harsing L. Regional blood flow and collateral circulation of the tongue in the dog studied by hydrogen polarography. *Oral Surg.* 46: 755-758, 1978.
- Fein JM, Lipow K, Marmarou A. Cortical artery pressure in normotensive and hypertensive aneurysm patients. *J Neurosurg* 59:51-56, 1983.
- Fein JM, Willis J, Hamilton J, et al. Polarographical measurement of local cerebral blood flow in the conscious and anesthetized primate. *Stroke* 6:42-51, 1975.
- Fick A. *Über die Messung des Blutquantums in den Herzventrikeln.* *Verhandl d phys - med Ges - u Würzburg* 2: xvi, 1870. (Quoted in its entirety by Hoff HE and Scott HJ, *N. Engl. J. Med.* 239:122, 1948)
- Fieschi C, Agnoli A, Battistini N, Bozzao L, Principe M. Derangement of regional cerebral blood flow and of its regulatory mechanisms in acute cerebrovascular lesions. *Neurology (Minneap)* 18:1166-1179, 1968.
- Fieschi C, Bozzao L, Agnoli A. Regional clearance of hydrogen as a measure of cerebral blood flow. *Acta Neurol. Scand.* 41 (Suppl. 14):46, 1965.
- Fieschi C, Bozzao L, Agnoli A, et al. The hydrogen method of measuring local blood flow in subcortical structures of the brain, including a comparative study with the <sup>14</sup>C-antipyrine method. *Exp. Brain Res.* 7:111, 1969.
- Flamm ES, Demopoulos HB, Seligman ML, et al. Free radicals in cerebral ischemia. *Stroke* 9:445-447, 1978.
- Fujishima M, Omae T. Lower limit of cerebral autoregulation in normotensive and spontaneously hypertensive rats. *Experientia* 32: 1019-1021, 1976.
- Fujishima M, Omae T. Carotid back pressure following bilateral carotid

- occlusion in normotensive and spontaneously hypertensive rats. *Experientia* 32: 1021-1022, 1976.
- Furlow TW. Cerebral ischemia produced by four-vessel occlusion in the rat: A quantitative evaluation of cerebral blood flow. *Stroke* 13:852-855, 1982.
- Garcia JH. Circulatory disorders and their effects on the brain. In: *Textbook of Neuropathology* (Davis RL, Robertson DM, eds), Baltimore: Williams and Wilkins, 1985.
- Garcia JH. Experimental ischemic stroke: A review. *Stroke* 15:5-14, 1983.
- Garcia JH, Mitchem HL, Briggs L, Morawetz R, Hudetz AG, Hazelrig J, Halsey JH, Conger KA: Transient focal ischemia in subhuman primates: Neuronal injury as a function of local cerebral blood flow. *J. Neuropath Exp Neurol* 42:44-60, 1983.
- Gilman AG, Goodman LS, Gilman A. *The Pharmacological Basis of Therapeutics, Sixth Edition*. MacMillan Pub Co, Inc, New York. 1980.
- Haining JL, Turner D, Pantall RM. Measurement of local cerebral blood flow in the unanesthetized rat using a hydrogen clearance method. *Circ Res* 23:313, 1968.
- Halsey JH, Capra NF. Physiological modification of immediate ischemia due to experimental middle cerebral occlusion - its relevance to cerebral infarction. *Stroke* 2:239-246, 1971.
- Halsey JH, Capra NF, McFarland RS. Use of hydrogen for measurement of regional cerebral blood flow - problem of intercompartmental diffusion. *Stroke* 8:351-357, 1977.
- Halsey JH, Clark LC. Some regional circulatory abnormalities following experimental cerebral infarction. *Neurology (Minneap)* 20:238-246, 1970.
- Heiss WD, Hayakawa T, Waltz AG. Cortical neuronal function during ischemia. *Arch Neurol.* 33:813-820, 1976.
- Hester RL, Granger JP, Williams J, Hall JE. Acute and chronic servo-control of renal perfusion pressure. *Am. J. Physiol.* 244:F455-F460, 1983.
- Hoffman WE, Miletich DJ, Albrecht RF. Cerebrovascular response to hypotension in hypertensive Rats: Effect of antihypertensive therapy. *Anesthesiology* 58:326-332, 1983.
- Hoffman WE, Miletich DJ, Albrecht RF. Maintenance of cerebral blood flow and metabolism during pharmacological hypotension in aged hypertensive rats. *Neurobiology of Aging* 3:101-104, 1982.
- Hossman KA, Mies G, Paschen W, Matsuoka Y, Schuir FJ, Bosma HJ. Experimental infarcts in cats, gerbils, and rats. In: Stefanovich V (ed) *Stroke: Animal models*. Pergamon Press, Oxford, England, pp 123-137, 1983.
- Hudetz AG, Conger KA, Halsey JH, McCormick J, Wilson TA, Roesel JF:

- Changes in regional cerebrovascular resistance during partial ischemia in rats. *Advances in Exp Med Biol*, Vol 180 (Eds.) Bruley HI & Reneau D, Plenum Press, New York, pp. 111-120, 1985.
- Hudetz, AG, Conger KA, Halsey JH, Pal M, Dohan O. Pressure distribution in pial arterioles under normal and ischemic conditions in the rat brain. In: *Proc. IUPS Satellite Symposium, "Structure-Function Relation in the Microcirculatory Network,"* Budapest, 1985, p. 155 (Abstract)
- Hunt HR. *A Laboratory Manual of the Anatomy of the Rat.* New York, MacMillan, 1924.
- Hyman ES. Linear system for quantitating hydrogen at a platinum electrode. *Circ. Res.* 9:1093-1097, 1961.
- Iannotti F, Hoff JT, Schielke GP. Brain tissue pressure in focal cerebral ischemia. *J Neurosurg* 62:83-89, 1985.
- Iversen LL, Iversen SD, Snyder SH. *Handbook of Psychopharmacology, Vol. 9: Chemical Pathways in the Brain.* London, Plenum Press, 1978.
- Jamieson AD, Halsey JH. Regional cerebral blood flow determination by the hydrogen clearance technique and comparison with oxygen availability in the rabbit. *Stroke* 4:904-911, 1973.
- Jones RH, Molitoris BA. A statistical method for determining the breakpoint of two lines. *Analytical Biochem.* 141:287-290, 1984.
- Kameyama M, Suzuki J, Shirane R, Ogawa A. A new model of bilateral hemispheric ischemia in the rat-three vessel occlusion model. *Stroke* 16:489-496, 1985.
- Kety SS. The theory and applications of the exchange of inert gas at the lungs and tissue. *Pharmacol. Rev.* 3:1-41, 1951.
- Klingenberg I. The effect of radium on blood flow in the human uterine cervix measured by local hydrogen clearance. *Acta Obstet. Gynecol. Scand.* 53: 7-11, 1974.
- Kummer RV, Herold S. Hydrogen clearance method for determining local cerebral blood flow. I. Spatial resolution. *J. Cerebral Blood Flow and Metab.* 6:486-491, 1986.
- Kummer RV, Kries FV, Herold S. Hydrogen clearance method for determining local cerebral blood flow. II. Effect of heterogeneity in cerebral blood flow. *J. Cerebral Blood Flow and Metab.* 6:492-498, 1986.
- Lassen NA, and Christensen MS. Physiology of cerebral blood flow. *Br. J. Anesth.* 48:719-734, 1976.
- Lawrence JH, Loomis WF, Tobias CA, Turpin FH. Preliminary observations on the narcotic effect of xenon with a review of solubilities of gasses in water and oils. *J. Physiol.* 105:197-203, 1946.
- Levine S. Anoxic-ischemic encephalopathy in rats. *Am. J. Pathol.* 36:1-17,

1960.

- Lubbers DW, Wodick R, Stosseck K, et al. Problems concerning the hydrogen inhalation technique to determine the cerebral blood flow by means of palladinized Pt electrodes. In Brock M, Fieschi C, Ingvar DH, et al (eds) *Cerebral Blood Flow*. Berlin-New York, Springer, pp39-41, 1969.
- Martin GR. Studies on the tissue distribution of ascorbic acid. *Ann. N.Y. Acad. Sci.* 92:141-147, 1961.
- Menelow R, Picozzi P, Russell RR. Reperfusion after cerebral ischemia: Influence of duration of ischemia. *Stroke* 17:460-466, 1984.
- Meyer JH, Fukuuchi Y, Kanda T, et al. Regional cerebral blood flow measured by intracarotid injection of hydrogen. *Neurology (Minneap)* 22:571-584, 1972.
- Michenfelder JD, and Theye RA. In vivo toxic effects of halothane on canine cerebral metabolic pathways. *Am. J. Physiol.* 229:1050-1055, 1975.
- Miletich, DJ, Ivankovich AD, Albrecht RF, Reimann CR, Rosenberg R, McKissic ED. Absence of autoregulation of cerebral blood flow during halothane and enflurane anesthesia. *Anesth. Analg. (Cleve.)* 55:100-109, 1976.
- Mishima Y, Shigematsu H, Horie Y, et al. Measurement of local blood flow of the intestine by hydrogen clearance method: Experimental study. *Jpn J. Surg.* 9: 63-70, 1979.
- Misrahy GA, Clark LC. Use of platinum black cathode for local blood flow measurements in vivo. *Proc. Intl. Cong. Physiol. (Brussels)*, XX:650, 1956.
- Morawetz RB, DeGirolami U, Ojemann RG, et al.: Cerebral blood flow determined by hydrogen clearance during middle cerebral artery occlusion in unanesthetized monkeys. *Stroke* 9:143-154, 1978.
- Nagata K, Watanabe Y, and Adachi J. Pancreatic local blood flow in experimental acute pancreatitis. *Jpn. J. Digestive Organs* 76: 2054, 1979.
- Pasztor E, Simon L, Dorsch NWC, et al. The hydrogen clearance method in assessment of blood flow in cortex, white matter and deep nuclei of baboons. *Stroke* 4:556-557, 1973.
- Pellegrino LJ, Pellegrino AS, Cushman AJ. A stereotaxic atlas of the rat brain. Second edition. Plenum Press, New York and London, 1979.
- Pulsinelli WA, Brierly JB. A new model of bilateral hemispheric ischemia in the anesthetized rat. *Stroke* 10:267, 1979.
- Roberts PJ, Woodruff GN, Iversen LL, (eds). *Advances in Biochemical Psychopharmacology*, Vol. 19: Dopamine. New York, Raven Press, 1978.
- Rosenblum WI. Regional cerebral blood flow in the anesthetized mouse as measured by local hydrogen clearance. *Stroke* 8:103-106, 1977.
- Salford LG, Plum F, Siesjo BK. Graded hypoxia-oligemia in rat brain.

- I. Biochemical alterations and their implications. *Arch. Neurol.* 29:227-233, 1973.
- Schaus R. The ascorbic acid content of the human pituitary, cerebral cortex, heart and skeletal muscle and its relation to age. *Am. J. Nutrition* 5:39-51, 1957.
- Senter HJ, Burgess DH, and Metzler J. An improved technique for measurement of spinal cord blood flow. *Brain Res.* 149: 197-203, 1978.
- Severinghaus J, Weiskopf R, Nishimura N, Bradley AF. Oxygen electrode errors due to polarographic reduction of halothane. *J Appl Physiol* 31:640-642, 1971.
- Siesjo BK. *Brain Energy Metabolism*. Chichester, UK, John Wiley, 1978.
- Smith AL, and Wollman H. Cerebral blood flow and metabolism. Effect of anesthetic drugs and techniques. *Anesthesiology* 36:378-400, 1972.
- Standgaard S, Olesen J, Skinhoj E, Lassen NA. Autoregulation of brain circulation in severe arterial hypertension. *Br Med J* 1:507-511, 1973.
- Stosseck K. Hydrogen exchange through the pial vessel wall and its meaning for the determination of local cerebral blood flow. *Pflugers Arch.* 320:111-119, 1970.
- Sunt TM, Sharbrough PW, Anderson RE et al. Cerebral blood flow measurements and electroencephalograms during carotid endarterectomy. *J. Neurosurg* 41:310-320, 1974.
- Tamura A, Graham DI, McCulloch J, Teasdale GM. Focal cerebral ischemia in the rat: I. Description of technique and early neuropathological consequences following middle cerebral artery occlusion. *J Cereb Blood Flow Metabol* 1:53-60, 1981.
- Todd NV, Picozzi P, Crockard HA, Russell RR. Duration of ischemia influences the development and resolution of ischemic brain edema. *Stroke* 17:466-471, 1986.
- Trojaborg W, Boysoen G. Relation between EEG, regional cerebral blood flow and internal carotid artery pressure during carotid endarterectomy. *Electroenceph. Clin. Neurophysiol.* 34:61-69, 1973.
- Whiteside LA, Lesker PA, and Simmons DJ. Measurement of regional bone marrow blood flow in the rabbit using the hydrogen washout technique. *Clin. Orthop.* 122:340-346, 1977.
- Will FG. Electrochemical oxidation of hydrogen on partially immersed platinum electrodes. *J. Electrochem* 110:145-152, 1963.
- Willis JA, Doyle TF, Ramirez A, Kobrine AI, Martins AN. A practical circuit for hydrogen clearance blood flow measurement. *AFRR Technical Note TN74-2*, March, 1974.
- Wollman H, Alexander SC, Cohen PJ, Chase PE, Melman E, Bahar MG:

Cerebral circulation during halothane anesthesia: effects of hypocarbia and d-tubocurarine. *Anesthesiology* 25:180-184, 1964.

Wollman H, Alexander SC, Cohen PJ, Smith TC, Chase PE, van der Molen RA: Cerebral circulation during general anesthesia and hyperventilation in man. Thiopental induction to nitrous oxide and d-tubocurarine. *Anesthesiology* 26:329-334, 1965.

Yamori Y, Horie R, Handa H, Sato M, Fukase M. Pathogenetic similarity of strokes in stroke-prone spontaneously hypertensive rats and humans. *Stroke* 7:46-53, 1976.

Young W. Hydrogen clearance measurement of blood flow. A review of technique and polarographic principles. *Stroke* 11:552-564, 1980.

Zuntz N. Zur Pathogenese und therapie der durch rasche Luftdruckanderungen erzeugten Krankheiten. *Fortschr. d. Med.* 15:632-639, 1897.

GRADUATE SCHOOL  
UNIVERSITY OF ALABAMA AT BIRMINGHAM  
DISSERTATION APPROVAL FORM

Name of Candidate Richard J. Boehme

Major Subject Biomedical Engineering

Title of Dissertation Computer Controlled Partial Ischemia  
in the Rat Brain

Dissertation Committee:

Virginia Campbell, Chairman \_\_\_\_\_

Martin McArthur \_\_\_\_\_

Paul A. Conger \_\_\_\_\_

Eric C. Shupard \_\_\_\_\_

Director of Graduate Program Eric C. Shupard

Dean, UAB Graduate School Anthony Kameel

Date June 2, 1987